

Geological Field Trips and Maps

2018
Vol. 10 (2.1)



ISSN: 2038-4947

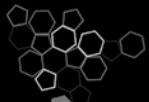


*Società Geologica
Italiana*



ISPRA

Dipartimento per il
SERVIZIO GEOLOGICO D'ITALIA
Organo Cartografico dello Stato (legge n°68 del 2-2-1960)



Sistema Nazionale
per la Protezione
dell'Ambiente

**Active volcanoes in southern Italy
(Etna, Stromboli, Vulcano and Lipari) and their multi-hazard**

IAVCEI Meeting - Naples, 2018

<https://doi.org/10.3301/GFT.2018.02>

GFT&M - Geological Field Trips and Maps

Periodico semestrale del Servizio Geologico d'Italia - ISPRA e della Società Geologica Italiana
Geol. F. Trips Maps, Vol.10 No.2.1 (2018), 106 pp., 56 Figs. (<https://doi.org/10.3301/GFT.2018.02>)

Active volcanoes in southern Italy (Etna, Stromboli, Vulcano and Lipari) and their multi-hazard IAVCEI Meeting, Cities on Volcanoes 10: "Millennia of Stratification between Human Life and Volcanoes: strategies for coexistence". September 2nd-7th, 2018 - Naples, Italy

Federico Lucchi¹, Eugenio Nicotra², Mauro Coltelli³, Gianfilippo De Astis⁴, Costanza Bonadonna⁵, Danilo Cavallaro³

¹ Dipartimento di Scienze Biologiche, Geologiche e Ambientali, Università di Bologna, Piazza Porta S. Donato 1, 40126 Bologna, Italy.

² Dipartimento di Biologia, Ecologia e Scienze della Terra, University of Calabria, Via P. Bucci 15/b, 87036 Arcavacata di Rende (CS), Italy.

³ Istituto Nazionale di Geofisica e Vulcanologia, Sezione di Catania, Osservatorio Etneo, Piazza Roma, 2, 95123 Catania, Italy.

⁴ Istituto Nazionale di Geofisica e Vulcanologia - Sezione di Sismologia e Tettonofisica, Via di Vigna Murata 605, 00143 Roma, Italy.

⁵ Section des sciences de la Terre et de l'environnement, Université de Genève, Rue des Maraîchers 13, CH-1205 Geneva, Switzerland.

Corresponding Author e-mail address: federico.lucchi@unibo.it; eugenio.nicotra@unict.it

Responsible Director

Claudio Campobasso (ISPRA-Roma)

Editor in Chief

Andrea Zanchi (Università di Milano-Bicocca)

Editorial Manager

Mauro Roma (ISPRA-Roma) - corresponding manager

Silvana Falchetti (ISPRA-Roma), *Fabio Massimo Petti* (Società Geologica Italiana - Roma),

Maria Luisa Vatovec (ISPRA-Roma), *Alessandro Zuccari* (Società Geologica Italiana - Roma)

Associate Editors

M. Berti (Università di Bologna), *M. Della Seta* (Sapienza Università di Roma),

P. Gianolla (Università di Ferrara), *G. Giordano* (Università Roma Tre), *M. Massironi*

(Università di Padova), *M.L. Pampaloni* (ISPRA-Roma), *M. Pantaloni* (ISPRA-Roma),

M. Scambelluri (Università di Genova), *S. Tavani* (Università di Napoli Federico II)

Editorial Advisory Board

D. Bernoulli, F. Calamita, W. Cavazza,
F.L. Chiocci, R. Compagnoni,

D. Cosentino, S. Critelli, G.V. Dal Piaz,

P. Di Stefano, C. Doglioni, E. Erba,

R. Fantoni, M. Marino, M. Mellini,

S. Milli, E. Chiarini, V. Pascucci,

L. Passeri, A. Peccerillo, L. Pomar,

P. Ronchi, B.C. Schreiber, L. Simone,

I. Spalla, L.H. Tanner, C. Venturini,

G. Zuffa.

ISSN: 2038-4947 [online]

<http://gftm.socgeol.it/>

The Geological Survey of Italy, the Società Geologica Italiana and the Editorial group are not responsible for the ideas, opinions and contents of the guides published; the Authors of each paper are responsible for the ideas, opinions and contents published.

Il Servizio Geologico d'Italia, la Società Geologica Italiana e il Gruppo editoriale non sono responsabili delle opinioni espresse e delle affermazioni pubblicate nella guida; l'Autore/i è/sono il/i solo/i responsabile/i.

INDEX

Information

Abstract	4
Program summary	4
Safety	6
Accommodation	6

Excursion notes

1. Introduction	7
2. Regional geological setting	8

Itinerary

3. The Aeolian Arc volcanoes	13
3.1 Stromboli	13
DAY 1st: the Stromboli itinerary	20
STOP 1.1	20
STOP 1.2	20
STOP 1.3	22
STOP 1.4	24
STOP 1.5	26
STOP 1.6	28
3.2 Lipari	31
DAY 2nd: the Lipary itinerary	37
STOP 2.1	37
STOP 2.2	39
STOP 2.3	41
STOP 2.4	44
STOP 2.5	45

3.3 Vulcano	49
--------------------------	----

DAY 3rd: the Vulcano itinerary. Ascent to the summit craters of the active La Fossa cone	57
STOP 3.1	57
STOP 3.2	59
STOP 3.3	61
STOP 3.4	62
STOP 3.5	65

DAY 4th: primary school of Vulcano	67
STOP 4.1	67

4. Mount Etna volcano	68
------------------------------------	----

DAY 5th: field itinerary to the summit craters of Etna and the NE-Rift volcanic system	79
STOP 5.1	80
STOP 5.2	84
STOP 5.3	88
STOP 5.4.1	89
STOP 5.4.2	91
STOP 5.4.3	92
STOP 5.4.4	92

DAY 6th: Osservatorio Etneo	94
STOP 6.1	94

References	97
-------------------------	----

Abstract

Southern Italy is a most active tectonic and volcanic setting comprising active (Stromboli, Vulcano) or dormant (Lipari) volcanic islands in the Aeolian Arc, and the majestic Etna volcano (together with the Campanian volcanoes). They have attracted the attention of a great number of volcanologists and can be rightfully considered the cradle of the scientific discipline of Volcanology. In the Aeolian Arc, the main features are the incessant and rhythmic Strombolian explosive activity of Stromboli and the Sciara del Fuoco collapse, together with the deposits of historical Vulcanian eruptions of Vulcano and its present-day intense fumarolic activity. The well-known Rocche Rosse obsidian lava flow and Mt. Pilato pumice are the traces of the Middle Ages activity of Lipari. On Etna, the geology of the valle del Bove depression and the summit craters and NE-Rift, and the 2001, 2002-03 and the 2011-2017 eruptive fissures and lava flow fields give an idea of the variability of its eruptive scenarios. The spectacular geology of these volcanoes and the INGV real-time monitoring network are the bases to discuss the main aspects of volcanic hazard and risk mitigation in case of future eruptions in a highly-urbanized territory characterized by intense tourism exploitation during the summer.

Key words: *Etna, Vulcano, Stromboli, Lipari, Active volcano, Hazard, Monitoring.*

Program summary

First Day: Stromboli - During the morning, a visit to the C.O.A. (Centre of Advanced Operativity) of the Department of Civil Protection to have a look on the real-time monitoring network of Stromboli, and to discuss the response of the Italian Civil Protection to the eruptive crises occurred between 2002 and 2014. The afternoon/evening will be dedicated to the ascent to the summit active craters of Stromboli, with a particular focus on the recurrent lateral collapses and phases of volcanism renewal in the evolution of this basaltic stratovolcano, and on the characteristics of the present-day activity as a typical example of Strombolian explosive eruptions and lava flows under control of volcano-tectonic structures.

Second Day: Lipari - In the second day a boat tour around the Lipari island will be carried out through a number of stop points where different features of its stratigraphy and volcanic evolution as an example of an active calcalkaline volcanic system can be observed. The main purpose will be to illustrate the complex

relationships between volcanism, crustal uplift and Late Quaternary sea-level fluctuations during the building up of an insular volcano, and to highlight the main features of its hazard evaluation. Along the different coastal sectors it will be possible to describe an articulated stratigraphic succession consisting of volcanic products and external tephra layers sourced from Aeolian and Campanian volcanoes, interlayered with different raised marine terraces formed during the last Interglacial (MIS 5, 124-81 ka). Special attention will be given to the observation and discussion of the main features of pumice pyroclastic deposits and obsidian lava flows relative to the most recent activity related to the Holocene up to the late Medieval ages during a short walk in the area between Porticello and Acquacalda

Third and Fourth Days: Vulcano - The third day will be dedicated to the ascent to the summit craters of La Fossa cone at Vulcano island. This will provide insights on the deposits produced by the typical Vulcanian explosive activity of AD 1888-90 and the dynamics of sedimentation and erosion in an active volcano. Moreover, the role played by the La Fossa caldera in conditioning the localization of the active vents and the distribution of volcanic products will be investigated. During the stops on the summit of La Fossa, we will also discuss the main critical infrastructure and facilities on the island and aspects of the associated systemic vulnerability. During the morning of the fourth day we will discuss aspects of assessment and management of volcanic risk with a particular application to Vulcano island. We will also have the opportunity to meet with the teachers and the children of the primary school of Vulcano with whom we have been running an experiential learning exercise on volcanic crisis management for the past 7 years.

Fifth and Sixth Days: Etna - The fifth day will be dedicated to the ascent to Mount Etna volcano. The main topics of the first part of the fieldtrip are the collapse-related Valle del Bove depression, where we will also discuss about the shifting of feeding system of the ancient volcanic centres and about recent lava fields produced by lateral and eccentric eruptive activities, and the active summit craters with their impressive fumarole fields. During the second part of the day, we will walk around the remnants of the Ellittico caldera and some eruptive fissures located along the NE-Rift, in particular the 2002 NE-Rift fissure.

The sixth day will focus on the visit of the control room of the volcano monitoring system of INGV - Osservatorio Etneo in Catania, where the volcanic plumes monitoring for the civil aviation safety will be also presented and discussed.

Safety

Field booths are suggested for most of the field activity, and a lamp is mandatory for climbing the Stromboli volcano (if you do not have one you have to rent it in Stromboli). Hat and sunscreen are useful given the commonly sunny and hot weather of Sicily during the summer. Please bear in mind that fieldwork on Stromboli and Etna will be carried out at high elevations (up to 3000 m asl), with rapidly changing, possibly cold and windy weather conditions, so that a rain-jacket is recommended.

Emergency contact numbers:

(+39) 112 – Carabinieri; (+39) 113 – Police; +39 (115) – Fire fighters; +39 (118) – First Aid.

Accommodation

Stromboli: Case La Giara. **Vulcano:** Hotel Conti. **Etna:** Hotel Biancaneve, Nicolosi (CT).



1. Introduction

This fieldtrip will focus on the geological, geochemical and petrological aspects of active volcanoes of Southern Italy (Aeolian Arc and Mount Etna), and the processes of hazard evaluation, and risk mitigation and management.

The Aeolian Arc is a unique geological area, well known all around the world as seat of some peculiar volcanic activities and related deposits. It consists of seven volcanic islands (Alicudi, Filicudi, Salina, Lipari, Vulcano, Panarea and Stromboli) and several seamounts (Eolo, Enarete, Sisifo, Lametini, Alcione and Palinuro) forming a volcanic arc controlled by regional faults. Among these, Stromboli and Vulcano have active volcanic manifestations, whereas Panarea and Lipari are presently dormant. They have attracted the attention of a great number of volcanologists, and can be rightfully considered the cradle of the scientific discipline of Volcanology, giving the name to the world-wide definitions of the 'Strombolian' and 'Vulcanian' styles of eruptive activity. At Aeolian Islands, attention will be focused on the processes and deposits related to the historic to present-day activities of the Stromboli, Vulcano and Lipari volcanic systems. Particular attention will be dedicated to the persistent and rhythmic Strombolian explosive activity of the Stromboli summit craters above the Sciara del Fuoco collapse scar, together with the INGV real-time monitoring network, which makes this volcano among the most observed and studied in the world. Then, the craters and deposits related to the AD 1888-90 Vulcanian explosive eruption of La Fossa cone on Vulcano will be observed, together with the main features of its present-day intense fumarolic activity. The geological outcrops will give the bases to discuss the main aspects of volcanic hazard, risk mitigation and crisis management of La Fossa possible future eruptions, whereas talks with the population and a simulation of the response of Italian Civil Protection and Institutions to an eruptive crisis (in collaboration with the Specialized CERTificate in assessment and management of Geological and Climate related Risk (CERG-C) of the University of Geneva, Switzerland) will provide the state of Community preparedness. Finally, the well-known Rocche Rosse obsidianaceous lava flow and Mt. Pilato pumice deposits will be investigated as the record of the latest activities of the Lipari volcanic system during the Middle Ages. Mount Etna is widely known as one of the most active volcanoes on Earth, and is a classical example of how a volcano interacts with activity of resident population and tourists. A geological walk towards the summit area of Mount Etna and the northern volcanic rift, will give the possibility to observe the variability of eruptive scenarios of this majestic volcano, and to investigate the volcanic products of the 2001 and 2002-03, and 2011-2017 paroxysms. The spectacular geological outcrops will give the bases to discuss the main aspects

of volcanic hazard, risk mitigation and crisis management of Etna's possible future eruptions in a highly-urbanized territory characterized by intense tourism exploitation.

2. Regional geological setting

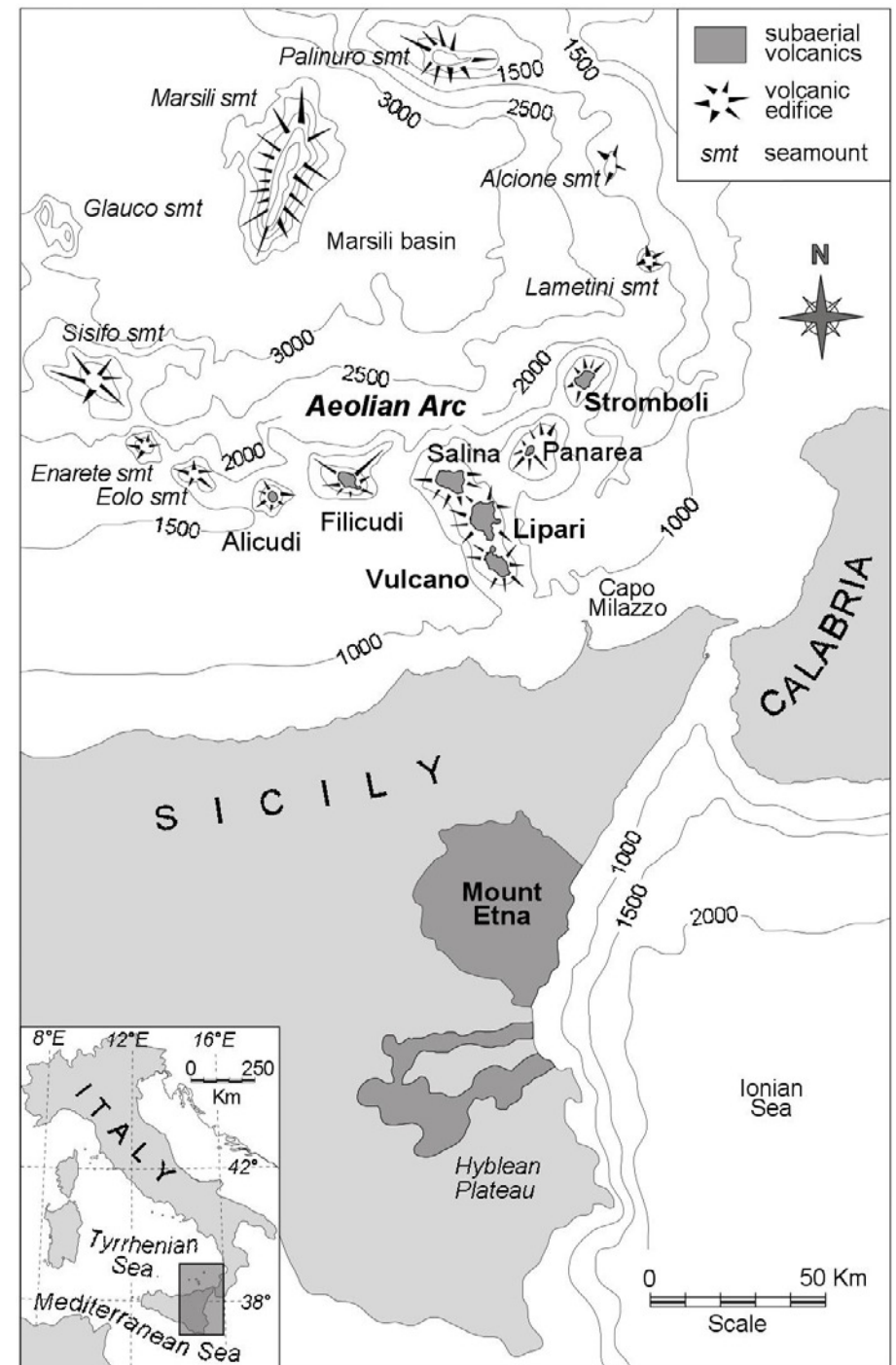
2.1 Aeolian Arc

The Aeolian Arc volcanic islands and associated seamounts form a ring-shaped structure around the subsiding Marsili basin and Marsili seamount (Fig. 1), emplaced on a 15-20 km thinned continental crust (Ventura, 2013 for a review). The Aeolian volcanism is generally assumed to have developed entirely during the Quaternary (c. 1.3 Ma for submarine lavas of Sisifo seamount; Beccaluva et al., 1985). The compilation of the available radiometric ages for the subaerial portions of the Aeolian Arc volcanoes - after discussion in the light of the reconstructed stratigraphy - shows that they mostly developed from c. 270-240 ka to the present (Fig. 2).

Based on structural, seismological and geochemical data, the Aeolian Arc is generally subdivided in three main structural/volcanological sectors (Fig. 1):

- the western sector extending from the Glauco seamount to Alicudi and Filicudi and the oldest part of Salina is controlled by a WNW-ESE striking fault system ("Sisifo-Alicudi") and is now considered extinct;

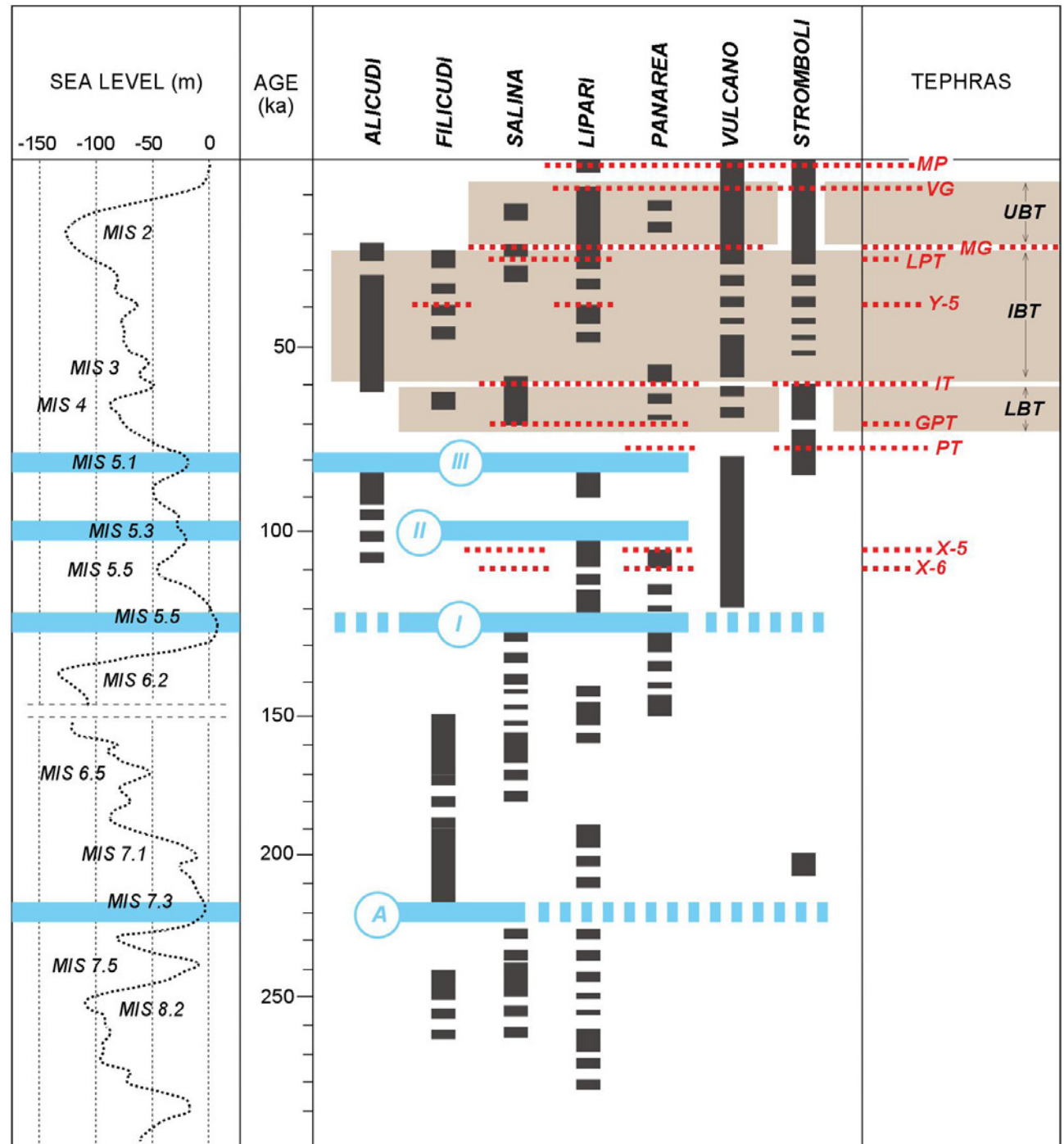
Fig. 1 - Sketch map of southern Italy showing the location of the Aeolian Arc and Mount Etna. Depth contour lines in metres below sea level (modified from Beccaluva et al., 1985).





- the central sector includes the volcanic systems of Salina, Lipari and Vulcano belonging to a NNW–SSE-oriented volcanic belt striking along the Tindari–Letojanni regional fault system that transversely intersects the arc-shaped structure of the Aeolian archipelago in its central sector; in this sector historical eruptions occurred at Lipari (last eruption in 1220 AD) and Vulcano

Fig. 2 - Schematic block diagram showing the chronology of eruptive activity in the Aeolian volcanic arc, as emerges from the available radiometric ages of volcanic products (vertical bars); see Lucchi et al., 2013c for a complete review of the ages and methods. The ages of marine paleoshorelines A, I, II and III (light grey horizontal bars) are displayed by comparison with specific peaks of the Late Quaternary sea-level curve of Waelbroeck et al., (2002). The main tephra layers recognized across the Aeolian arc are also shown: X-6 and X-5 tephra layers (Campanian); PT=Petrazza Tuffs (Stromboli); GPT=Grey Porri Tuffs (Salina); IT=Ischia-Tephra (Campanian); Y-5 tephra layer (Campanian); LPT=Lower Pollara Tuffs (Salina); MG=Monte Guardia (Lipari); VG=Vallone del Gabelotto (Lipari); MP=Monte Pilato (Lipari); LBT, IBT, UBT=Lower, Intermediate, Upper Brown Tuffs (Vulcano).





(last eruption in 1888-90 AD), the latter currently characterized by intense gas emissions, and fumaroles, hot springs and shallow seismicity are recognized in large submarine areas (Gamberi et al., 1997);

- the eastern sector extending from Panarea and Stromboli to the Alcione and Palinuro seamounts is controlled by a NNE-SSW to NE-SW striking fault system and is characterized by the persistent eruptive activity of Stromboli and gas emissions at Panarea, together with very shallow seismicity along the seamounts.

From a petrological point of view, calcalkaline (CA) and high-K calcalkaline (HKCA) rocks occur throughout the arc but dominate at Alicudi, Filicudi, Salina, Lipari and Panarea, whereas shoshonites (SHO) are spatially restricted to the peripheral central-eastern islands of Vulcano and Stromboli during their mature to late stage of volcanic activity (Peccerillo et al., 2013 for a review). The degree of magma evolution increases from the external to the central islands. Basalts to andesites were erupted during the older stages of evolution (except for Stromboli), while shoshonitic and some undersaturated leucite-bearing lavas have been emitted since c. 40 ka. These K-rich magmas are associated both in space and time to rhyolites and dacites and minor trachytes. Rhyolites and dacites were emitted at Panarea, Vulcano, Salina and Lipari, and were generally associated with an increase of the energy and magnitude of the eruptions. A number of Subplinian explosive eruptions occurred at Lipari (Monte Guardia: 27–24 ka; Vallone del Gabellotto: 8.7–8.4 ka), Stromboli (Petrazza: 77–75 ka) and Salina (Grey Porri Tuffs: c. 70–67 ka; Lower Pollara: 27.5 ka). Rhyolites were also emitted as lava flows and domes at Lipari and Vulcano (obsidian lavas and endogenous dome), and Panarea (Basiluzzo dome) or low-energy pumice deposits at Lipari (Monte Pilato: AD 776).

A regional framework for stratigraphic correlations in the Aeolian archipelago is provided by widespread tephra layers and Late Quaternary marine terrace deposits combined with the available radiometric ages (Fig. 2; Lucchi et al., 2013c). Several tephra layers of Campanian and Aeolian provenance dated back to c. 110 ka, were reported. The most important key-layers are the X-6 (110 ka) and X-5 (105 ka) tephra layers and the so-called "Ischia Tephra" (56 ka, likely corresponding to the Y-7 marine tephra layer) from the Campanian area, the Grey Porri Tuffs (70–67 ka) and the Lower Pollara Tuffs (27.5 ka) from Salina island, the Monte Guardia pyroclastics (27–24 ka) from Lipari island and the Brown Tuffs (c. 70–8 ka) from Vulcano island. Late Quaternary marine terrace deposits are recognized along the coastal slopes of most of the Aeolian archipelago (except at Vulcano and Stromboli). They record distinct interglacial sea-level peaks during marine isotope stages (MIS) 5 and 7 in a context of prevalent long-term crustal uplift. Key erosional unconformities bounding the terrace deposits are the ravinement surfaces formed at the onset of MIS 7.3 (F_1), MIS 5e (U_1) and MIS 5c interglacial peaks (L_3), and the subaerial unconformity formed during the MIS 5a



sea-level fall up to the emplacement of Brown Tuffs (U_{II}) (Lucchi, 2009). These unconformities are adopted as important regional-scale markers for chronostratigraphic classification and correlation between the different islands of the Aeolian Arc (Fig. 3).

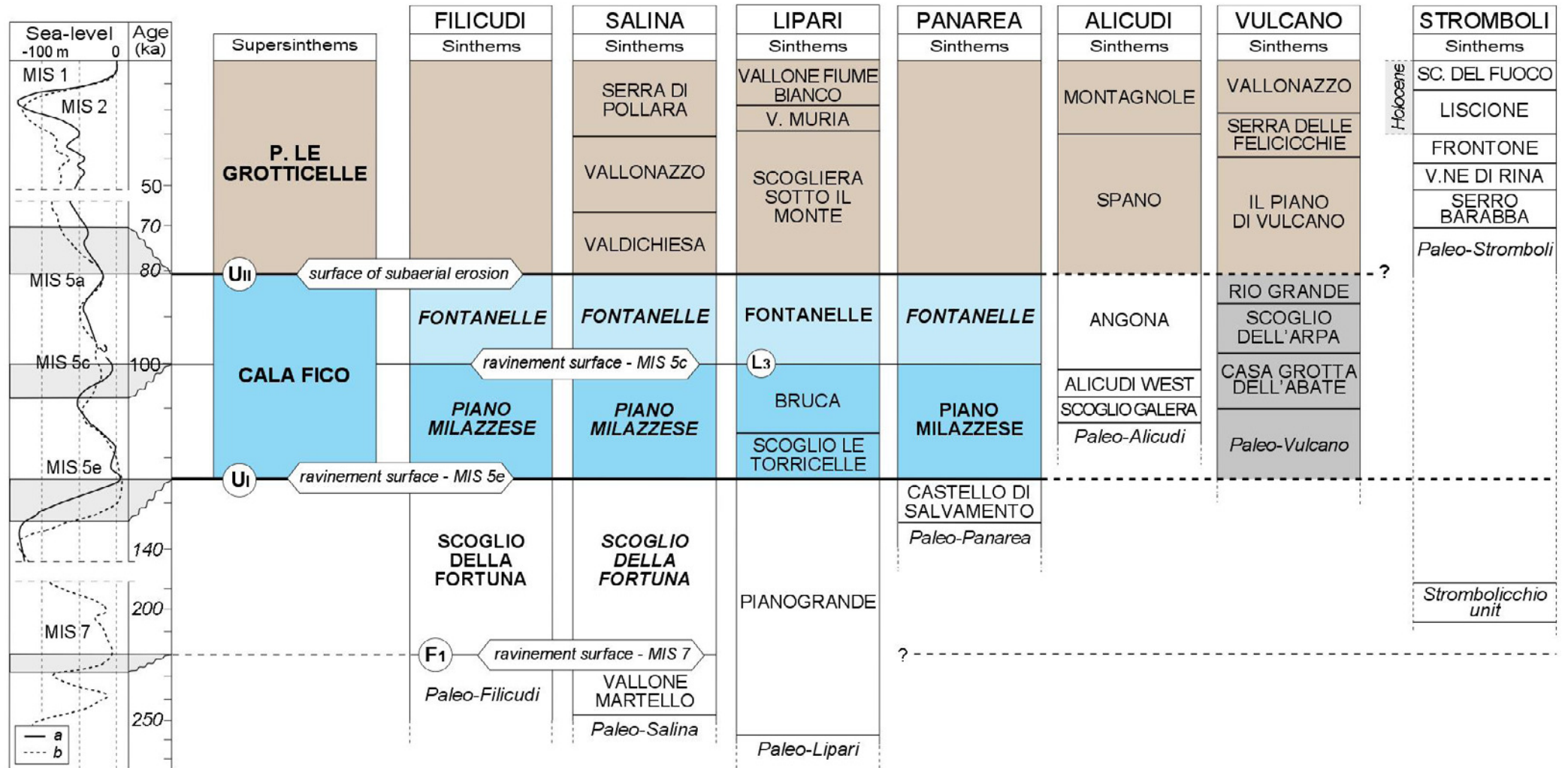


Fig. 3 - Generalized stratigraphic framework of unconformity-bounded units across the Aeolian archipelago (from Lucchi et al., 2013c). The time interval of formation of the correlative major unconformities is outlined by linking with the sea-level curves (a=Chappell and Shackleton 1986; b= Waelbroeck et al., 2002).



2.2 Mount Etna

Mount Etna is a basaltic composite volcano, whose activity began during the middle Pleistocene in eastern Sicily, in a complex geodynamic setting, resulting from the Neogene convergence between the European and African plates. Etna volcanism developed in a sector where the front of the Apenninic-Maghrebian Chain overlaps the foreland Hyblean (Fig. 1) domain succession belonging to the African continental plate margin (Lentini et al., 2006). Hence, the volcano basement is made up of the Apenninic units, cropping out on the western and northern Etna boundaries, and by the Plio-Pleistocene Gela-Catania foredeep sediments to south and southeast (Di Stefano and Branca, 2002), deposited on the flexured margin of the foreland Hyblean Plateau.

Etna volcanism is considered the northern extension of that one occurring from the Late Trias up to Quaternary (Carbone et al., 1982) on the Hyblean Plateau. The most recent volcanism occurred during Pliocene-lower Pleistocene (1.6 Ma, De Beni et al., 2011) along the northern margin of the plateau, producing lavas with tholeiitic and alkaline affinity (Carveni et al., 1991). A thick volcanic succession, buried within the foredeep Pleistocene sediments of Catania Plain, was detected by magnetic anomalies and sampled by drilling (Longaretti et al., 1991; Grasso and Ben Avraham, 1992).



3. The Aeolian Arc volcanoes

3.1 Stromboli

The Stromboli volcano is well known for its persistent state of mild explosive Strombolian activity, which has attracted both scientists and travellers since the ancient times (see Rosi et al., 2013 for a review).

The island of Stromboli (total area of 12.6 km²) is the north-easternmost of the Aeolian archipelago and represents the subaerial culmination of a broad, largely submerged, cone-shaped, slightly NE–SW-elongated volcanic edifice rising c. 2400–2700 m above the seafloor (Fig. 4), with a maximum base diameter of c. 16 km at the –1500 m isobath and a subaerial peak of 921 m above sea level (a.s.l.) at “I Vancori”.

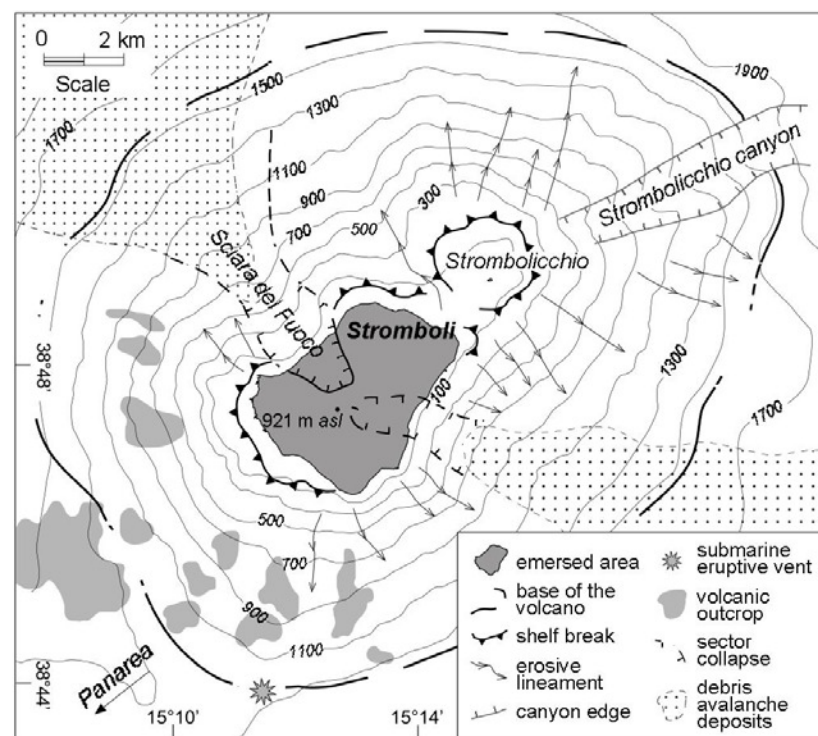


Fig. 4 - Morpho-structural sketch map of the submerged flanks of Stromboli (modified from Romagnoli et al., 2013). Depth contour lines are in metres below sea level; elevation between contour lines is 200 m.

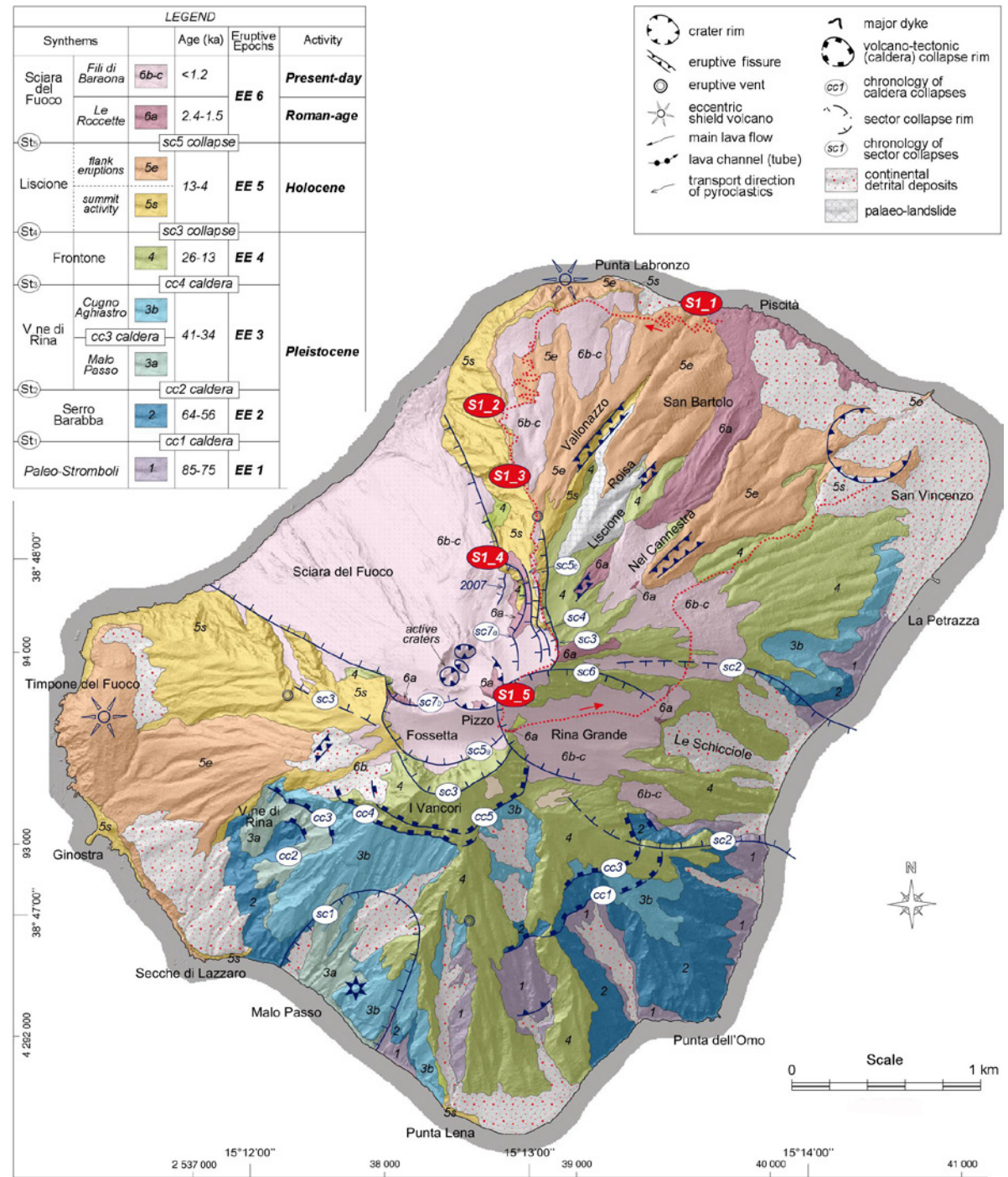
The structural pattern is dominated by the NE–SW regional system as demonstrated by the orientation and distribution of dikes and sheets, eruptive fissures, secondary vents and the active summit craters (Fig. 5). A sequence of lateral collapses with estimated volumes varying from 0.7 to 2 km³ have been recognized occurring during the last 13 ka along the NW flank of the island, giving rise to the multistage Sciara del Fuoco collapse structure (Francalanci et al., 2013). Five concentric caldera collapses are recognized along the southern flank of Stromboli (Fig. 5), and mark the most important erosional unconformities during the older to intermediate cycles of activity of Stromboli. Several dikes and eruptive fissures over the entire history of Stromboli (up to the present) are exposed along the southern flanks of the volcano (Fig. 5; Hornig-Kjarsgaard et al., 1993; Corazzato et al., 2008). Erupted products display large variations from CA basaltic-andesites, to potassic (KS) trachybasalts and shoshonites, through HKCA basalts and andesites and SHO basalts and few trachytes (Fig. 6). This petrochemical variability indicates that magmas underwent variable and complex differentiation processes (cf. Francalanci

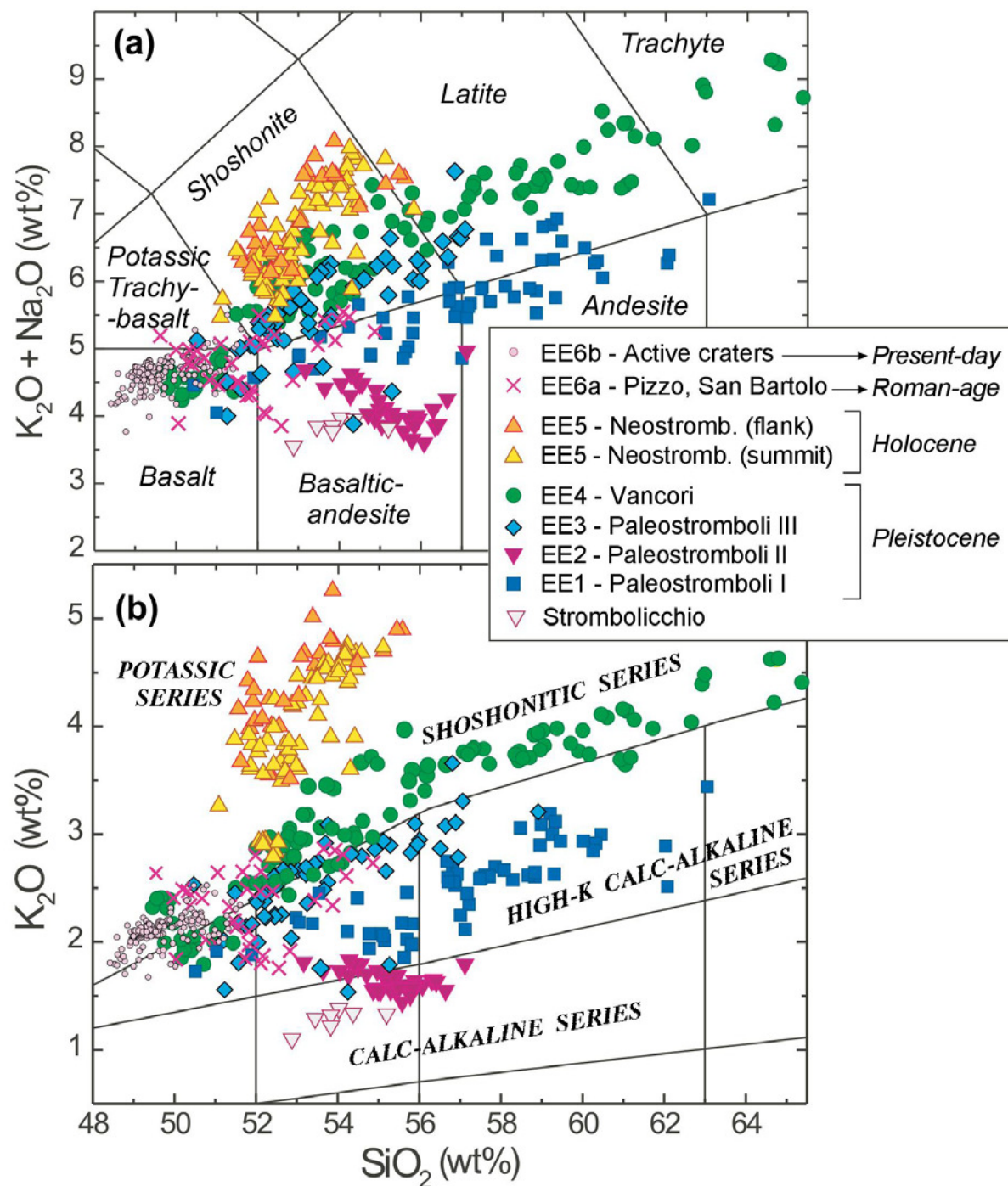


et al., 2013 for a review). Simple fractional crystallisation mainly affected SHO and HKCA magmas, KS melts evolved by crustal assimilation associated to crystallisation, whereas mixing and a combination of the previous processes occurred in different types of magma. Two major magma reservoirs and other minor batches were present at different depths during all the Stromboli history. Variable partial melting degrees of a heterogeneous mantle wedge have been also proposed in order to explain the genesis of the different parental magmas.

A major effort in improving the knowledge on the Stromboli volcano and its eruptive and magmatic conditions of activity has been produced after the 2002-2003 eruption (more than 400 papers since 2004). This was one of the most intense and dangerous eruptive

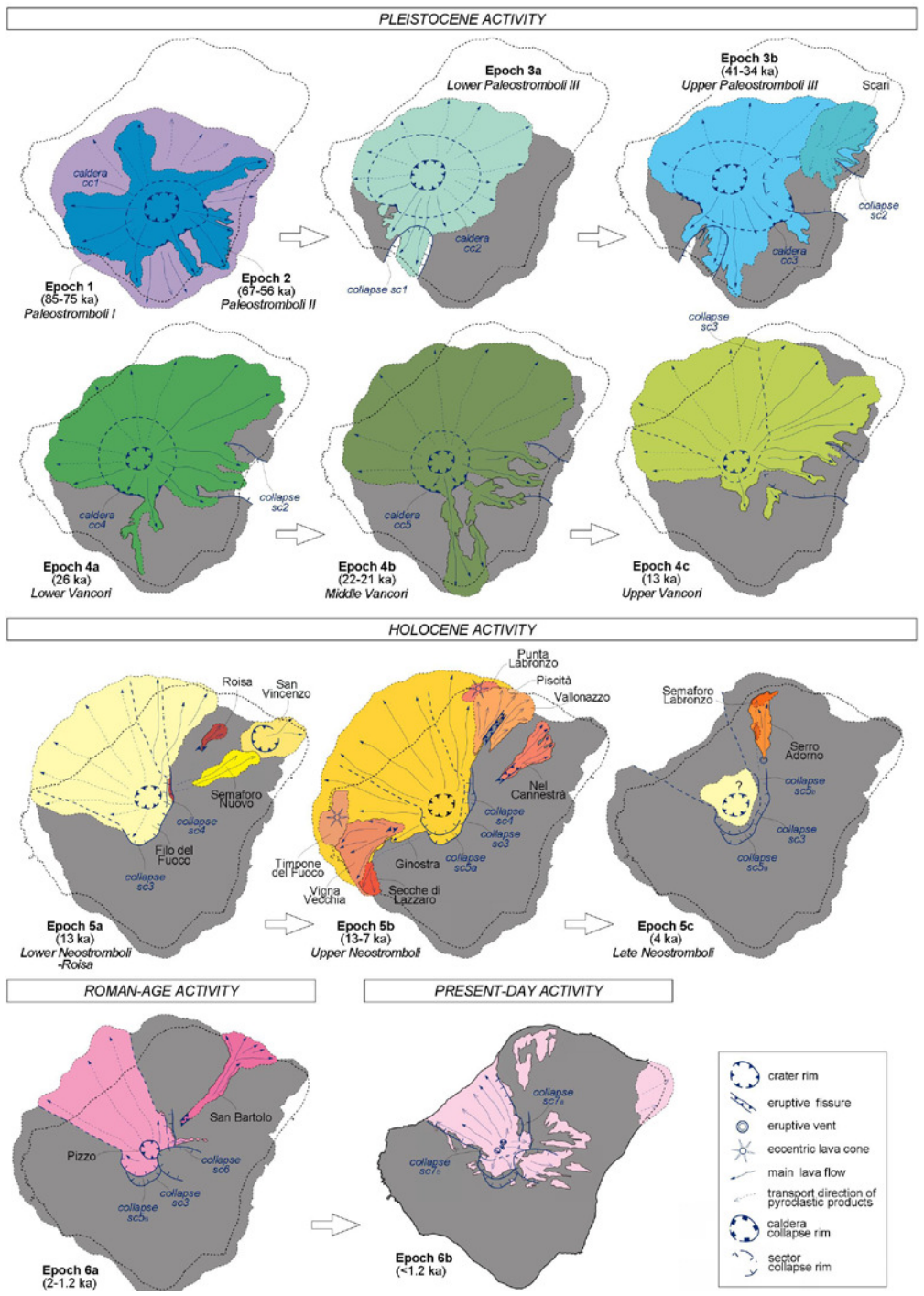
Fig. 5 - Sketch geological map of Stromboli in terms of the main unconformity-bounded units and corresponding Eruptive Epochs (modified from Lucchi et al., 2013b). Kilometric coordinates conform to the Gauss-Boaga system (Sistema Nazionale - Fuso Est) and geographic coordinates are related to Greenwich meridian. DEM-shaded relief image courtesy of DICEA, Università di Roma La Sapienza (research project funded by the Italian Department of Civil Protection). The trace of the Semaforo Labronzo footpath and location of the main stops of the fieldtrip are shown in red.





crisis of the past three centuries, consisting of the combination of a slope failure along Sciara del Fuoco, effusive activity and a paroxysm explosion that culminated in a landslide-driven tsunami wave hitting the village of Stromboli (see Bonaccorso et al., 2003 for a review). As a result of the threat connected with paroxysmal explosions, slope failure and tsunami, there were a rapid expansion of the monitoring system and a substantial change in the conditions of turistic approach to the volcano set by the Italian Civil Protection. Principal current networks include: broadband seismic network (INGV), seismic-acoustic network (Univ. of Firenze), continuous ground gas emission (INGV), continuous gas streaming from the summit craters (INGV), Radon monitoring (Univ. of Torino), ground-based, Linear SAR (Lisa) (JRC Ispra - Univ. of Firenze), total station

Fig. 6 - Classification of Stromboli rocks in the (a) Total Alkali v. Silica (TAS; Le Maitre et al., 1986) and (b) K_2O v. SiO_2 (Peccerillo and Taylor 1976) diagrams. Rocks are subdivided into groups conforming to the recognized synthems, Eruptive Epochs (EE) and main lithosomes (Neostromboli includes all the lithosomes of the summit activity and flank eruptions) Data are plotted on LOI-free basis. Data source from Francalanci et al., (2013) and references therein.



(INGV), continuous GPS stations (INGV), Tiltmeters (INGV), Ondameters (National Civil Protection), optic and thermal videocameras (INGV). Periodic topographic and bathymetric surveys have been also conducted by the Universities of Rome "La Sapienza" and Bologna, and by the IGM - CNR of Bologna.

3.1.1 Eruptive history

The eruptive, magmatic and volcano-tectonic history of Stromboli is here synthetically described according to the most recent stratigraphy and geological map by Francalanci et al. (2013) and Lucchi et al. (2013b). Based on the reconstructed unconformity-bounded stratigraphy (Fig. 5), the eruptive history of Stromboli is described by six successive Eruptive Epochs in the time interval between ca. 85 ka and present times (Fig. 7). The Strombolicchio lava neck (ca. 204 ka), representing the remnants of the activity of an independent eruptive centre located 1.7 km off the north-eastern coast of Stromboli, is out of this time-stratigraphic framework. The Eruptive Epochs of Stromboli generally developed over tens of thousand of years and were interrupted by destructive (erosional) phases driven by recurrent vertical caldera-type (cc1-5) and lateral (sector and flank) collapses (sc1-7), generally associated with periods of volcanic quiescence. Eruptive vents and fissures have been mostly concentrated in the

Fig. 7 - Sketch maps showing the location and structural control of the eruptive vents (and relative volcanic products) during the successive Eruptive Epochs of Stromboli.



summit area of Stromboli, either within successive caldera structures (Pleistocene activity) or at the top of the Sciara del Fuoco (Holocene activity). The eruption style was almost invariably Strombolian-effusive, beside minor hydromagmatic events.

Most of the subaerial growth of Stromboli occurred during the Pleistocene through Epochs 1 (Paleostromboli I, 85–75 ka, HKCA), 2 (Paleostromboli II, 64–56 ka, CA), 3 (Paleostromboli III, 41–34 ka, HKCA transitional to SHO) and 4 (Vancori, 26–13 ka, SHO), progressively leading to the construction of a 950–1000 m high composite volcano, registering a general discontinuous increase through time of potassium and silica contents. The Pleistocene activity was homogeneously of central-type with alternating effusive and Strombolian eruptions from vents constantly located in the summit area of Stromboli (within-caldera). A major collapse (sc3) occurred at 13 ka as a result of a combination of oversteepening and overloading of the growing cone together with recurrent dike emplacement along the NE–SW structural zone crossing the cone (Tibaldi 2001). This was a voluminous, deep-seated, horseshoe-shaped failure structure that truncated the Upper Vancori volcano in the area presently occupied by the Sciara del Fuoco, interrupting the Pleistocene development of Stromboli and playing a pivotal role in conditioning the location of active vents and the development of the successive lateral collapses during the subsequent eruptive history of Stromboli.

Afterthat, the Holocene activity of Stromboli (Epoch 5) developed from vents mostly located in the upper portion of the collapse depression along the north-western flank of the edifice, producing volcanic products with a distinctive KS magma composition (Neostromboli series). The activity is subdivided into three successive sequences of mostly effusive eruptions producing dominant lava flow successions from the summit vents, Lower Neostromboli (Epoch 5a, c. 13–12 ka), Upper Neostromboli (Epoch 5b, c. 13–8 ka) and Late Neostromboli (Epoch 5c, c. 4 ka), developed in alternation with recurrent NW-dipping lateral collapses (sc4, sc5a–b) along Sciara del Fuoco (cf. Francalanci et al., 2013 for more details). During the Holocene, a number of flank (explosive and effusive) eruptions occurred from vents and NE-trending fissures located along the north-eastern and western (buttressed) flanks of the cone, together with some hydromagmatic eruptions and PDCs likely induced by successive lateral collapses (Francalanci et al. 2013 and ref. therein).

The Recent Stromboli activity (Epoch 6, c. 2.4 ka) occurred from summit vents and fissures located near to the presently active craters, with subordinate flank activity producing the San Bartolo lava flow field along the NE flank of the island. The erupted products mostly filled the multi-stage collapse structure corresponding to the present Sciara del Fuoco, and were characterized by a substantial shifting of magma composition to SHO and HKCA mafic compositions (Francalanci et al., 2013). A minor SE-dipping flank collapse (sc6) truncated the



summit and south-eastern flank of the Pizzo cone constructed during the Roman-age activity (Francalanci et al., 2013). Starting from the 8th century, the Present-day activity of Stromboli has been characterized by an eruption style similar to that of the currently active craters of Stromboli (Rosi et al., 2013 for a review). The erupted products are typically characterized by the occurrence of coexisting bimodal juvenile fragments, which are the SHO and high-K basaltic, highly-porphyrific (HP) black scoriae and low-phenocryst (LP) golden pumices derived from mingling between HP- and



Fig. 8 – (a) Aerial overview of the crater terrace located at elevations of c. 750 m asl in the upper part of the Sciara del Fuoco collapse (after the 2002-2003 eruption). The footpath to the active craters is put in evidence (arrow) together with the summit of the Pizzo cone (c. 920 m asl) representing the best viewpoint of the eruptive activity at the end of the ascent (photo courtesy of P. Lo Cascio). (b) Snapshot of the eruptive jet (with a ground-hugging pyroclastic flow cloud at the bottom) relative to the 5 April 2003 paroxysm (modified from Rosi et al., 2013). (c) Active lava flow field (and lava delta) during the 2007 eruption along the coastline near the NE border of the Sciara del Fuoco collapse (photo courtesy of C. Romagnoli).



LP-magmas (Francalanci et al., 2013). The active craters are clustered in a NE-SW-elongated, roughly elliptical crater terrace lying about 750 m (a.s.l.) in the upper portion of the Sciara del Fuoco collapse. Their activity is characterized by persistent and mild (Strombolian) explosive eruptions and intermittent more energetic explosions (paroxysms), with episodic lava effusions within the Sciara del Fuoco depression (Fig. 8). Lava flows are emitted either as overflows from the active craters or by vents and fissures located inside the Sciara del Fuoco collapse at lower elevations than the current crater area, most frequently under control of the major NE-SW structural trend. The vents opened along the Sciara del Fuoco frequently produce voluminous lava flow fields able to reach the sea, e.g. in 2002–2003 and 2007 (see Calvari et al., 2005, 2010 for a review) and 2014.



DAY 1st: the Stromboli itinerary

Ascent to the summit active craters of Stromboli along the old footpath of Semaforo Labronzo (which was abandoned after the 2002-2003 eruptive crisis) running aside the northern border of the Sciara del Fuoco collapse and visit to the C.O.A. (Center of Advanced Operativity) of the Italian Civil Protection and INGV (Fig. 5).

STOP 1.1: (38°48'8"N, 15°14'2"E)

Locality: COA (Advanced Operational Center) of the Italian Civil Protection and INGV (National Institute of Geophysics and Volcanology)

Focus: Eruptive crisis at Stromboli during the last 20 years. INGV real-time monitoring network.

Description: During the 2002-2003 eruption occurred at Stromboli, the Department of Civil Protection established on the island an Advanced Operational Center (in Italian COA), located in the upper part of the Scari-San Vincenzo village and aimed to support scientific and logistic operations. The COA collects signals from the multi-parameter monitoring networks (seismic, acoustic, geochemical, ground deformation, magnetic, gravimetric, optical and thermal cameras) installed on the island and managed by the INGV and the Department of Earth Sciences of the University of Florence. Particularly, radar interferometers (SAR) are installed to monitor the active deformations and landlised processes along the Sciara del Fuoco collapse scar, together with a warning system for tsunami waves offshore the island. In emergency phases, the COA welcomes personnel from the Civil Protection Department, and the scientific community, together with all the possible organizations that can play a role during the eruptive "crisis", thus becoming the place where decisions on the mitigation of volcanic risk and the safety of the population are taken in real time.

Points-for-discussion

- Hazard and Risk Mitigation at Stromboli: the role of INGV and the Italian Civil Protection.

STOP 1.2: (38°48'36"N, 15°13'39"E)

Locality: Piscità

Focus: NE-trending flank eruptions of the Holocene activity



Description: The ascent to the Stromboli summit is performed along the old footpath of Semaforo Labronzo. In the first part of the footpath, passing along the NE flank of Stromboli, there is the field evidence of some of the NE-trending flank fissures that characterized the latest phases of the Upper Neostromboli activity (c. 8-7 ka) (Fig. 9). The Nel Cannestrà fissure (8-7.5 ka) is made evident by a NE-elongated ridge at elevations between 300 and 470 m made up by welded Strombolian-Hawaiian fallout scoriaceous agglomerates and lava flows, the latter descending the lower slopes of the volcano near to the San Vincenzo scoria cone (on which there is the main village of San Vincenzo). Similarly, the Vallonazzo fissure (7-6.5 ka) is recognized by a NE-trending linear gorge at elevations of c. 200–300 m and a laterally-extensive, fountain-fed welded scoria blanket that mantles both sides of the valley.



Fig. 9 - Aerial view of the north-eastern flank of Stromboli hanging on the Piscità village where the morphological evidence of deposits from flank eruptions of the Holocene activity is shown: RO=Roisia (c. 13 ka); NC=Nel Cannestrà (8-7 ka); VA=Vallonazzo (7-6.5 ka). The part at higher elevations of the San Bartolo lava flows (SB; 2.3-2 ka) is also shown, with its well developed lava channel. The location of the corresponding NE-trending eruptive fissures is put in evidence (*).

A most important feature is represented by the San Bartolo lava flow field (c. 2.4-2 ka) originated from a NE-trending fissure exposed at elevations of 600–650 m asl (Fig. 9). The lava flow field descended along a palaeovalley of the north-eastern slope of Stromboli forming two parallel lava channels and a tube in the area of the San Bartolo church, then fanwise opening at the outlet of the palaeo-valley and forming a voluminous flattish lava delta (c. 20 m thick, 1.2 km wide) in the coastal sector of Piscità-Ficogrande. The San Bartolo lavas, well exposed in the Piscità beach, are HKCA basalts to basaltic andesites, rich in olivine, clinopyroxene and plagioclase phenocrysts, and include mafic and ultramafic cumulitic xenoliths of different mineralogical assemblages (olivine-gabbro, gabbro-norite, anorthosite, dunite, wehrlite and clinopyroxenite; Laiolo and Cigolini 2006).



Points-for-discussion:

- Sources of volcanic hazard along the more inhabited areas of the Stromboli island.

STOP 1.3: (38°48'20"N, 15°12'52"E)

Locality: Stop point at elevation of 300 m asl

Focus: Sciara del Fuoco collapse

Description: At elevation of 300 m asl the footpath opens on the impressive view of the Sciara del Fuoco multi-stage collapse structure and the active craters of Stromboli (Fig. 10a). This is a voluminous, deep-seated failure structure bordered by a large horseshoe-shaped escarpment cutting the NW flank (and summit) of Stromboli. Sciara del Fuoco was formed in its present appearance through several lateral collapses during the last 13 ka, with major collapse rims recorded during the Holocene (sc3, 4, 5) and in late Medieval times (sc7). The collapse has a total volume up to c. 2 km³ (in its subaerial portion) estimated by Tibaldi (2001) for the early collapse truncating the summit of the Upper Vancori volcano, with vertical displacements up to a few hundreds of metres. Subsequent collapses had volumes of 0.5-1 km³ suggesting a general decrease through time after the first collapse event, as also demonstrated by the coaxial geometry of the collapse scars (Tibaldi, 2001). Slope inclination within the collapse is up to 35-40° with a flattish area immediately below the presently active craters.

Along the north-eastern, steep shoulder of Sciara del Fuoco the Lower and Upper Neostromboli (c. 13-8 ka) products are exposed thanks to erosion and truncation by subsequent collapses during the Holocene (Fig. 10a), as a record of successive phases of infilling and failure of the collapse depression. They are represented by thin, laterally persistent pahoehoe to aa lava flows (with well evident phenocrysts of clinopyroxene, olivine and plagioclase, and leucite in the groundmass or as microphenocrysts), embedded within a thick autoclastic breccia deposit, dipping with a slight component toward the Sciara del Fuoco (following the original slope of the pre-collapse volcano) or to the NNE, with bedding inclination of 15-30°. They have been emitted from the summit craters and flowed down the steep slopes of the early Upper Vancori collapse, progressively piling up and occasionally overflowing its lateral rims and invading the north-eastern (and western) sector of Stromboli, before they were truncated by recurrent lateral failures occurred during the Holocene. The Neostromboli lava successions are cut by several intersecting dikes (Fig. 10a), either feeding the summit activities over the younger stages of eruptive history of Stromboli (radial dikes) or following the walls of the



Fig. 10 – View of the active craters and Sciara del Fuoco collapse from the stopping place at elevation of 300 m asl (a); this is located on the NE border of the collapse that truncates (and allow exposure of) the products of the summit Holocene activity (Lower and Upper Neostromboli), represented by thick successions of lava flows embedded in autoclastic breccias and crossed by several intersecting dikes. In the lower part of the collapse, the lava delta produced during the latest 2014 effusive eruption is visible (b).

collapse reflecting the tensional debuttressing associated with the collapse formation (circum-sector collapse dikes; Tibaldi 2001).

The Neostromboli lavas emerge from the cover of the most recent lava flows and scoriae cropping out within the collapse depression and dipping dominantly parallel to the present collapse scar. They are the products erupted from the summit active craters during the whole Present-day activity subsequent to the latest collapse (sc7) in late Medieval times. From this point of view, the lava flows erupted in August 2014 are well visible, mantling the collapse-filling sequence and forming a lava delta (Fig. 10b). These lava flows were originated from a lateral fissure opened at the base of the presently active craters and formed a lava flow field according



to the typical behaviour described for the 2002–2003 (and 2007) effusive activity (cf. Spampinato et al., 2008), with stacked lava flows with pahoehoe to aa characteristics that run along the steep slopes of the collapse frequently reaching the sea.

Points-for-discussion

- The role of the Sciara del Fuoco collapse structure in conditioning the location of the active vents and fissures and the direction of volcanogenic flows during the Present-day activity.

STOP 1.4: (38°48'11"N, 15°12'53"E)

Locality: Stop point at elevation of 400 m asl.

Focus: Paroxysmal spatter deposits and scoriae of the Present-day activity of Stromboli.

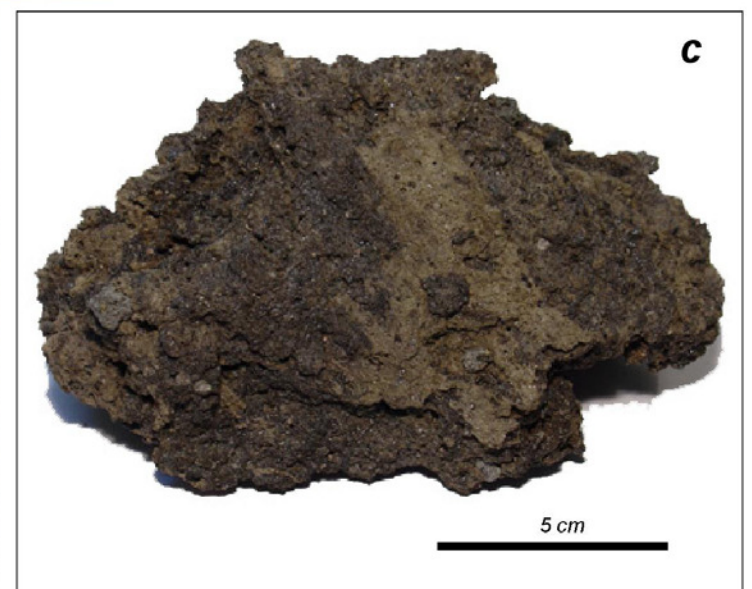
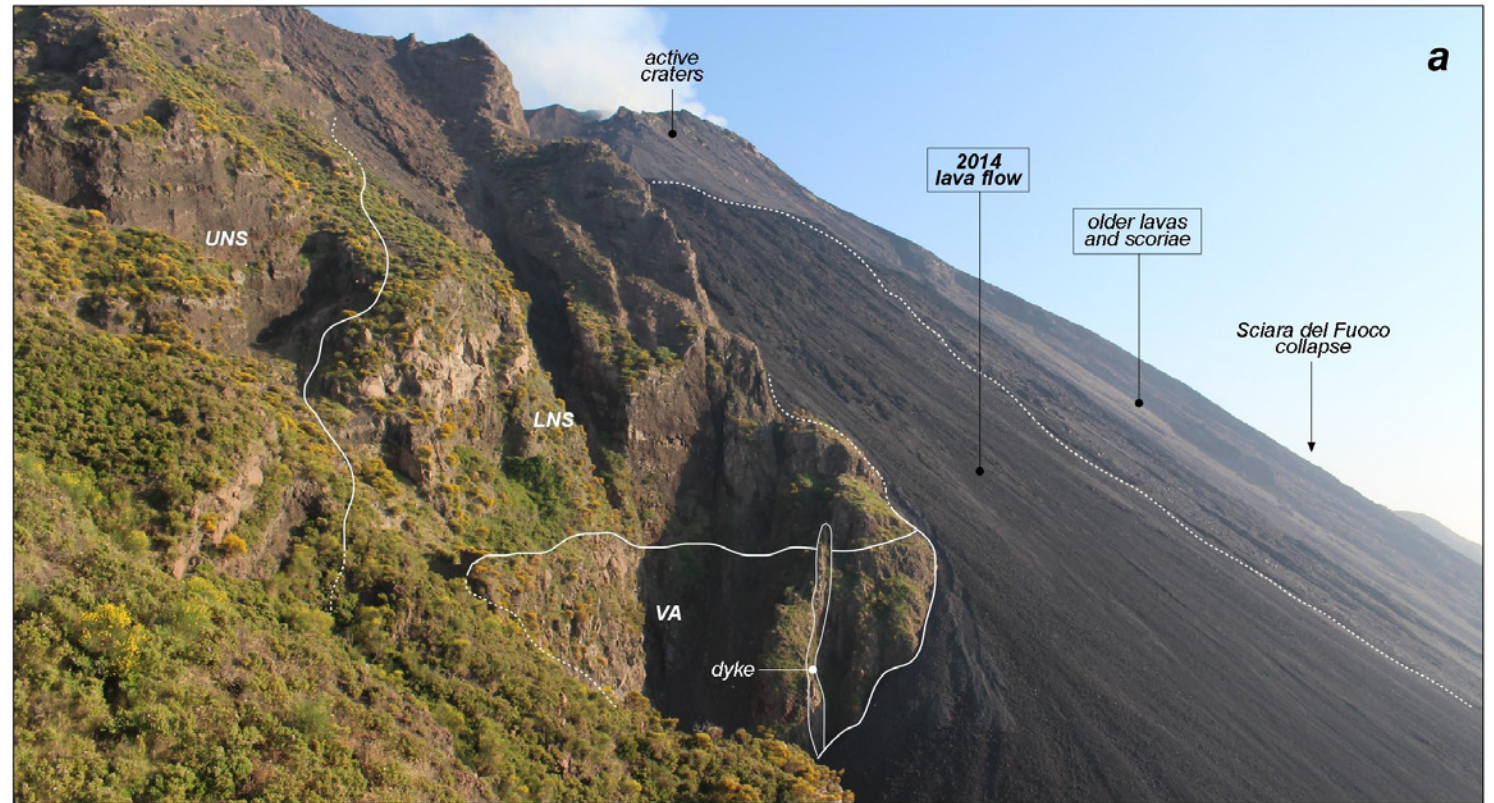
Description: This stop point provides another spectacular view on the Sciara del Fuoco collapse structure and the active craters of Stromboli (Fig. 11a). Along the NE shoulder of the collapse the succession of products truncated by the successive collapses of Sciara del Fuoco is exposed, with the Middle-Upper Vancori lavas and breccias (26–13 ka) unconformably covered by the Lower and Upper Neostromboli (c. 13–8 ka) lava successions (Fig. 11a). Within the collapse depression, the lava flow field produced during the 2014 effusive eruption is well exposed (Fig. 11a), together with the other lavas and scoriae originated from the summit active craters.

The stop point is located above the massive lava flows of Serro Adorno erupted from a flank fissure at an elevation of c. 550 m during the Late Neostromboli activity (c. 4 ka). These lava flows occupy the top portion of the Sciara del Fuoco collapse shoulder and are truncated by the late Medieval collapse (sc7). Above these lavas, a pyroclastic succession consisting of loose lapilli-tuffs with sparse pumices and scoriae (HK shoshonites) and abundant accretionary lapilli is discontinuously exposed along the footpath when the stopping place is left behind (Fig. 11b). This is the Semaforo Labronzo hydromagmatic pyroclastic succession interpreted as the product of directed PDCs originated from a summital (undefined) eruptive vent, likely associated with a lateral failure at the end of Neostromboli.

In several outcrops along the footpath, these products are sealed by a dm-thick layer of welded spatter and scoriae that mantles and plasters the pre-depositional topography (Fig. 11b). They are the fountain-fed fallout deposits produced during the well-known AD 1930 paroxysmal eruption, and are the typical lithofacies of the paroxysms that punctuated the historical activity mostly in the 16th century and in 1907, 1919, 1930 and



Fig. 11 – The stopping place at elevation of 400 m asl offers a spectacular view of the active craters and the Sciara del Fuoco collapse (a), with a best exposure on the lava flow field of 2014 (and older lava and scoriae). On the collapse shoulder, the Middle-Upper Vancori lavas and breccias (VA) are visible in the lower stratigraphic portion, and are covered in unconformity by the Lower (LNS) and Upper Neostromboli (UNS) lava successions. Along the footpath leaving behind the stopping place (b), a stratigraphic section across the most recent products of the summit activity of Stromboli is exposed, with the following units visible from the base to the top: LB=Semaforo Labronzo hydromagmatic succession; SP=spatter stack relative to the AD 1930 paroxysmal explosive eruption; SC=loose scoriae and bombs of the 2002-2003 and 2007 eruptions with HP scoria-LP pumice mingled bombs. (c) Detail of a HP scoria-LP pumice mingled bomb of distal fallout deposits relative to the 2003 paroxysm (from Rosi et al., 2013, modified).





1944. The paroxysmal eruptions of Stromboli typically generate eruptive columns with heights of 1000-4000 metres producing metre-thick welded spatter deposits extending laterally to the lower slopes of the volcano down to elevations of c. 350-400 m asl, whereas widespread ballistic blocks may be distributed downwind also causing damage in the lower inhabited flanks of the volcano. This is a common behaviour during the most powerful paroxysms, as demonstrated in AD 1930 (cf. historical reports of Rittman, 1931) and the most recent paroxysms of 2003 and 2007 (Rosi et al., 2013).

Above the 1930 welded spatter stack, there are discontinuous outcrops and patches of scattered HP scoriaceous lapilli and HP scoria-LP pumice mingled bombs related to the most recent paroxysms of 2003 and 2007 (Fig. 11b-c).

Points-for-discussion:

- Occurrence of collapse-driven phreatomagmatic directed PDCs along the lower slopes of the volcano with implications for volcanic hazard.
- The explosive paroxysms of Stromboli and their triggers in the evaluation of volcanic hazard and risk.

STOP 1.5: (38°47'51"N, 15°12'59"E)

Locality: Le Roccette saddle, elevation of 680 m asl.

Focus: Holocene collapse rims of Sciara del Fuoco.

Description: The saddle of Le Roccette is sited along the northeastern inner border of the Sciara del Fuoco collapse structure. There is a spectacular panoramic view on the active craters of Stromboli and the higher portion of Sciara del Fuoco. Moreover, along the shoulder of Sciara del Fuoco, a natural stratigraphic section is exposed across the products related to distinct and successive phases of piling up and lateral failure in the Holocene history of Stromboli (Fig. 12a).

The oldest exposed products are the lava flows and breccias of the Upper Vancori unit (13 ka) representing the remnants of collapse sc3 that truncated the Pleistocene volcano. These are unconformably covered by the Lower Neostromboli lavas, represented by a thick succession of thin, laterally persistent pahoehoe to aa lava flows embedded within autoclastic breccias, passing upwards into a series of m-thick massive lava flows with blocky carapaces. These lavas are assumed to have progressively piled up within the collapse depression (as demonstrated by their low-dipping to subhorizontal bedding attitude) which were filled up to the rim at elevations

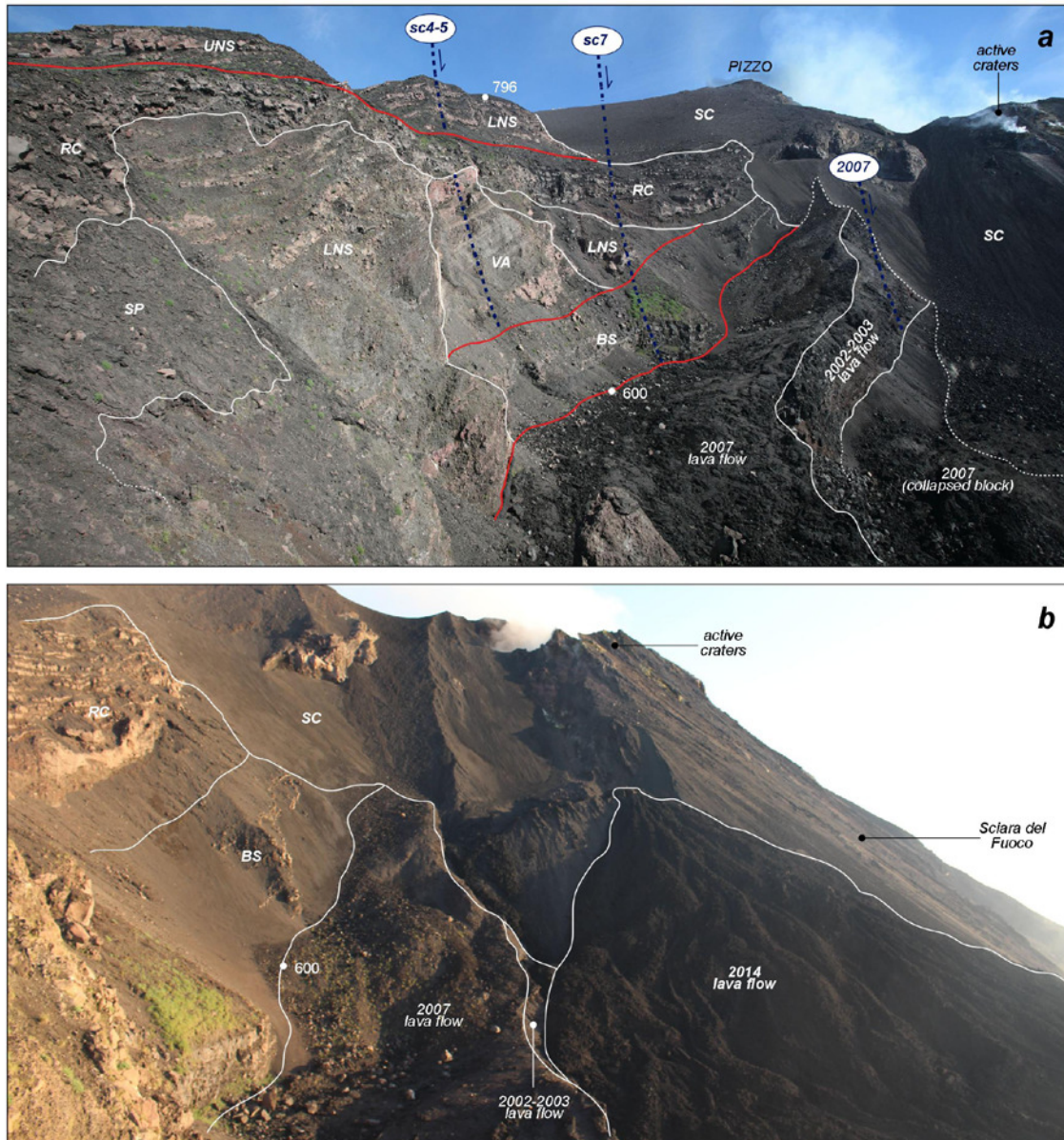


Fig. 12 – (a) Panoramic view from Le Roccette saddle of the Sciara del Fuoco collapse inner border in the area of Bastimento (in 2012). A natural stratigraphic section is exposed across the products related to distinct and successive phases of piling up and lateral failure in the recent history of Stromboli. The oldest exposed products are those of the Vancori unit (va) of Epoch 4, representing the border of sc3 collapse (Upper Vancori collapse, 13 ka). This collapse was filled up by the Lower Neostromboli lavas (LNS) of Epoch 5a, subsequently truncated by the collapse sc4. The rim of this collapse was overflowed by the Upper Neostromboli lava flows (UNS) of Epoch 5b (13-8 ka). Both the Lower and Upper Neostromboli lava successions are cross-cut by the collapse sc5 (c. 7 ka). Its morphological scar was progressively filled up by the successive lava successions of Bastimento (BS), related to Epoch 6a (1.7-1.5 ka), and Le Roccette (RC), related to Epoch 6b (c. 0.7 ka). These are visible along the border of the collapse, in lateral contact on the older (pre-collapse) products and hanging above the 2002–2007 lava flow fields. The Bastimento and Le Roccette lava successions (and the older units) are truncated by the collapse rim sc7 in late Medieval times. This collapse rim is covered by the present-day scoriae (SC), and particularly by a spatter stack near Le Roccette (SP) dated at the 17th century. The collapse sc7 is filled by the most recent lava flow fields of 2002–2003 and 2007, both truncated by the minor collapse that developed during the 2007 eruption. The lateral contacts between the distinct units are displayed by red lines. (b) The morphostructural setting of this area is presently largely modified after the effusive eruption of August 2014 that produced a large lava flow field from a fissure opened at the base of the active crater area. The numbered points in the figure indicate metres asl.

of c. 780–790 m, from where the lava flows descended along the north-eastern flank of Stromboli towards the Vallonazzo gorge. The Lower Neostromboli lavas were truncated by the collapse sc4, coalescent to and concentric with the older



Upper Vancori collapse. The rim of this collapse was overflowed by the Upper Neostromboli lava succession (13–8 ka) composed of thin laterally persistent lava flows embedded within autoclastic breccias fanwise distributed along the N sector of Stromboli. Both the Lower and Upper Neostromboli lava successions are cross-cut by the collapse sc5_b that runs along the trace of the previous collapses. This collapse scar was progressively filled up by the successive lava successions of Bastimento (c. 1.7–1.5 ka) and Le Rocchette (c. 0.7 ka) related to the Roman-age to present-day activity of the summit craters (Fig. 12a). These crop out as lava terraces at different elevations documenting distinct levels of filling up of the collapse. Rocchette lavas, in particular, document the latest episode of collapse overflow in the history of Stromboli in correspondence of the saddle near Bastimento at elevations of 630–680 m. Both the lava successions (and the older units) are truncated by the collapse rim sc7a, the latest episode of major lateral failure in the history of Stromboli leading to development of the Sciara del Fuoco in its present morphology. The rim of this collapse is covered by a spatter stack dated to the 17th century (Speranza et al., 2008), which constrains its development to a late Medieval age.

The present Sciara del Fuoco collapse depression is filled by scoriae and lavas relative to the most recent eruptions of the Present-day activity. In particular, the lava flow fields of 2002–2003 and 2007 are visible near the border of the collapse (Fig. 12a), whereas the latest lavas of the 2014 eruption presently crop out aside of the minor collapse rim formed during the 2007 eruption. The 2014 lavas were originated from a fissure opened near the base of the active crater area (Fig. 12b), possibly associated with a drop in magma level within the main conduit (as demonstrated by the associated prolonged interruption of the normal Strombolian activity).

Points-for-discussion

- Dynamics of recurrent lateral collapse and volcanism renewal in a steep basaltic stratovolcano as a fundamental feature for its eruptive development and volcanic hazard.
- Opening of fissures and vents at lower elevations along the Sciara del Fuoco collapse feeding the main lava flow fields during the Present-Day activity.

STOP 1.6: (38°47'32"N, 15°12'52"E)

Locality: Stromboli summit.

Focus: Active craters and present-day Strombolian activity.



Description: The end of the ascent is located on the top of the Pizzo scoria cone (c. 920 m asl) built up during the Roman-age activity and truncated by the latest NW-dipping collapse sc7 (and the SE-dipping collapse sc6). The remnants of the cone after this collapse are made up of planar beds of Strombolian scoriaceous lapilli that are largely altered by strong hydrothermalization.

The stop point is located c. 150 m above the active craters, and makes it possible (with good weather conditions) to have an impressive view of the typical Strombolian explosions and the active crater area (Fig. 13a). This is a flattish crater terrace at c. 750 m asl consisting of three main sectors (Southwest, Central and Northeast craters) and other minor vents or fissures (5–15 according to Harris and Ripepe, 2007) along the main NE–SW structural trend, continuously degassing and alternatively (or contemporaneously) erupting. The most active vents are generally the NE and SW craters. The morphology and dynamics of the active crater area, however, are subjected to changes with time related to periods of more intense activity or possible collapses of the crater floor (see Rosi et al., 2013 for a review).

As recently summarized by Rosi et al., (2013), the normal Strombolian activity consists of rhythmic, mild to moderate explosions lasting a few seconds that eject scoriaceous lapilli and bombs, ash and lithic blocks (Fig. 13a-b). The explosive bursts are particularly well visible in the night, when it is possible

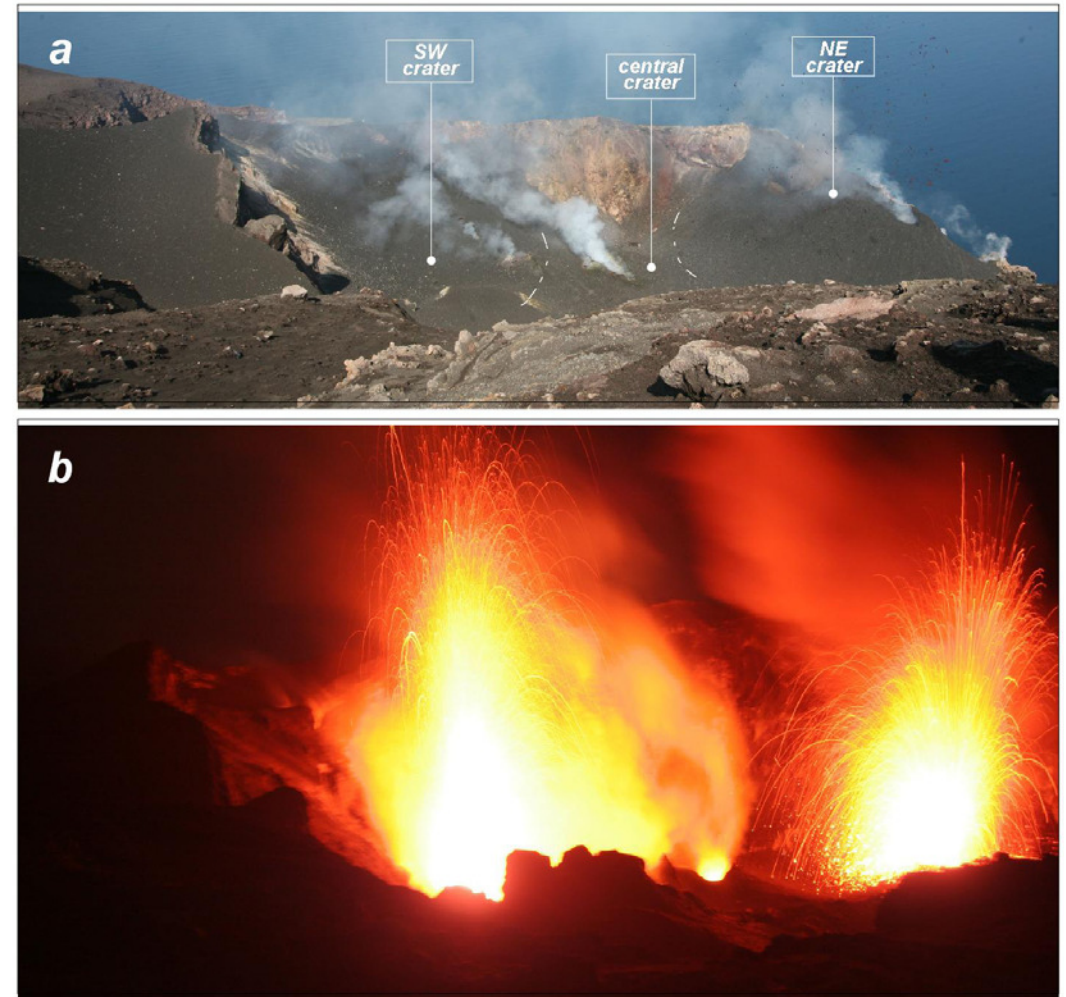
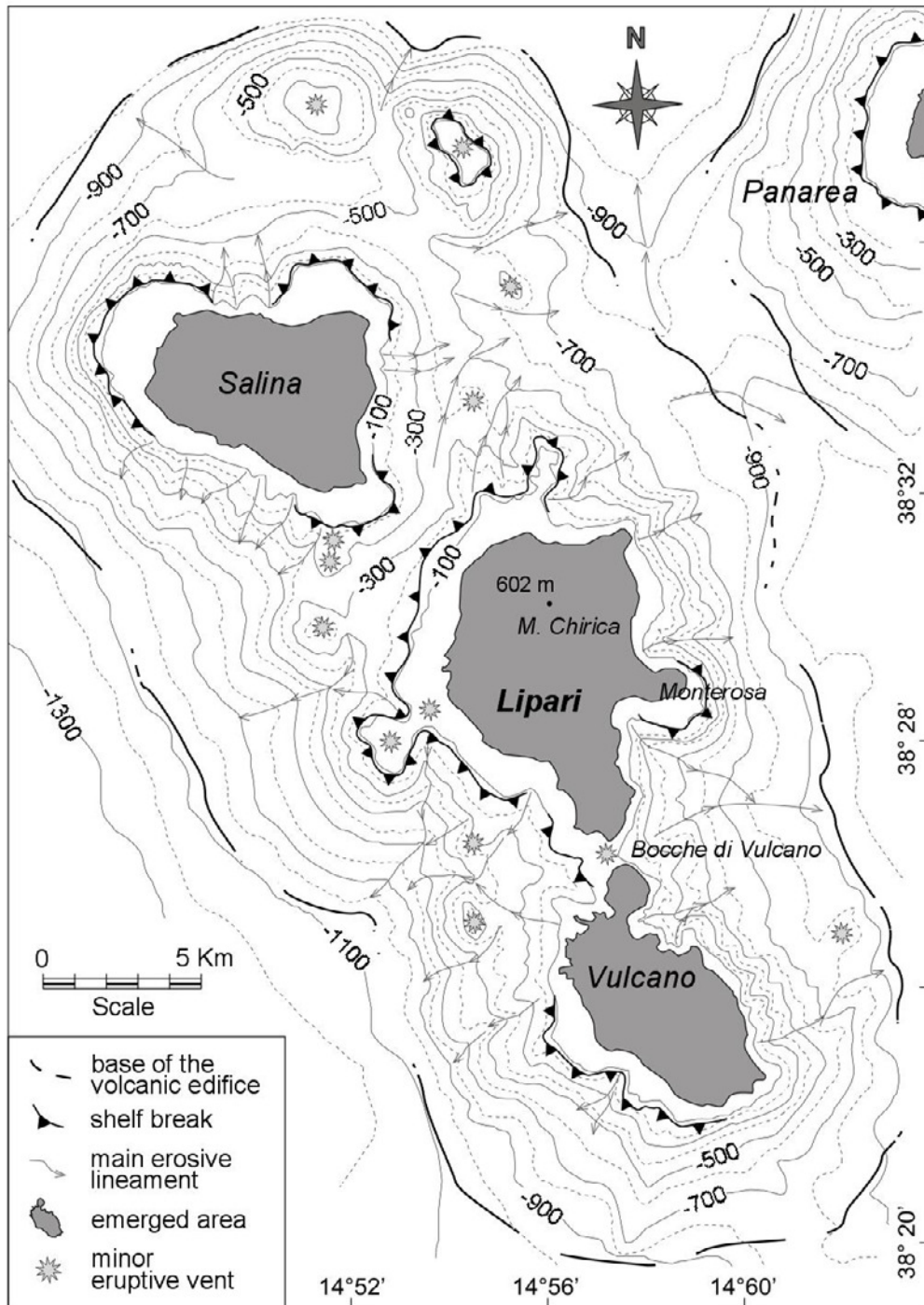


Fig. 13 – (a) View in the daylight of the crater terrace area from the peak of Pizzo Sopra la Fossa showing the three main sectors (NE, central, SW) in which active vents and craters are usually localized at Stromboli (in 2009). The NE crater was erupting scoriae and bombs in a small Strombolian explosion, whereas the other vents were degassing and puffing. (b) Night view from the Pizzo Sopra la Fossa peak of two contemporaneous Strombolian explosions in the SW and central crater sectors (in 2007; photo courtesy of L. Mugellesi).



to estimate the real size and shape of the different lava fountains and explosive jets (Fig. 13b). During periods of low-level activity, the lava level tends to drop in the vents and explosions become weaker and fewer. During periods of more intense activity the lava level raises, the number and energy of explosions increase and jets are charged with incandescent fragments. Eruption frequencies range between 7 and 17 events per hour, with duration of emissions ranging from 4 to 30 s (Delle Donne et al., 2006), ejecta rising c. 50–400 m above the vents (Patrick et al., 2007) and ballistic clasts falling anywhere between tens of metres and 200–250 m from the vents. An average eruption rate in the order of m^3/sec has been recently estimated for the normal Strombolian activity (Marsella et al., 2012). The Strombolian explosions are usually associated with a continuous 'passive' streaming of gas from the crater area through diffuse degassing of the fumarole fields and low-energy active degassing (puffing), during which discrete small bursts of gas (every 1–2 sec) sometimes eject small amounts of incandescent material (Ripepe, 1996).

The scoriae are black with high phenocryst (HP) content (c. 50 vol% of plagioclase, clinopyroxene and olivine crystals), and coexist (mingling with) with light-coloured ('golden') pumices with low phenocryst (LP) content (c. 5–10 vol% of crystals; Francalanci et al., 1999). Black scoriae and light-coloured pumices are often mingled in a same ejecta. The coexistence of HP scoriae and LP pumices is the distinctive field characteristic of the deposits of the Present-day activity. HP scoriae and LP pumices display quite similar whole-rock compositions (SHO to HKCA basalt), although the pumices have lower Sr isotope ratios and slightly different geochemical characteristics (e.g. lower K_2O contents, Bertagnini et al., 2008). They are representative of a polybaric multi-reservoir plumbing system, with a degassed HP magma of shallow-level origin (depths of 1–3 kms) erupted as scoriae (and lavas) and a volatile-rich LP magma of deeper derivation (depths of c. 10 km) erupted as pumices only during the major eruptions and paroxysms (Francalanci et al., 2013 for a review).



3.2 Lipari

The island of Lipari (total area of 38 km²) is the largest in the Aeolian archipelago and represents the above-sea-level culmination of a broad, largely submerged volcanic complex belonging to the Vulcano–Lipari–Salina volcanic belt. This volcanic complex rises c. 1700 metres above the seafloor and reaches a subaerial peak of 602 m above sea level (a.s.l.) at Monte Chirica (Fig. 14), with average slope angles ranging from 30° to a few degrees. Both the subaerial and submerged portions of Lipari are assumed to be directly controlled by the NNW–SSE-oriented Tindari–Letojanni Fault System (Mazzuoli et al., 1995).

Marine terrace deposits and fossils occur mostly along the western coast of Lipari, representing the evidence of three paleoshorelines at elevations of 43–45 metres asl (I order), 23–27 m (II order) and about 12 m (III order). These are the record of the main Late-Quaternary eustatic highstands of MIS 5e, 5c and 5a, dated to 124, 100 and 81 ka, respectively (Lucchi et al., 2004). All the terraces of Lipari are found at elevations higher than the sea-level heights during the corresponding high sea-level peaks, as the consequence of a long-

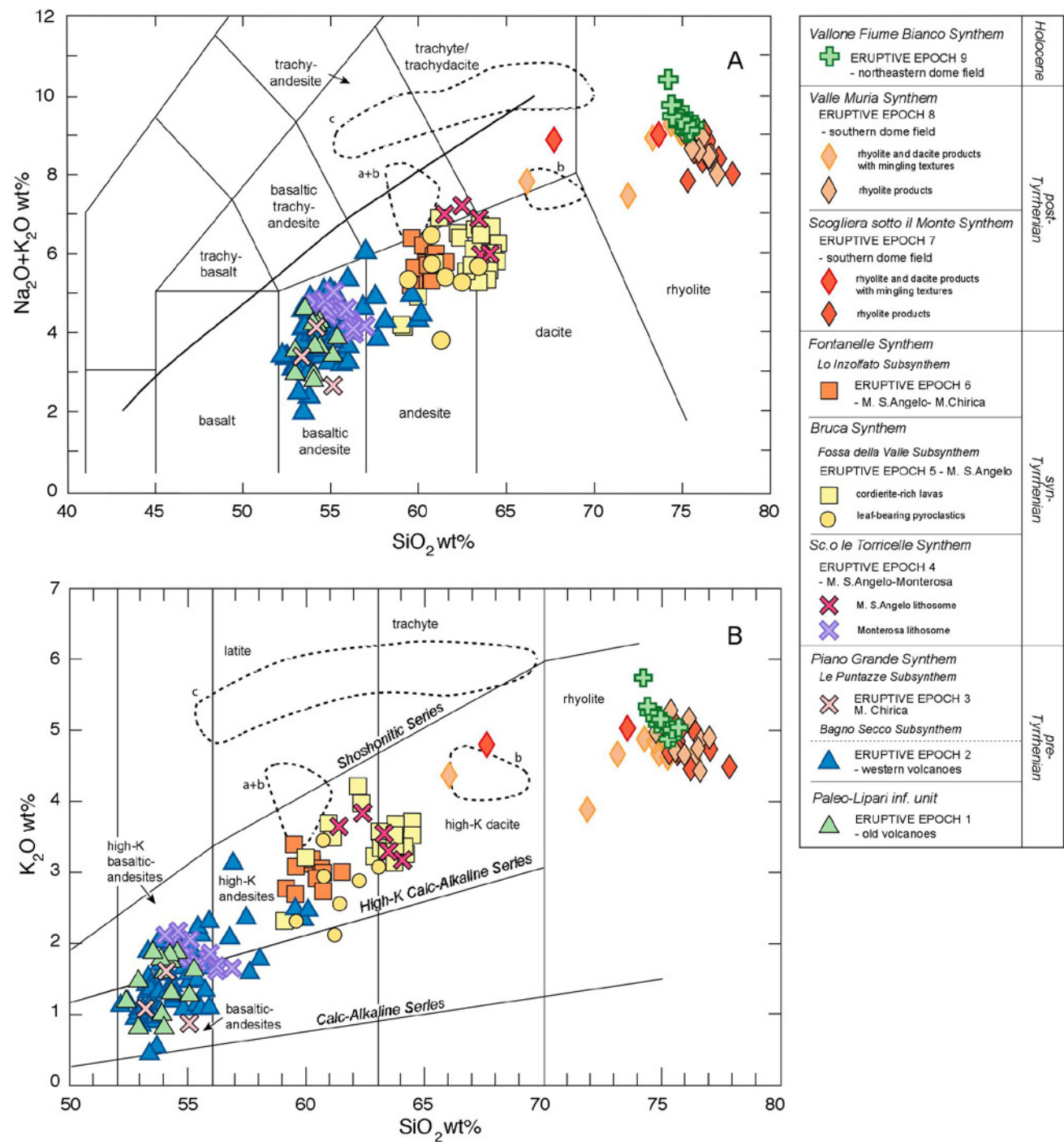
Fig. 14 - Morphostructural bathymetric sketch map of the Vulcano–Lipari–Salina volcanic belt aligned along the NNW–SSE direction of the major Tindari–Letojanni structural system (simplified from Romagnoli et al., 1989, 2013). Depth contour lines in metres below sea level.



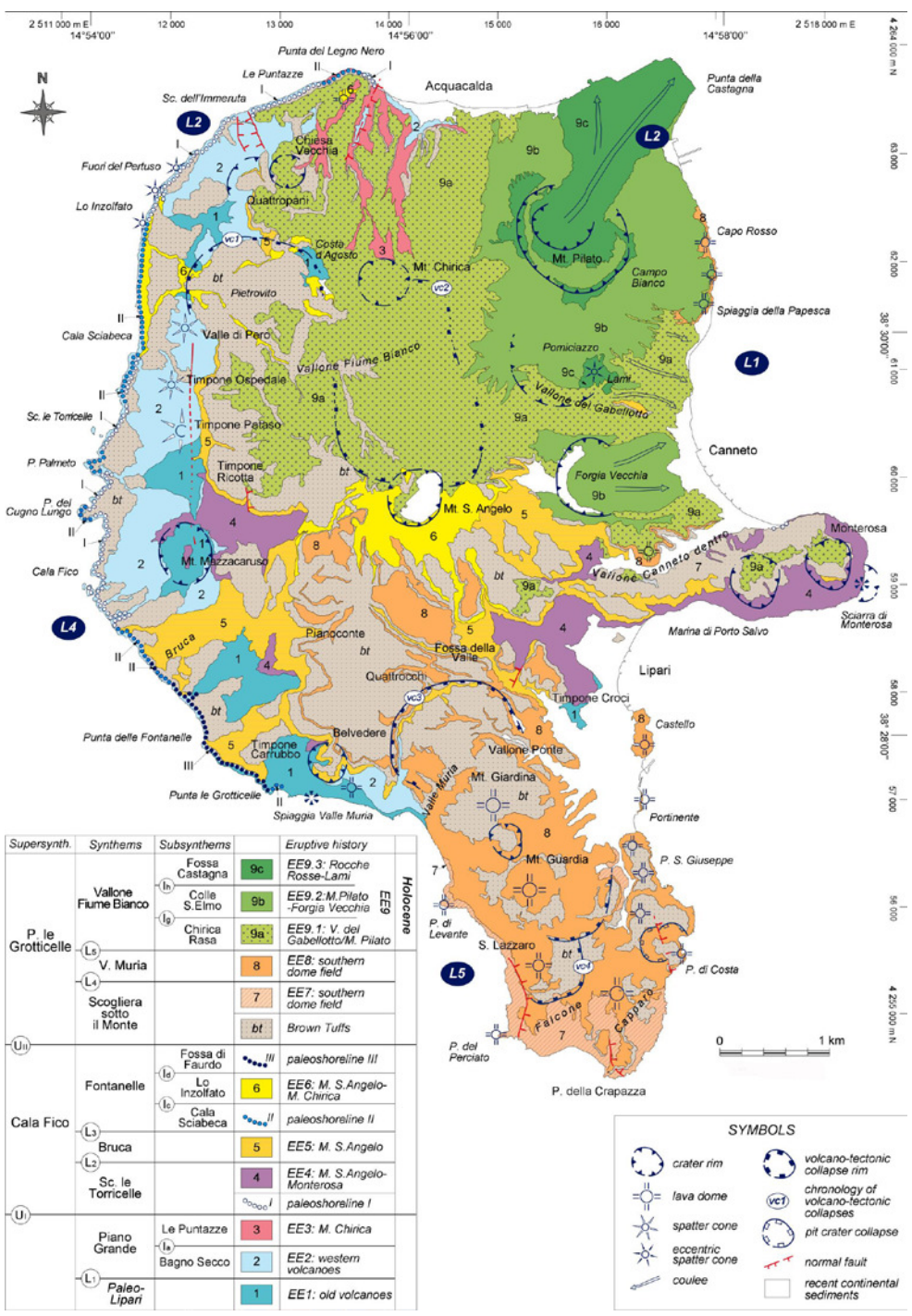
term crustal uplift that affected the volcanic complex during its growth history superimposed on the glacio-eustatic sea-level oscillations and tectonic vertical movements.

The volcanic rocks of Lipari cover a wide compositional interval from CA and HKCA basaltic andesites to rhyolites (with a significant gap in the dacite field), evolving parallel to its eruptive history (Fig. 15). K_2O increases very steeply from mafic to intermediate rocks. Some samples, especially among HKCA dacites and rhyolites, notably

Fig. 15 - (A) Total alkali v. silica (TAS) diagram (Le Maitre et al., 1989) and (B) K_2O v. SiO_2 classification diagram (Peccerillo and Taylor 1976) for the volcanic rocks of Lipari (see Figure 16 for the stratigraphic units and epochs of activity). Geochemical data relative to the leaf-bearing pyroclastics (Epoch 5) are from Ricci Lucchi et al., (1988). Dashed lines enclose compositional fields of the mafic magmas involved in the mixing with rhyolitic melts: a, mafic enclaves within the rhyolite lavas of Falcone and P. S. Giuseppe fms (Epochs 7–8) from Gioncada et al., (2003); b, grey pumices of the M. Guardia Formation (Epoch 8) from De Rosa et al., (2003); c, mafic enclaves within the Fossa della Rocche Rosse Formation (Epoch 9) from Davì et al., (2009).



<https://doi.org/10.3301/GFT.2018.02>



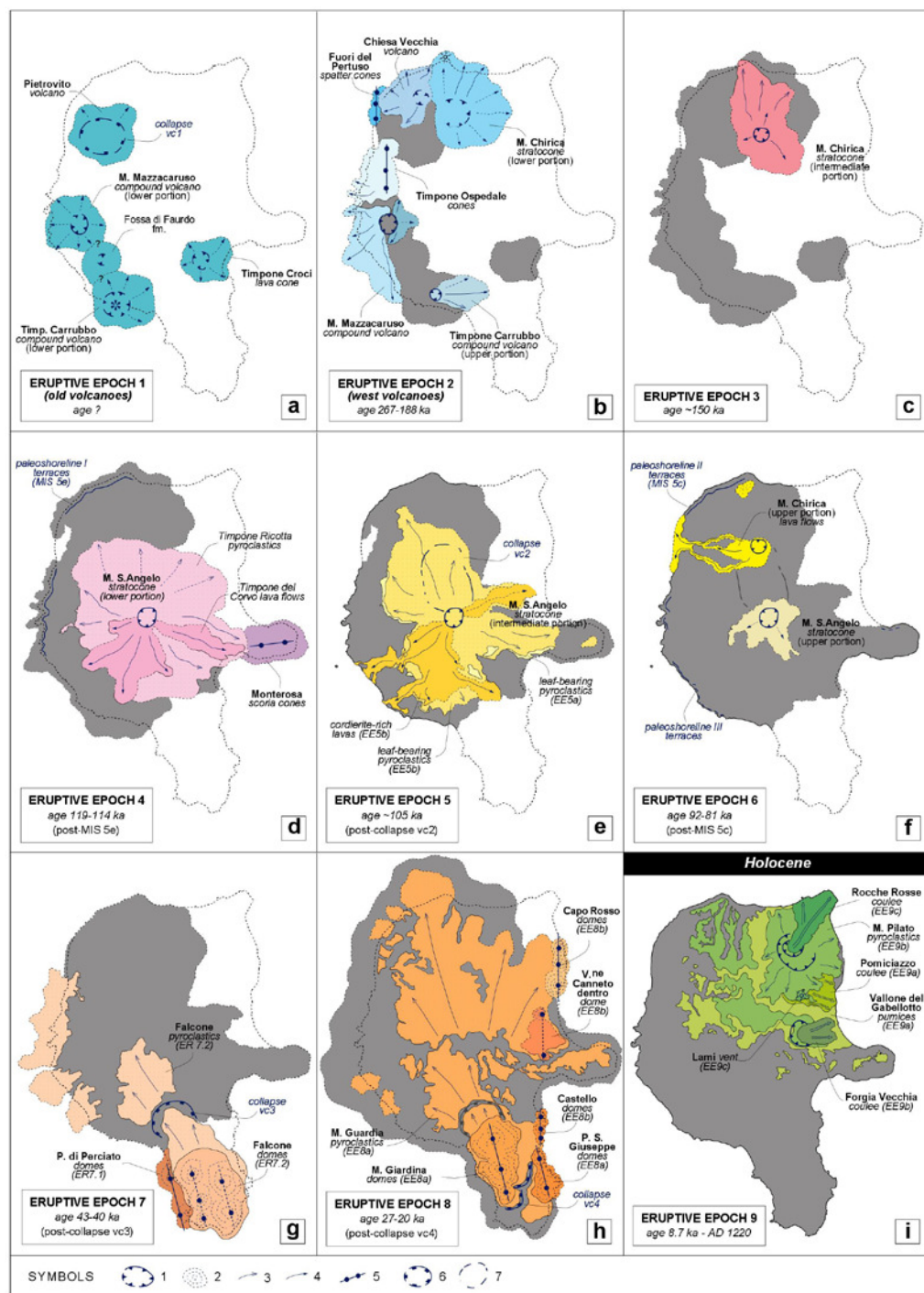
display evidences of mingling such as the occurrence of mafic enclaves and xenocrysts (Forni et al., 2015). The magmatic evolution of Lipari is related to different mantle-derived magmas mostly differentiated through AFC processes and magma mixing, with a variable contribution of the crust through time in the frame of a polybaric plumbing system (Di Martino et al., 2010).

3.2.1 Eruptive history

According to the most recent 1:10.000 geological map of the island and the relative stratigraphic succession (Fig. 16), the eruptive (and magmatic) history of Lipari is arranged into nine successive Eruptive Epochs developed between c. 270 ka and medieval ages (Forni et al., 2013; Lucchi et al., 2013d). The successive Epochs were interrupted by quiescence periods associated with the major volcano-tectonic collapses, shifts of the eruptive vents, major chemical changes or the episodes of marine ingression and erosion which occurred during the recurrent sea-level oscillations of MIS 5 (Fig. 17; cf. Forni et al., 2013 for more details).

The oldest products of Lipari (Epochs 1-3, 270-150 ka) are CA and high-K basaltic andesite to andesite lava flows and pyroclastic units related to a series of eruptive

Fig. 16 - Simplified geological map of Lipari according to the main UBUs. The main steps of eruptive history of Lipari (EE, Eruptive Epochs) are also shown by comparison with the unconformity-bounded units. Kilometric coordinates conform to the Gauss-Boaga System (IGM). Modified from Lucchi et al. (2013d). The location of the fieldtrip-stops is also shown.



centres of both central-type (from north to south: Monte Chirica, Chiesa Vecchia, Pietrovito, Monte Mazzacarusu and Timpone Carrubbo stratocones) and fissural-type (early Monte Chirica, Fuori del Pertuso and Timpone Ospedale cones), mostly distributed along NNW-SSE to N-S lineaments. They crop out along the western sector of Lipari and are related to hydromagmatic and magmatic (Strombolian and effusive) phases of activity in shallow marine to subaerial environments. All the products of these Epochs are cut by marine terraces corresponding to paleoshorelines I (MIS 5e, 124 ka), II (MIS 5c, 100 ka) and III (MIS 5c, 81 ka).

The intermediate stages were fundamentally characterized by the construction of Monte S. Angelo (Epochs 4-6, 119-81 ka) (Fig. 17). This is a large, polygenetic central-type stratocone characterized by hydromagmatic and (minor) Strombolian phases of activity that produced great volumes of pyroclastic deposits from PDCs and fallout, followed by the emission of high aspect-ratio blocky lava flows. The cone growth was interrupted by two major (c. 10-ka-long) periods of volcanic inactivity and minor quiescences, and

Fig. 17 - Sketch maps showing the distribution and structural control of the active eruptive vents during the successive Epochs of activity, sequences of eruptions (EE) and eruptions (ER) of the Lipari volcanic complex (modified from Forni et al., 2013). Symbols: 1, crater rim; 2, lava dome foliation; 3, presumed transport direction of pyroclastic products; 4, main lava flow; 5, volcanic alignment; 6, caldera-type collapse rim; 7, collapse rim of uncertain origin.



recurrent phases of subaerial and marine erosion driven by the episodes of marine ingression during the high sea-level peaks of MIS 5e (124 ka), 5c (100 ka) and 5a (81 ka) (Lucchi et al., 2004). The W-E-aligned Monterosa scoria cones along the central-eastern coast of Lipari were constructed contemporaneously with the early phases of activity of Monte S. Angelo (Epoch 4, c. 119–114 ka). The bulk of Monte S. Angelo was built up during Epoch 5 (105 ka) by means of voluminous “leaf-bearing” pyroclastic products and cordierite-rich lava flows (Di Martino et al., 2011). During the latest phases of Vulcanian activity of Monte S. Angelo (Epoch 6, 92–81 ka), the Monte Chirica stratocone was also active in the northern sector of Lipari, and produced a series of three thick lava flows from the western side of its summit crater.

The youngest stages of development of Lipari occurred after a c. 40-ka-long quiescence period following the end of Monte S. Angelo and Monte Chirica activity (Fig. 17). During this inactive period, corresponding to MIS 4 to 3, Lipari has long remained in conditions of relative sea-level fall and lowstand, which triggered intense subaerial erosion and reworking of the existing volcanic reliefs that produced thick epiclastic accumulations, together with deposition of a thick succession of tephtras from the outside of Lipari (Lucchi et al., 2008; Lucchi et al., 2013c).

Renewed activity in southern Lipari marked the onset of rhyolitic magmatism (Epochs 7–8, 43–20 ka), associated with the development of highly explosive eruptions to generate great volumes of pumice pyroclastic products and the emission of alignments of endogenous lava domes (Fig. 17). A voluminous dome-field was thus constructed to the south of the volcano-tectonic collapse (vc3) cutting the southern flanks of Monte S. Angelo in the area of Quattrocchi. Three successive growth stages of this dome-field occurred following a recurrent eruptive scenario characterized by Subplinian explosive phases of activity followed by dome effusion, with late explosive phases sometimes resulting in the partial destruction of the dome surface (cf. Forni et al., 2013 for details). The emission of the latest domes of Monte Giardina-Monte Guardia-San Lazzaro was preceded by the reknown high-energy Monte Guardia explosive eruption (27–24 ka) producing a widespread pumice succession representing a fundamental stratigraphic marker on the whole of Lipari (De Rosa et al., 2003; Colella and Hiscott 1997), and across most of the Aeolian archipelago (Lucchi et al., 2013c). This succession is composed of rhyolite hornblende-bearing pumice deposits from fallout and dilute PDCs, with an estimated volume of $4.75 \times 10^8 \text{ m}^3$ (Sheridan et al., 1987). The Monte Guardia unit is dated at between 27 and 24 cal ka as derived from calibration of the radiocarbon ages for charcoal fragments embedded within the Intermediate and Upper Brown Tuffs found below and above (Crisci et al., 1981, 1983; Lucchi et al., 2008, 2013c). A series of scattered lava domes were erupted during late Epoch 8 (~20 ka) by north–south tectonic fissures along eastern Lipari



(Castello, V.ne Canneto dentro, Capo Rosso, from south to north). This marked a change in the structural control on volcanic activity, and signalled a progressive shift to the north of the active vents.

The Holocene activity (Epoch 9, 8.7 ka-1220 AD) occurred in the north-eastern sector of Lipari (Fig. 17). A composite volcanic system composed of rhyolitic pumice successions and viscous obsidian lava flows developed through three successive sequences of eruptions that followed a recurrent eruptive pattern with initial Strombolian to Sub-plinian explosions and late obsidian flow effusion. The Vallone del Gabellotto pumices and Pomiciazzo obsidian lava flow were emitted at c. 8.7 ka, whereas most of the Monte Pilato pumice cone and (likely) the Forgia Vecchia obsidian lava flow were erupted in AD 776. The Rocche Rosse obsidian lava flow and (likely) the Lami eccentric cone in AD 1220 were the latest phases of activity of the Lipari volcanic complex.



DAY 2nd: the Lipary itinerary

Counterclockwise tour by boat around the island of Lipari (Fig. 16) devoted to the observation and description of the main stratigraphic features of the volcanic succession, and its most important volcanic and volcanotectonic structures. Particular attention will be devoted to the north-eastern coast where the obsidian lava flows and pumice pyroclastic products of the Holocene to historic eruptive activity of Lipari crop out.

STOP 2.1: (38°30'1"N, 14°57'45"E)

Locality: Spiaggia della Papesca-Canneto.

Focus: Holocene obsidian lava flows and pumice deposits (Vallone del Gabellotto, Pomiciazzo, Forgia Vecchia).
Description: The north-eastern coastal sector of Lipari is mostly composed of rhyolitic pumice successions and viscous obsidian lava flows related to the Holocene to medieval-age activity. At the base of the exposed succession there are the hydrothermally-altered Capo Rosso N-S-aligned lava domes (~20 ka) (Fig. 18a). They are covered by the discordant, widely-distributed Vallone del Gabellotto pumices (dated at 8.7-8.4 by tephrochronology) and the Pomiciazzo obsidian lava flow, on which the asymmetric Monte Pilato pumice cone is constructed.

The widespread Vallone del Gabellotto pumice succession is the result of the initial high-energy explosive phases of the Holocene activity of Lipari. They are best exposed along the Vallone del Gabellotto gorge as a 130 m thick succession of massive to planar and cross-stratified lapilli-tuffs with large-scale wavy bedforms and a variable content of lithics, derived from deposition of dilute, dry-type PDCs and subordinate fallout (Fig. 18b). The activity was driven by both hydromagmatic processes and magmatic fragmentation as recorded in highly vesicular pumices combined with moderately vesicular, blocky and equant pumiceous clasts. Thickness and grain-size of either the whole succession or the individual beds and wavelength of the bedforms gradually decrease in radial directions from the vicinity of the Vallone del Gabellotto gorge. This is thus considered the source area, although there are no traces of a tuff-cone and/or crater due to the cover of younger deposits and intense erosion of the loose primary deposits. The Vallone del Gabellotto pumice succession is recognized across the whole central-northern parts of Lipari and represents an important marker for correlations, with distal layers found on Panarea and Vulcano (Lucchi et al., 2008, 2013c) and the South Adriatic and Tyrrhenian cores (E1 tephra layer; Zanchetta et al., 2011). The large Pomiciazzo obsidian lava flow was then emitted from the eastern rim of the Vallone



Fig. 18 – Vents and products of the Holocene activity of Lipari. a) Panoramic view along the north-eastern coast of Lipari in the area of Canneto where the main pyroclastic and lava products of the Holocene activity are visible. b) Outcrop exposure of the Vallone del Gabelotto PDC deposits along the Vallone del Gabelotto gorge (thickness of the unit about 130 m).

del Gabelotto crater during the late stages of this activity (8.6 ka). The lava flow reached the coastal sector of Lipari as three lobes in the area of Spiaggia della Papesca (Fig. 18a), and flowed down the submarine slope for a total length of 4.5 km (Gamberi and Marani, 1997).

Behind the village of Canneto, the tongue-like, bilobate obsidian lava flow of Forgia Vecchia is well visible above the Vallone del Gabelotto pumice succession (Fig. 18a). The Forgia Vecchia lava flow is thought to have been emitted contemporaneously with the Monte Pilato activity (AD 776), although the fission track age of 1.6 ka (Bigazzi and Bonadonna 1973) is not perfectly consistent. The lava flow emission was preceded by low-energy magmatic explosive phases recorded in massive to normal-graded, and planar to cross-stratified (vesicular) pumiceous lapilli-tuffs with a variable content of lithics deposited from fallout and dilute



PDCs of limited dispersal. These products constructed a low-profile crater in the area of Pirrera, from the eastern rim of which the Forgia Vecchia lava flow was outpoured.

Points-for-discussion

- Control of tectonic activity on the development of Holocene to late Medieval activity on Lipari
- Volcanic hazard of low-energy explosive phases in currently inhabited areas

STOP 2.2: (38°31'3"N, 14°57'34"E)

Locality: Walk along the road from Porticello to Acquacalda

Focus: Pumice deposits and obsidian lava flow related to the historic to medieval activity of Lipari (Monte Pilato, Rocche Rosse)

Description: In the area of the Porticello quarry, there is a spectacular view on the internal structure of the Monte Pilato pumice cone. This is a 350 m high pumice cone open to the NE, with a 1 km large crater rim and average slope angles of 25-30°, constructed by a hundred of metres thick sequence of whitish pumice deposits exposed in the quarries deeply cutting its crater rims (Fig. 19). These consist of thick layers of aphyric pumice lapilli, bombs and ash with scattered lithic clasts and abundant accretionary lapilli towards the top produced from fallout and dilute to concentrate PDCs. A significant part of the succession can be interpreted as due to secondary volcanoclastic processes along the steep slopes of the growing cone. The Monte Pilato succession is composed of highly vesicular pumices coexisting with poorly vesicular blocky clasts, which indicates that this explosive activity was driven by both end-member fragmentation mechanisms (Dellino and La Volpe, 1995), with magmatic fragmentation occurred during the initial phases of the eruption, and magma-water interaction occurred during the subsequent phases particularly along the outer portions of the conduit. The Monte Pilato activity is dated at AD 776 on the basis of a ¹⁴C calibrated age for short-lived carbonized plant fragments contained within the basal portion of the Monte Pilato succession (Keller, 2002). Consistently, the Monte Pilato pumices cover Greco-Roman ruins in the archeological site of Contrada Diana near the village of Lipari, which provides a generic Late Roman age (AD 4–5th century). Moreover, the historical report by monk Gregorius travelling through Lipari in AD 787 likely described the ongoing explosive activity of Monte Pilato. The M. Pilato succession crops out over most of the north-eastern sector of Lipari, mantling the topography above a laterally persistent palaeosol affecting the Vallone del Gabelotto pumice succession. Distal layers are also recognized on the islands of Vulcano, Panarea



and Stromboli (Lucchi et al., 2008, 2013c).

In the inner crater zone, there is an erosional contact between the Monte Pilato pumices and the pyroclastic deposits that preceded the effusion of the Rocche Rosse obsidian lava flow from the NE side of the crater. This is a tongue-like rhyolite coulee (up to 60 m thick) with spectacular ramps and flow foliation, and blocky and rough surface, representing one of the best examples of an obsidian-rich lava flow (cf. Cas and Wright 1987). The thick basal carapace and internal structure characterized by steep, subvertical, flow ramp structures and folds (Fig. 19b-c) curving down to subhorizontal flow foliation are exposed in the area of Porticello. The coulee surface, well

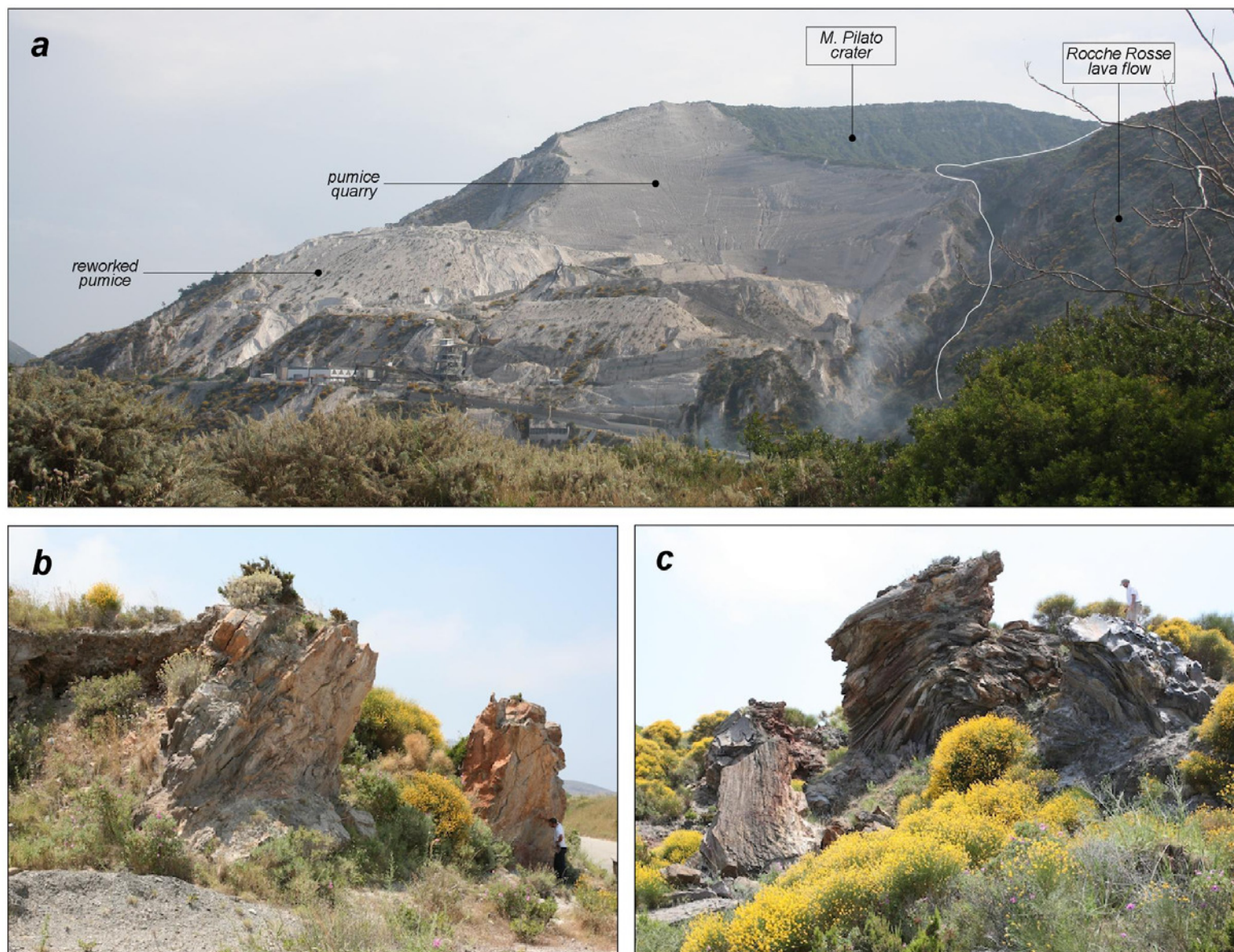


Fig. 19 – (a) View from Porticello of the M. Pilato crater rim and Rocche Rosse obsidian lava flow. To be noted that the M. Pilato crater rim is deeply cut by quarry activity. The surface of Rocche Rosse lava flow is visible along the road from Porticello to Acquacalda, where fold (b) and rampart (c) structures are exposed, together with lava microfoliation.



visible along the coast road from Porticello to Acquacalda, is typically blocky and rough with concentric curved cracks, with exposures of rampart terminations. Several outcrops of the inner lava flow show that its foliated structure consists of dense interbanding of obsidian, pumiceous and lithic rhyolite layers and is frequently folded. Pure obsidian portions are visible, although it is largely spherulitic (mm- to cm- rounded fibrous bodies of k-feldspar crystals resulting from cooling processes and glass devitrification) or perlitized (amorphous volcanic glass typically formed by hydration of obsidian interacting with atmospheric water).

Points-for-discussion

- Factors favouring the increased mobility and anomalous length of obsidian-rich lava flows.

STOP 2.3: (38°31'22"N, 14°55'39"E)

Locality: Scoglio dell'Immeruta

Focus: Tephra layers from outside Lipari (e.g. Brown Tuffs) and Last Interglacial marine terraces.

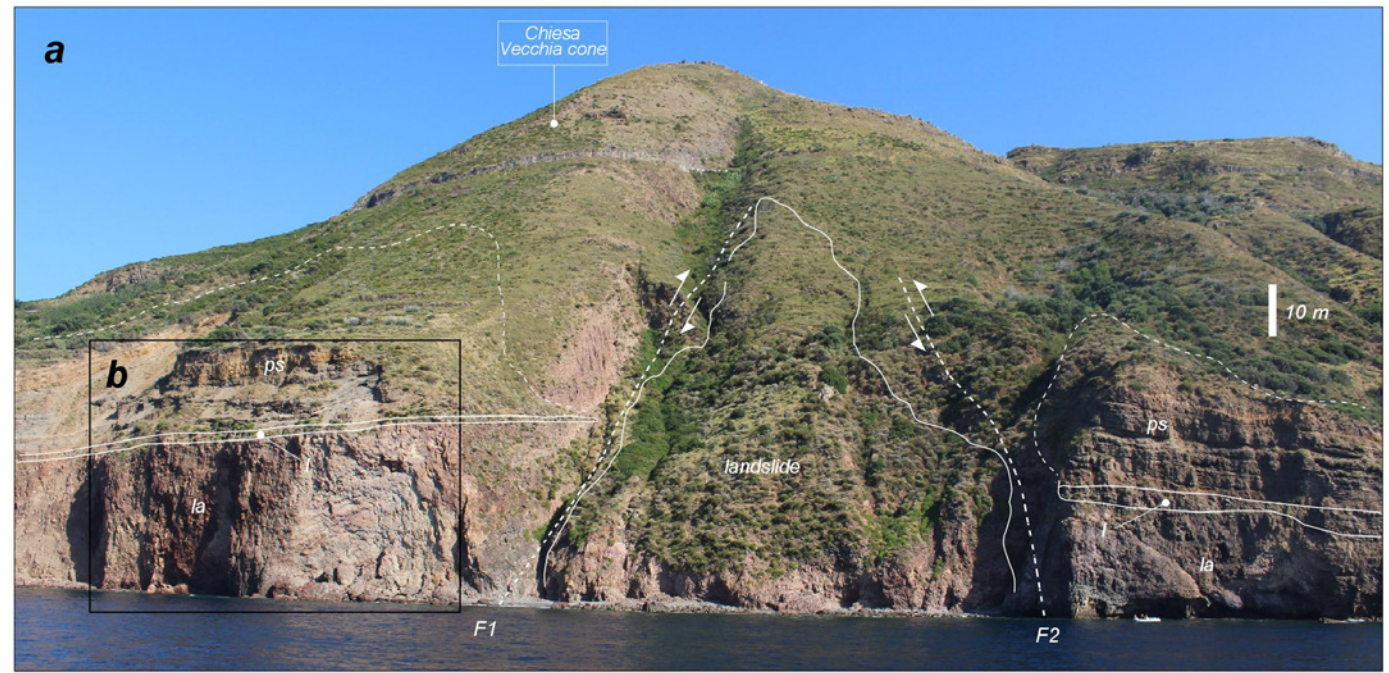
Description: Along the whole western coast of Lipari, the stratigraphic motif is that of marine terraces cutting the older volcanic products (267-150 ka). The marine terraces are recognized at varying elevations representing the evidence of the paleoshorelines I (43-45 metres asl, MIS 5e=124 ka), II (23-27 m, MIS 5c=100 ka) and III (about 12 m, MIS 5a=81 ka). Their most visible features are metre-thick, laterally persistent horizons of coarse transgressive conglomerates consisting of well-rounded pebbles to boulders lying above sharp marine erosional surfaces (Fig. 20a), representing the transverse to longitudinal sections of the terraces. Cross- to planar-laminated sands deposited in late transgressive to highstand conditions of paleoshoreline II are exposed at Cala Sciabeca. The terraces are generally arranged in a downstepping pattern with older terraces located at higher elevations as a result of a long-term tectonic crustal uplift on a regional scale affecting Lipari at a relatively constant mean rate of 0.34 m/ka from the Last Interglacial (Lucchi 2009).

All the terraces are homogeneously sealed by a thick pyroclastic succession of tephra layers of external provenance extending back to c. 70 ka (Lucchi et al., 2008, 2013c) (Fig. 20a-b), together with some pyroclastic layers related to the southern activity of Lipari during Epochs 7-8. The external tephras recognized on Lipari are the distal fallout layers originated from high-energy eruptions with source in the Campanian area or other Aeolian volcanoes. Most of them are the subaerial equivalents of widespread tephrostratigraphical marker beds in the deep-sea and lake sediment records (see Wulf et al., 2004 for a wider review). The most prominent products are brownish ash deposits



known as Brown Tuffs (Crisci et al., 1983), recognized on most of the Aeolian islands (Lucchi et al., 2008, 2013c). They mantle most of the surface of Lipari with thickness variations controlled by the pre-depositional topography, ranging from a few tens of centimetres on the palaeo-reliefs to a maximum of c. 20 m in the morphological depressions. They have a typical lithological and textural appearance

Fig. 20 – View of the stratigraphic succession along the western coastal cliff of Lipari in the area of Scoglio dell’Immeruta. a) Blocky and brecciated lava flows (la) originated from the Chiesa Vecchia cone (Epoch 2) are cut by a marine terrace of the paleoshoreline I (MIS 5e, 124 ka). This is covered by a pyroclastic succession (ps) including local and external tephra layers dated back to c. 70 ka. This stratigraphic motif is well exposed on the sides of a couple of conjugate normal faults (F1 and F2) that bound a NW–SE-oriented graben. b) Detail of the tephra succession including different layers of Brown Tuffs, the Grey Porri Tuffs and Lower Pollara Tuffs from Salina, the Ischia Tephra and the Monte Guardia pyroclastic products of Lipari.





of massive, unstratified, weakly coherent tuffs composed of glass fragments and minor crystals, with distinctive trachy-andesitic glass composition. Previously interpreted as “tuffloess” wind-reworked products or palaeosoils, they are now assumed as the distal fallout ash accumulations of large-scale hydromagmatic explosive eruptions from the area of La Fossa caldera on Vulcano (Lucchi et al., 2008, 2013c; De Rosa et al., 2016), with some layers deposited from dilute PDCs in south Lipari and Vulcano (near to the source). They are stratigraphically subdivided into the Lower (70–56 ka), Intermediate (56–27 ka) and Upper Brown Tuffs (24–8 ka) based on interlayered (dated) tephtras. An estimated volume in the range of hundreds of million cubic meters is estimated for The Upper Brown Tuffs (Dellino et al., 2011), which constrains, in terms of magma volume, the maximum eruptive potentiality of the past eruptions of Vulcano. Accordingly, this is the highest magnitude eruption of the Aeolian volcanoes, with important implications on the quantitative assessment of the volcanic risk and eruptive scenarios over the short and long term.

Other tephra layers are interlayered within the Brown Tuffs succession. Not all of them are visible in the area of Scoglio dell’Immeruta, as in most of the outcrops of this pyroclastic succession, due to discontinuous processes of emplacement and subsequent erosion of fine ash products. One of the main marker beds is the Ischia Tephra, recognized on most of the Aeolian archipelago and in Mediterranean region (Lucchi et al., 2008; 2013c). This is a distinctive titanite and acmite-bearing alkali-trachytic ash bed, Ar/Ar dated at 56 ± 4 ka (Kraml et al., 1997) and correlated with the deep-sea Y-7 tephra (Keller et al., 1978), reaching on Lipari a maximum thickness of 20 cm. This is the distal fallout layer related to the Monte Sant’Angelo Unit of the Epomeo Green Tuff Cycle from the island of Ischia in the Campanian area (Keller et al., 1978; Keller 1981; Wulf et al., 2004). A couple of tephra layers from the island of Salina are also interlayered: Grey Porri Tuffs and Lower Pollara Tuffs. The Grey Porri Tuffs, dated at 70–67 ka, consist of a 15 m thick (NW-to-SE decreasing) succession of grey pumices and scoriae produced by fallout and PDCs related to the initial explosive phases of activity of Monte dei Porri (Keller 1980; Lucchi et al., 2013a), with a typical CA basaltic andesitic to andesitic bulk composition. The Lower Pollara Tuffs, dated at 27.5 cal ka, are the initial explosive products of the Pollara crater on Salina (Keller 1980; Calanchi et al., 1993; Lucchi et al., 2013a), and are represented on Lipari by a distal fallout layer of dark basaltic andesitic scoriae upwards passing to light-coloured andesitic to rhyolitic pumices, widely distributed on most of the island with thickness SEwards decreasing from 45 to 30 cm.

Three distinct layers of pumice pyroclastic deposits relative to the distinct phases of rhyolitic activity in southern Lipari (Punta di Perciato, Falcone, Monte Guardia) are interlayered within the Brown Tuffs succession, although they are not invariably visible. The most important and clearly visible is the Monte Guardia pyroclastic unit,



widely distributed across most of Lipari and representing one of the most voluminous successions of the island. Distal Monte Guardia fallout layers of pumiceous ash and lapilli with obsidian fragments are recognized on Salina, Vulcano, Panarea and Stromboli.

Points-for-discussion

- Long-term hazard scenario for widespread explosive eruptions from La Fossa cone of Vulcano
- Recognition of distal tephra layers in a terrestrial stratigraphic record and their potential for stratigraphic correlation and hazard evaluation

STOP 2.4: (38°29'18"N, 14°53'59"E)

Locality: Bruca-Cala Fico.

Focus: Older volcanic edifices and marine terraces of MIS 5 (Tyrrhenian stage) and interlayered volcanic products.

Description: The oldest Lipari products (c. 270-190 ka) are exposed along the west coast of the island. They are lava flows and hydromagmatic pyroclastic products with minor scoriae that built up a number of centres mostly aligned in N-S direction. The fissural-type lava-scoria cones with steep slopes of Timpone Pataso (334 m), Timpone Ospedale (352 m) and Valle di Pero (333 m) are particularly visible. The M. Mazzacarusu stratocone (Fig. 21a) is characterized by thick accumulations of chaotic pyroclastic-breccias composed of moderately vesicular to scoriaceous clasts and interlayered thin lava flows related to Strombolian and effusive phases of activity, and subsequent re-deposition along the steep volcanic slopes (leading to abrasion, rounding and breakage of the loose lava and scoriaceous fragments). Highly brecciated lava products crop out in the isolated Pietra del Bagno islet located off the west coast of Lipari, representing the remnants of generic volcanoclastic units originated from the M. Mazzacarusu edifice. Thick, massive lava flows with evident jointing are exposed in the capes of Scoglio le Torricelle, Punta Palmeto and Punta di Cugno Lungo. Overall, these products are homogeneously CA basaltic andesites, which represent the most primitive rock types on Lipari.

In the coastal sector between Bruca and Cala Fico there is the best field exposure of the sequence of Tyrrhenian marine terraces and interlayered volcanic products. Metre-thick, laterally persistent horizons of coarse transgressive conglomerates consisting of well-rounded pebbles to boulders lying above sharp marine erosional surfaces are well visible, terminating landwards in terrace inner margins best exposed at P. delle Grotticelle (paleoshoreline II) and Cala Fico (paleoshoreline I; Fig. 21a). Carbonate buildups consisting of calcareous algae



and serpulids englobing mollusc shells (and corals) are associated with the boulder conglomerates in some places near to Cala Fico. The stacking pattern of terraces at different elevations is well exposed between Cala Fico and P. del Cugno Lungo where the terrace of palaeoshoreline I is bordered by an inner margin at c. 45 m and is cross-cut by the paleoshoreline II terrace found at lower elevations (inner margin at c. 25 m).

In the sector of Bruca (Fig. 21b), the terraces are interlayered with the Monte S. Angelo products of Epochs 5 (105 ka). There, the paleoshoreline I marine terrace deposits formed during MIS 5e (124 ka) are found at elevations of 5-15 m asl (lower than usual) as a consequence of local tectonic vertical displacement along a series of normal faults. This terrace is directly covered by the cordierite-rich lavas (and leaf-bearing pyroclastics) relative to Monte S. Angelo (Epoch 5, 105 ka). These products are in turn cut by terraces related to paleoshorelines II (MIS 5c=100 ka) and III (MIS 5a=81 ka). The most feasible scenario implies that the successive sea-level transgressions of MIS 5c and 5a partly or completely flooded the older paleoshoreline I terrace as a consequence of its vertical displacement, thus generating a (not-typical) vertical stacking succession. The stratigraphic relationships between the cordierite-rich lavas and successive terraces are recognized because the terraces of palaeoshorelines II and III are almost entirely composed of clasts with a distinctive cordierite-bearing lithological and petrochemical appearance, which are instead completely absent in the terrace deposits of palaeoshoreline I.

Points-for-discussion

- Interplay between volcanic activity, sea-level fluctuations and crustal uplift in the evolution of a coastal volcano during the Late Quaternary

STOP 2.5: (38°27'1"N, 14°56'30"E)

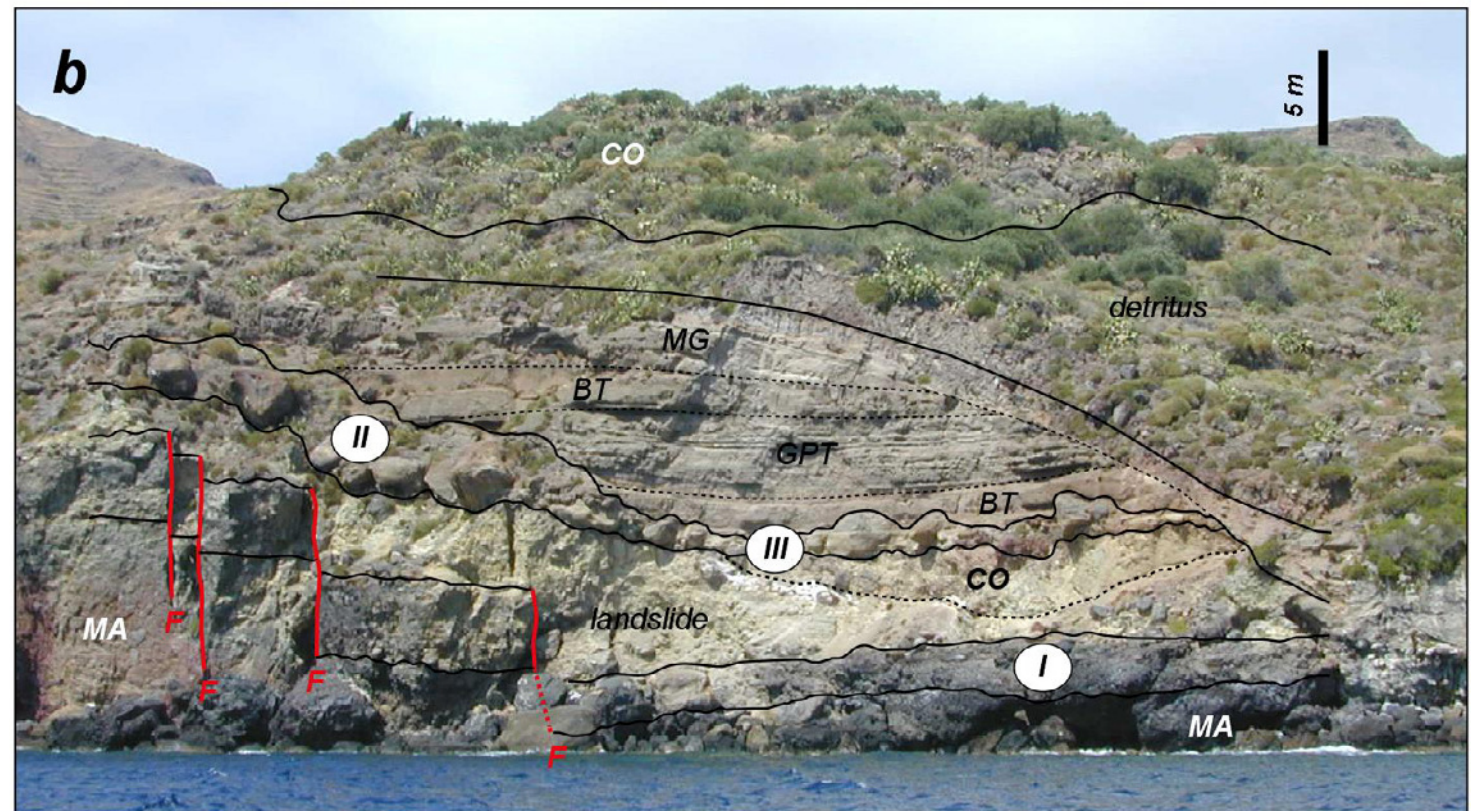
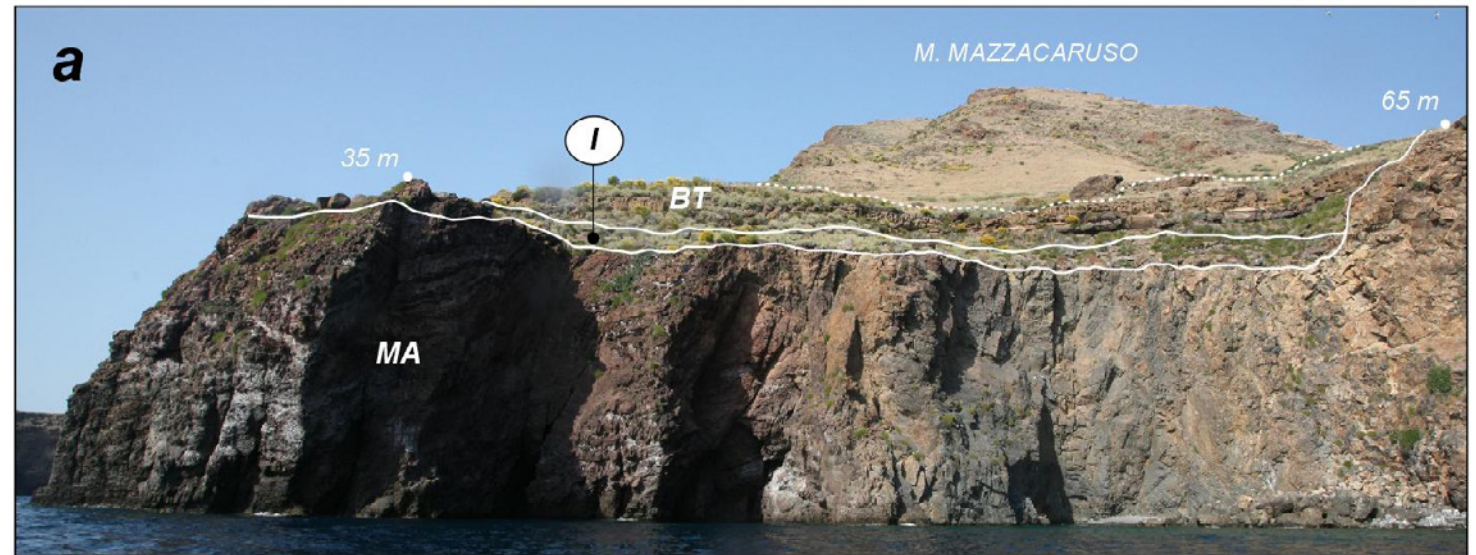
Locality: Scogliera sotto il Monte (south-west Lipari)

Focus: Southern rhyolitic dome-complex

Description: The southern sector of Lipari is entirely constructed by a voluminous NNW-SSE-elongated rhyolitic dome-field constituted by an alternance of pumice deposits and endogenous lava domes. In the area of Spiaggia V. Muria, the pyroclastics products related to the dome-field climb over the collapse (vc3) that affected the south-eastern flank of Timpone Carrubbo, marking a primary unconformity. A natural stratigraphic section across the products of the southern dome-field is particularly exposed along the western side of this dome-field between Spiaggia V. Muria and P. della Crapazza (Fig. 22).



Fig. 21 - (a) Best exposure of the terrace of paleoshoreline I along the coastal cliff of Cala Fico, west Lipari, with field evidence of the main features and inner margin at c. 45m asl. The terrace is carved into lavas of the M. Mazzacarusu cone (MA), visible in the background, and is sealed by a continuous pyroclastic cover including Brown Tuffs, Grey Porri Tuffs and M. Guardia pyroclastics. (b) The coastal cliff of Bruca shows a natural stratigraphic section across the succession of MIS 5 terraces and interlayered volcanic products. From the base to the top, the following units are recognized: (i) volcanic products of M. Mazzacarusu (MA, 270-190 ka); (ii) palaeoshoreline I terrace deposits (124 ka), displaced along a series of normal faults (F); (iii) a landslide and the flow front of the cordierite-rich lavas of M. S. Angelo (CO, 105 ka), which are also visible in the background; (iv) palaeoshorelines II and III terrace deposits (100–81 ka), set in a downstepping stacking pattern; (v) pyroclastic succession including the Brown Tuffs (BT), Grey Porri Tuffs (GPT) and M. Guardia pyroclastic unit (MG).

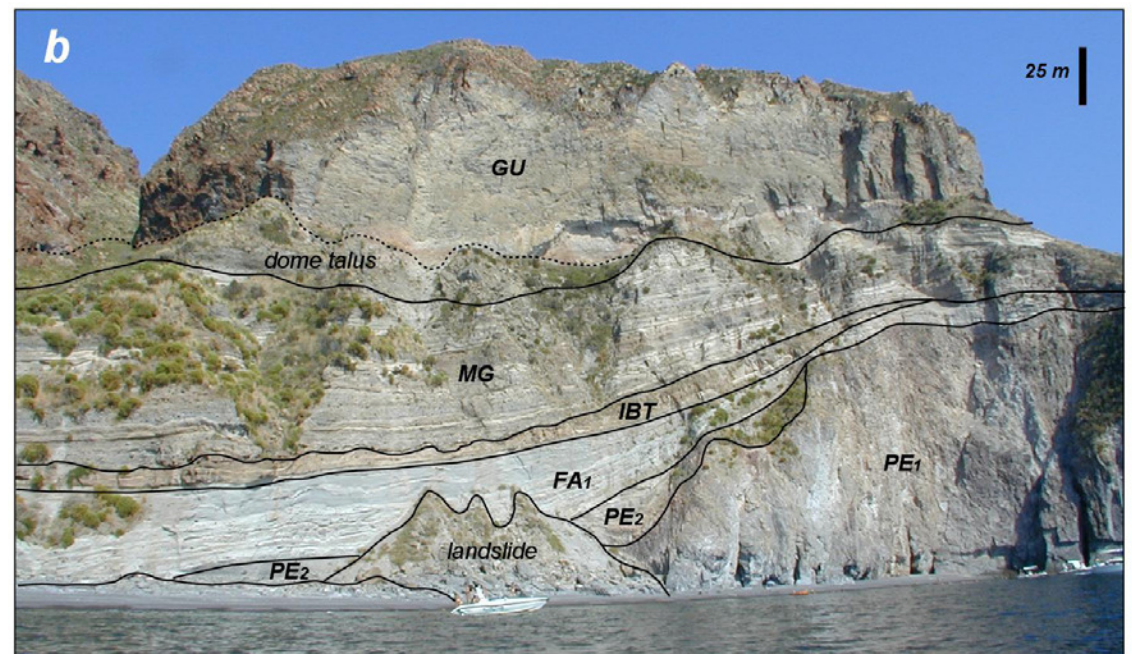




The oldest products in this sector are the remnants of the two endogenous NNW–SSE-aligned lava domes of P. del Perciato (Fig. 22a) and P. di Levante (Fig. 22b), together with the isolated rocks of le Formiche, Pietralunga and Pietra Menalda (known as “Faraglioni”) representing the remnants of eroded domes. These domes are discontinuously surmounted by a whitish pumiceous pyroclastic succession of massive to cross-stratified lapilli-tuffs related to explosive phases that partially destroyed the underlying domes (as inferred by the occurrence of abundant dome-type lithics in proximal areas). Renewed activity occurred from vents in the area of Falcone (43-40 ka). Initial explosive activity



Fig. 22 – Along the coastal cliffs of P. del Perciato (a) and Punta di Levante (b) a natural stratigraphic section is exposed across the rhyolitic products building up the southern dome-field of Lipari. From the base to the top, the following units are visible: i) lava domes of P. del Perciato (PE_1) and overlying pumices (PE_2); ii) pumiceous succession of Falcone (FA_1) and the overlying domes (FA_2); iii) pyroclastic succession of M. Guardia (MG) and lava domes of San Lazzaro, M. Guardia and M. Giardina (GU). A layer of Intermediate Brown Tuffs from Vulcano (IBT) and the embedded Y-5 tephra layer is interlayered contributing to the definition of the stratigraphic relationships between distinct levels of domes and pyroclastics. A spectacular view on the onion-skin foliated inner structure of one of the endogenous domes of P. del Perciato (PE_1) is visible at the P. di Perciato cape (a).





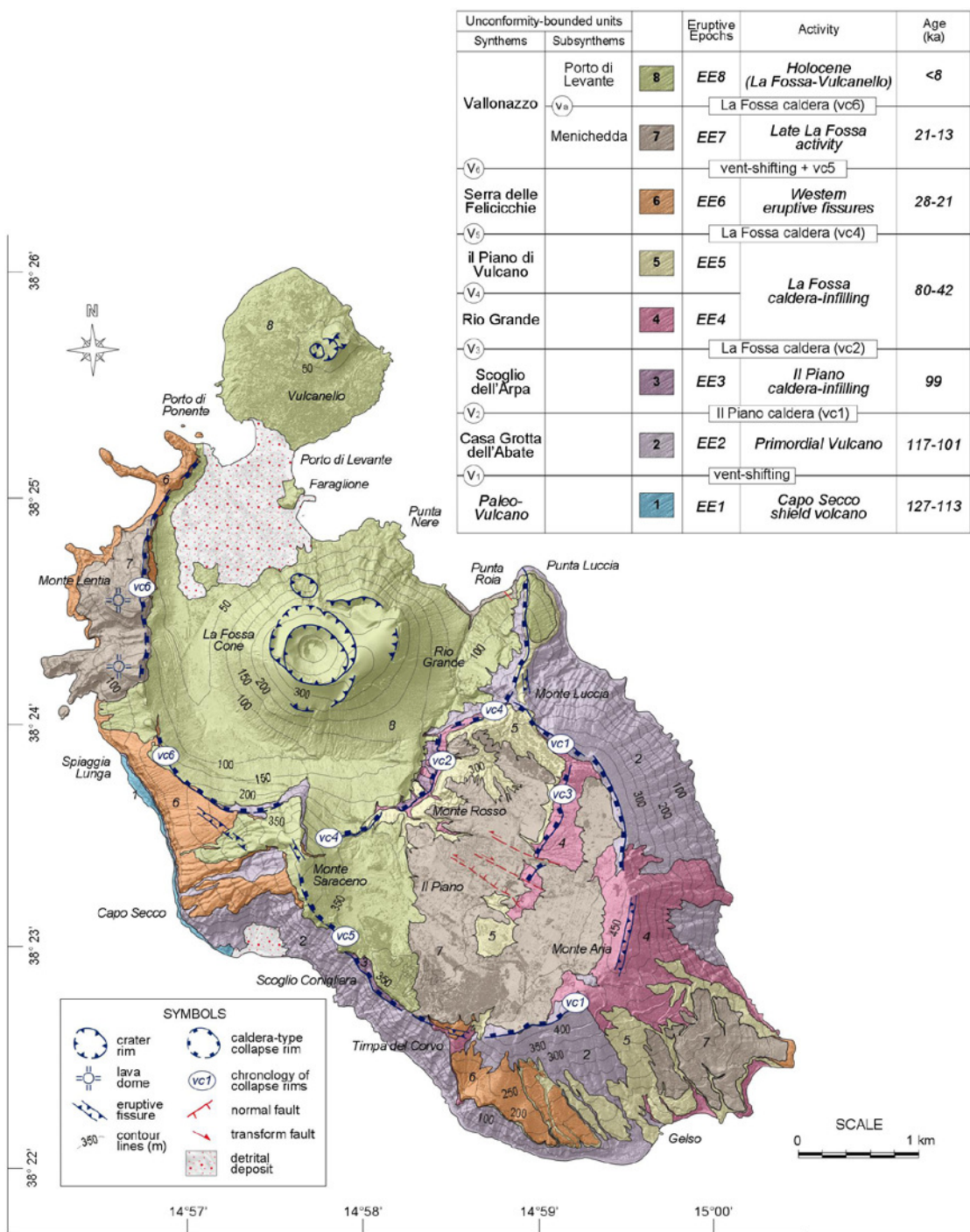
produced a thick whitish pumiceous succession consisting of multiple depositional units from dilute PDCs characterized by a typical northward facies variation from massive to cross-stratified lapilli-tuffs (Fig. 22a-b). These products constructed a large tuff-ring that was subsequently filled by the endogenous domes of Falcone, Capparo and Capistello (Fig. 22a). Related to these domes, near Punta della Crapazza a small high-K dacite black lava dome crops out, fed by a dike running along the trace of a north-south-trending normal fault. The lavas of this small dome are characterized by the presence of mafic xenoliths and flow structures, suggesting interactions between latitic and rhyolitic magmas (Gioncada et al., 2003). A caldera-type collapse (vc4) truncated the summit of this dome-field during a subsequent prolonged quiescence period, which was also characterized by deposition of several layers of Brown Tuffs from Vulcano, exposed along most of the coastal cliff within the rhyolitic pyroclastic and dome sequence (Fig. 22b).

The Monte Guardia-Monte Giardina activity (c. 27-24 ka) was the most intense in southern Lipari. The early explosive eruptions occurred from a vent localized within the morphologic depression of collapse vc4 and produced the Monte Guardia pyroclastic succession (Fig. 22b). In this sector, this is a thick pumiceous pyroclastic succession of multiple depositional units from dilute PDCs (showing the typical lateral and vertical facies variations) and minor fallout from an associated eruption plume. The succession is mostly made up of highly vesicular white rhyolitic pumices, with a subordinate content of moderately vesicular latitic pumices and banded pumices, that provide evidence of mingling-mixing processes when a fresh mafic (latite) magma entered into a shallow rhyolite chamber (De Rosa et al., 2003). This gave rise to a Subplinian eruption mostly driven by mechanisms of magmatic volatile fragmentation, with periodic episodes of hydromagmatic interaction when seawater had access to the vent that was located near sea level. The Monte Guardia succession is covered by the NNW-SSE-aligned, endogenous, obsidian-rich lava domes of S. Lazzaro, Monte Guardia and Monte Giardina (Fig. 22b), named in order of progressive effusion from south to north. To the side of this dome-alignment, the coeval NNW-SSE-aligned endogenous lava domes of P.S. Giuseppe occupy the eastern side of the southern dome-field, revealing the activity of two parallel eruptive fissures fed by different magma batches.

The whole southern dome-field is cut by major NNW-SSE-oriented strike-slip to normal faults exposed along the southern coast of Lipari near P. del Perciato by c. 100-m-high subvertical fault scarps with triangular to trapezoidal facets.

Points-for-discussion

- Features controlling the transition of eruptive style from explosive to effusive during the southern dome-field evolution



3.3 Vulcano

The island of Vulcano (21.2 km²) is the southernmost of the Aeolian Arc and is the exposed summit of an active volcanic complex that rises from the sea floor (c. 1000 m b.s.l.) up to the maximum height of 500 m a.s.l. at Monte Aria, as part of the NNW–SSE-elongated volcanic belt including also Lipari and Salina (Ventura, 2013 for a review) (Fig. 14).

The structural pattern of Vulcano (Fig. 23) is conditioned by the formation of the intersecting multi-stage calderas of Il Piano and La Fossa (average diameter 2.5–3 km) in the time interval between c. 100 ka and 13–8 ka. The younger La Fossa caldera, in particular, is the result of (at least) three major collapse events occurred at c. 80 ka (vc2, south-eastern border), at some point between 42 and 24 ka (vc4, central-eastern border) and at 13–8 ka (vc6, western border), and presently occupies the northern part of Vulcano, partly below the sea-level (Casalbore et al., 2018).

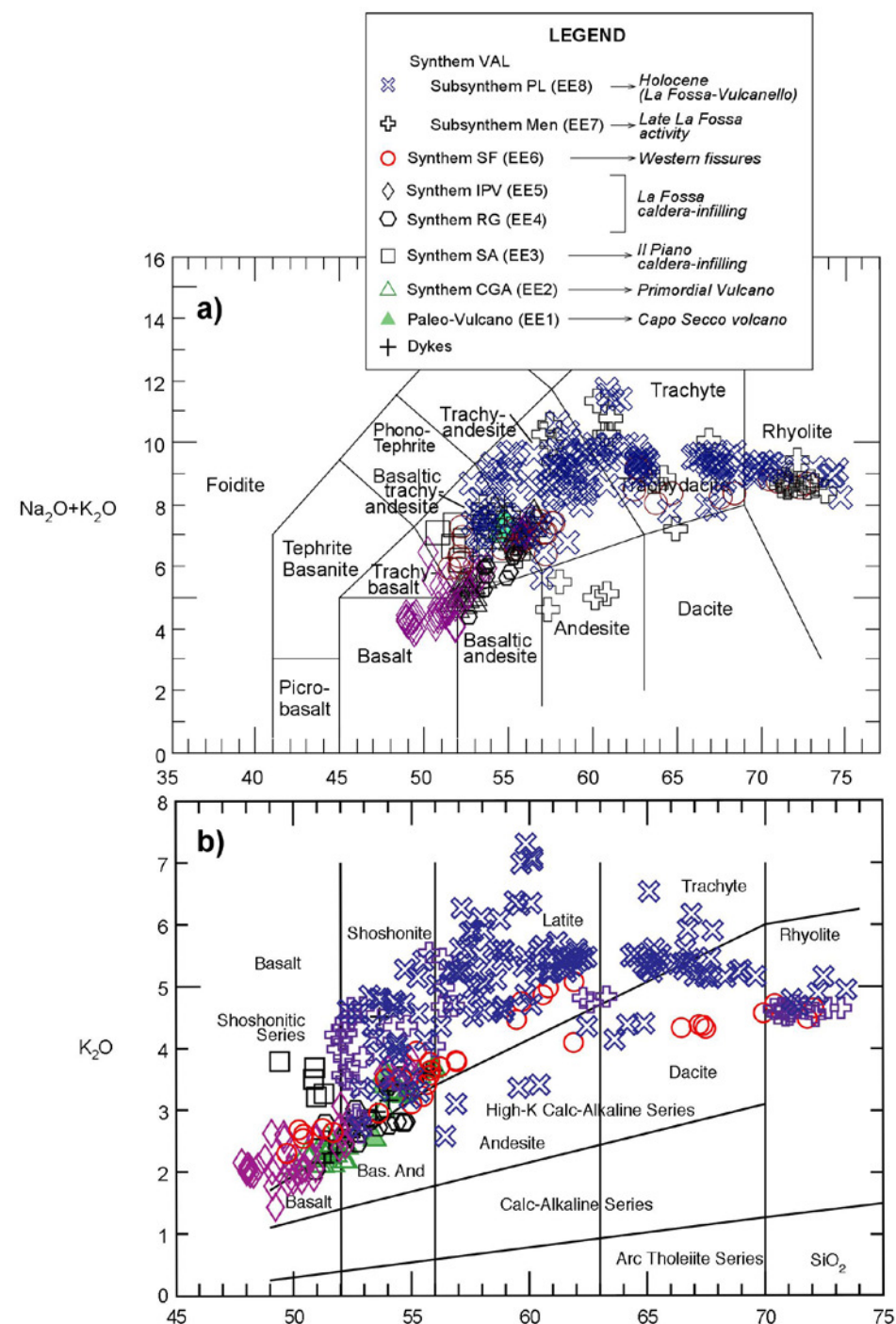
Fig. 23 - Sketch geological map of Vulcano (modified from De Astis et al., 2013a, b) merged on a shaded-relief DEM of the island, showing the areal distribution of the designated UBUs and the corresponding Eruptive Epochs (EE) as well as the collapse rims corresponding to the multi-stage formation of the Il Piano and La Fossa calderas. Coordinates conform to the Gauss-Boaga System (IGM) with reference to the Greenwich meridian.



The La Fossa caldera has been recently assumed as the source area of the high-energy hydromagmatic explosions giving rise to the widespread Brown Tuffs (Lucchi et al., 2008, 2013c). The calderas on Vulcano are basically related to magma chamber dynamics under direct control of the regional Tindari-Letojanni fault System, as particularly outlined by the general NNW-SSE elongation of the calderas and progressive shifting towards the NNW, causing the development of the calderas in the Lipari-Vulcano complex along the NNW-SSE direction.

Vulcano rocks display a wide spectrum of compositions ranging from basalts to rhyolites with HKCA and SHO affinity, and most rocks plot in the compositional fields of the SHO series (Fig. 24). Both total alkali and potassium generally increase with increasing silica up to the intermediate compositions, then dropping slightly in the most silicic products. The SHO rocks notably display a wide range of K_2O contents and K_2O/Na_2O ratios and some of them are slightly undersaturated in silica, implying that they may be related to potassium alkaline rocks (KS). The variability of magmatic compositions recorded along the eruptive history

Fig. 24 - Total alkali v. SiO_2 (TAS) and K_2O v. SiO_2 (Peccerillo and Taylor 1976) classification diagrams for the products of Vulcano. Oxides are expressed as weight percent (wt%). Compositions are normalized on a LOI (Loss On Ignition)-free basis. Legend of the synthems (see Fig. V1): CGA, Casa Grotta dell'Abate; SA, Scoglio dell'Arpa; RG, Rio Grande; IPV, Il Piano di Vulcano; SF, Serra delle Felicicchie; Val, Vallonazzo (Men, Menichedda; PL, Porto di Levante). The attribution to Eruptive Epochs (EE) is also shown. Modified from De Astis et al. (2013b).





of Vulcano reflects both shallow-level evolutionary processes and differentiation in a polybaric magmatic system consisting of separated, but often interconnected, magma reservoirs, and the occurrence, of geochemically distinct types of primary melts generated in different mantle sources (see De Astis et al., 2013b for a review). Products erupted during the last 1000 years have latitic to rhyolitic compositions (also in the same eruptive event, as enclaves), which have been related to the selective activation some magma reservoirs at different composition, located between 15 to 3 km of depth (Nicotra et al., in press).

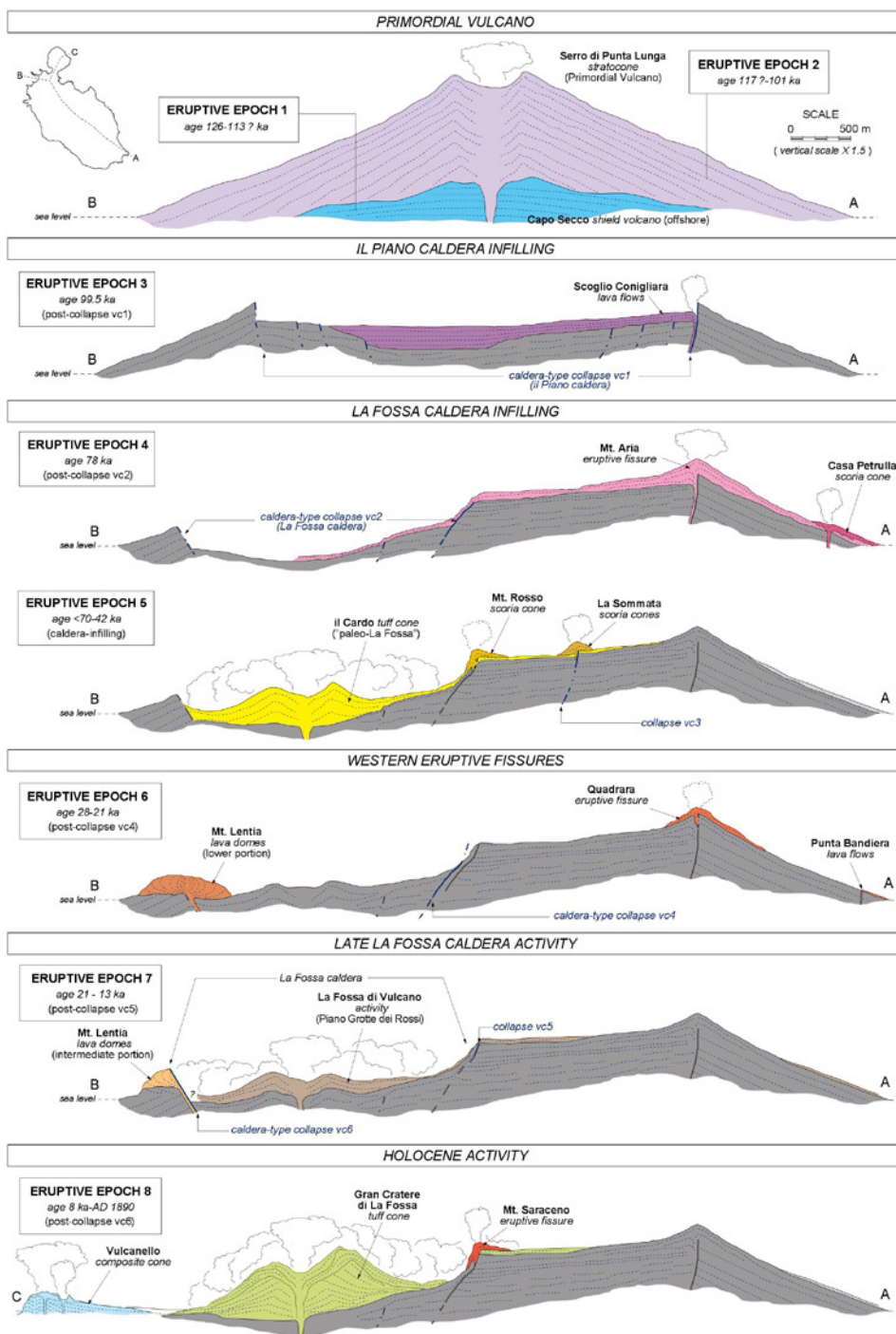
Starting from the '80s, the Aeolian Islands seismic network has been improved with several stations covering all the archipelago and equipped with seismometers with short period. In the 2000s, all the stations (12, of which 4 at Vulcano) have been substituted with 3-components-seismometers.

Since the end of '90s a permanent GPS network with 6 CGPS stations has been active. The degassing is monitored from the Palermo and Catania sections of INGV, with periodic campaigns and continuous measuring. Geochemical monitoring is performed through an automatic station registering the CO₂ flux, the temperature gradient and the determination coefficient (R²) on vertical profiles of soils, the chemical and physical parameters of water, the total pressure of gas dissolved in water, the temperature and flux of SO₂ of the fumarolic field in Vulcano. At Vulcano a meteorologic station for the measurement of global parameters is also present, together with a thermal camera on the crateric fumaroles.

3.3.1 Eruptive history

According to the most recent 1:10.000 geological map of the island and the relative stratigraphy (De Astis et al., 2013a, b), the eruptive and volcano-tectonic (and magmatic) history of Vulcano is described as the result of eight successive Eruptive Epochs in the time interval between c. 127 ka and historical times (AD 1888–1890) (Fig. 23). These Epochs were separated by periods of quiescence, erosion and dismantling or collapse events (vc1–vc6) forming the il Piano and La Fossa caldera-type structures. Volcanism during each Epoch was characterized by a distinctive localization of eruptive centres erupting products with different chemical compositions.

The oldest rocks exposed on Vulcano are dated at c. 127–113 ka (Epoch 1) and consist of lava flows representing the east-dipping outer flank of the small Capo Secco shield volcano located offshore of the western coast of the present island, and presently almost entirely submerged. The c. 700 m high Primordial Vulcano stratocone (Epoch 2, c. 117–101 ka) was then constructed to the east of Capo Secco volcano by HKCA basaltic andesite to shoshonite lava flows and scoriae related to phases of Strombolian and effusive activity (Fig. 25). At c. 100 ka, the summit



of this stratocone was truncated by the Il Piano caldera (collapse vc1). After the caldera formation, the eruptions of Epochs 3 (99.5 ka) and 4 (c. 78 ka) occurred from fissures and vents mostly located along its southeastern and western edges (Scoglio Conigliara, Monte Aria, Timpa del Corvo) and produced the progressive caldera in-filling by means of SHO basalt to leucite-bearing shoshonite lava flows and pyroclastic products. The transition from Epoch 3 to 4 occurred at c. 80 ka, marked by the first collapse (vc2) event related to the development of the southeastern border of the multi-phase La Fossa caldera. This collapse signalled the early step of the NW-wards shifting of volcanic and tectonic activity.

Renewed volcanism during Epoch 5 (between c.70 and ka) was mostly characterized by the emplacement of thick grey to varicoloured, planar- to cross-bedded pyroclastic successions of deposits from Strombolian fallout and dilute PDCs (Monte Molineddo 1, 2 and 3) presently exposed within the Il Piano caldera. Based on west-to-east decrease of thickness and grain size, these successions are related to an eruptive vent(s) located within the La Fossa caldera, almost entirely dismantled by the subsequent volcano-tectonic collapses. These pyroclastic successions are suggested by Lucchi et al., (2008, 2013c) to be the more

Fig. 25 - Schematic geological sections of the volcanic products emplaced during the Eruptive Epochs of Vulcano (modified from De Astis et al., 2013b), where the control exerted by the successive caldera-type collapses on the localization of active eruptive vents is evident.



proximal facies of the Intermediate Brown Tuffs. They are interlayered with Strombolian scoriaceous deposits and lava flows related to the Monte Rosso scoria cone and the Monte Luccia and Passo del Piano fissures along the eastern border of La Fossa caldera (c. 53-48 ka). Minor Strombolian activity within the Il Piano caldera formed the two NNE-SSW-aligned, scoria cones of La Sommata. All the products of Epoch 5 have high-K basalt to shoshonite compositions, and the basaltic magma feeding the Sommata activity is the most primitive ever erupted from the plumbing system of Vulcano. Epoch 5 was interrupted by the volcano-tectonic collapse vc4 (between c. 42 and 24 ka) forming the central-eastern branch of La Fossa caldera.

Between c. 28 and 13 ka (Epochs 6-7) three phases of rhyolitic (and trachytic) dome growth occurred in the Monte Lentia area building up a N-S elongated dome-field (Fig. 25). Volcanic activity from eruptive fissures and vents located along the western border of the La Fossa and Il Piano calderas produced minor volumes of mafic to intermediate products (Spiaggia Lunga, 24 ka; Quadrara, 21 ka) giving rise to the emplacement of widespread scoria blankets. Effusive activity along the south-eastern border of La Fossa caldera also produced the Punta Roia latite lava flows (c. 14-13 ka). Important activity during Epoch 7 (21-13 ka) emplaced Piano Grotte dei Rossi tuffs, representing the proximal counterpart of the Upper Brown Tuffs (Lucchi et al., 2008, 2013c). They are a thick succession of massive to laminated, pale-brown to brown-grey fine-coarse ash deposits from dilute PDCs and associated fallout processes. Accordingly, they are related to high-energy hydromagmatic eruptions of an eruptive vent(s) located within the La Fossa caldera, possibly constructing a tuff-cone similar to the present-day La Fossa cone (now entirely dismantled by a subsequent caldera collapse). Epoch 7 activities were interrupted by the collapse (vc6) that formed the current western border of La Fossa caldera, which directly offset the Monte Lentia dome-field. A total vertical displacement of c. 1000 m is estimated in the northern sector of La Fossa caldera (Gioncada and Sbrana, 1991).

The Holocene activity of Vulcano (Epoch 8) occurred from different vents located along the margins and inside the La Fossa caldera, in the time span from c. 8 ka to the historical activities of Vulcanello and Gran Cratere di La Fossa (Fig. 25). The early activities produced three small rhyolitic domes (c. 8.5 ka) relative to the Monte Lentia dome-field and Strombolian-Hawaiian scoriaceous products and lava flows with shoshonite composition from the Monte Saraceno fissure at the junction between the il Piano and La Fossa caldera structures. Also, the most recent layers of the Piano Grotte dei Rossi tuffs (c. 8.5 ka) and the interlayered Vallone del Gabellotto tephra from Lipari were deposited. Most important among the eruptive centres active in the Holocene period are the active La Fossa cone and Vulcanello, active in the time interval from c. 5.5 ka up to historical times. The 56-m-high stack of il Faraglione, located just in front of the Porto di Levante harbour, consists of hydrothermally



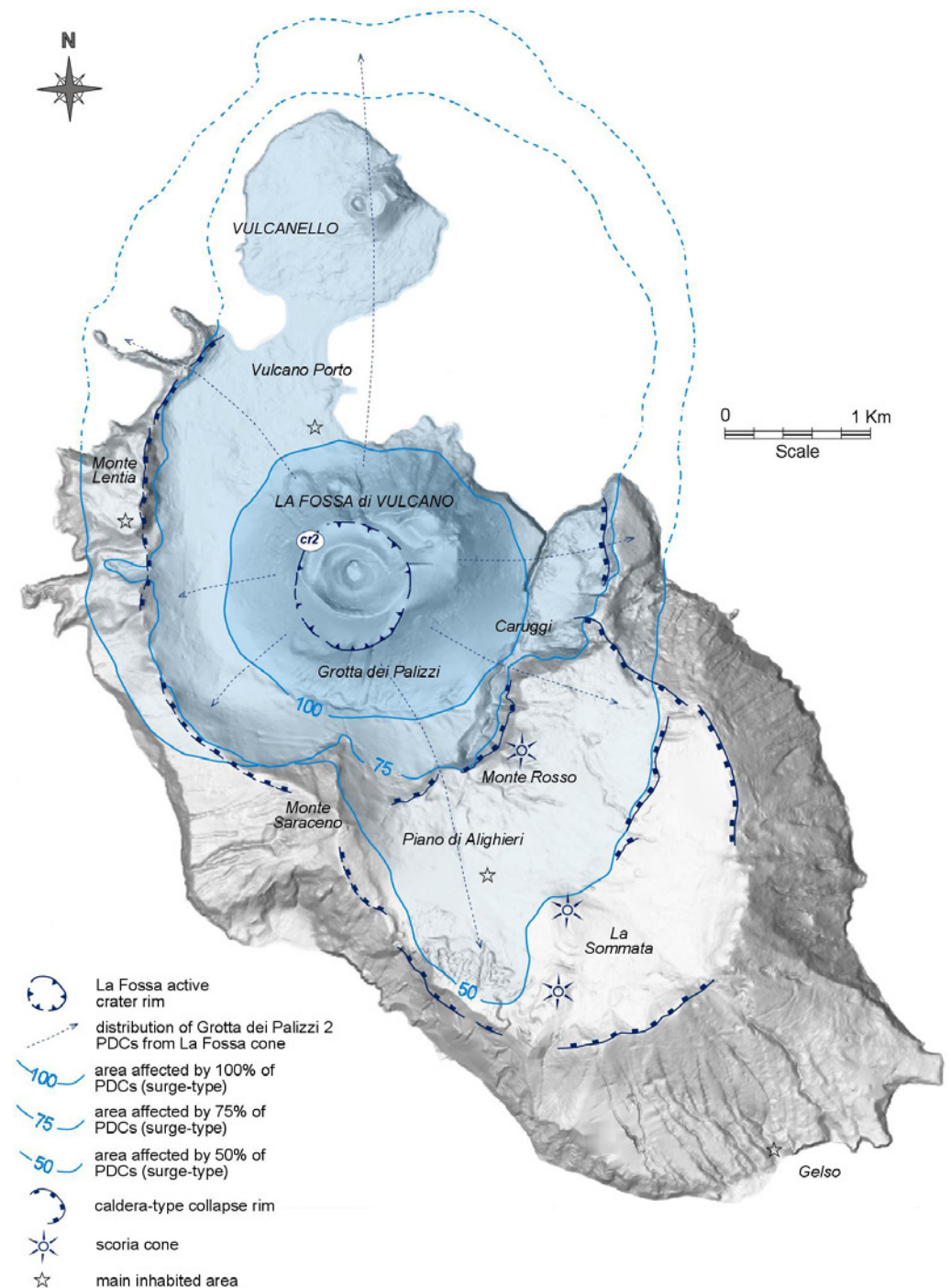
altered and locally hardened pyroclastic deposits representing the remnants of an undated small tuff cone. The Vulcanello composite cone consists of a lava platform encircling three small coalescent NE–SW-aligned scoria cones (c. 123 m high) and was constructed during the time interval between ca. 2.0 ka and 0.4 ka (De Astis et al., 2013b and references therein) through three distinct phases of explosive and effusive activity occurred along the northern edge of La Fossa caldera (Fig. 25). Recent papers proposed a different chronology for the construction of Vulcanello mostly during the last 1000 years (Fusillo et al., 2015), and further studies are developing. Vulcanello is the summit of a largely submerged volcanic edifice, progressively grown through the accumulation of submarine pillow lavas presently recognized along the north-eastern submarine slopes of the islet (Romagnoli et al., 2013). A lava platform is formed by compound aa-type to pahoehoe lava flows, and its surface is typically characterized by several few-metres-high rootless cones. Diffusion modeling on plagioclase crystals showed a very rapid magma ascent for the early eruptive products of Vulcanello (<2 years), with no storage in the shallow crust (<11 km) and direct magma ascent from the magma reservoir ponding at the Moho (Nicotra et al., in press). The Vulcanello islet is presently connected to the main island of Vulcano as the result of the progressive accumulation of volcanic material in the isthmus area mostly during the Middle Ages (c. AD 1550). Vulcanello is presently quiescent, although fumarolic activity has persisted until AD 1878.

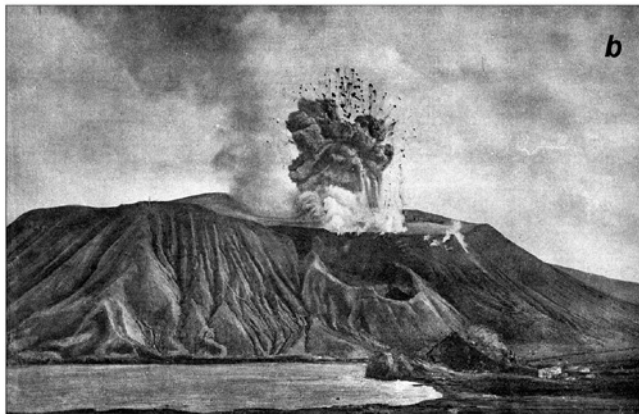
The currently active La Fossa cone has been constructed during the last 5.5 ka in the middle of La Fossa caldera through recurrent hydromagmatic to Vulcanian explosive phases of activity producing dilute PDC and fallout deposits alternating with a few viscous lava flows (Fig. 25). The La Fossa stratigraphic succession is hereafter synthetically described conforming with Dellino and La Volpe (1997) and De Astis et al., (2013a, b), although a different time-stratigraphic reconstruction has been recently proposed (Di Traglia et al., 2013). The lower portion (c. 5.5–2.9 ka) is mostly represented by the Punte Nere pyroclastic products (latites to trachites) that built up the framework of La Fossa cone up to elevations of c. 300 m (crater cr1). The planar varicoloured Grotta dei Palizzi 1 (c. 2.9 ka) lapilli-tuffs were deposited from a number of dilute PDCs and minor fallout relative to a new coalescent crater (cr2) slightly shifted to the SW along a NE–SW axis. Two minor craters were also active along the northern flank of La Fossa in the sector of Forgia Vecchia. The intermediate portion of La Fossa cone (c. 2.2 ka–AD 776) is related to volcanic activity following the typical eruptive scenario with initial hydromagmatic eruptions driving the generation of dilute PDCs or fallout processes and late effusion of (viscous) lava flows. The Grotta di Palizzi 2 activity (c. 2.2–2.1 ka) mostly produced massive to planar and cross-stratified grey latitic tuffs from dilute PDCs and a stubby rhyolitic lava flow exposed on the southern flank of La Fossa cone. Due to their wide areal distribution, these tuffs are considered the marker bed for the short-term maximum



expected eruptive event at La Fossa (Dellino and La Volpe 1997; Dellino et al., 2011) (Fig. 26). The Grotta di Palizzi 3 activity (c. 1.6-1.5 ka) instead produced planar to cross-stratified tuffs from dilute PDCs and a tongue-like trachyte lava flow mostly exposed on the southern flank of the cone. After a few hundred years of dormancy, the renewed Caruggi (Commenda) activity produced pyroclastic products from a block-and-ash flow and dilute PDCs originated from the new crater cr3, which is coalescent to and concentric with the older craters. In some outcrops a rhyolitic tephra layer from Lipari is interbedded, correlated with either the AD 776 Monte Pilato succession (De Astis et al., 2013b) or the AD 1220 Rocche Rosse activity (Di Traglia et al., 2013). The upper portion of La Fossa cone includes the products relative to the latest Vulcanian eruptions occurred through discrete pulses from AD 1739 (Pietre Cotte) to the last paroxysmal biennium of AD 1888–1890. The Pietre Cotte eruption produced thin planar varicoloured pyroclastics from dilute PDCs and fallout distributed around the summit area of La Fossa and an obsidian rhyolite lava flow along the NW flank of La Fossa, presently hanging over the Vulcano Porto village. Afterthat, in the last two centuries, the

Fig. 26 – Sketch map of Vulcano on a shaded-relief DEM image showing the areal distribution of the Grotta dei Palizzi 2 dilute PDCs, which are taken as a benchmark for the maximum expected eruptive event at La Fossa in a short-term hazard scenario (modified from De Astis et al., 2013a, b).





La Fossa cone was characterized by recurrent hydromagmatic-Vulcanian eruptions from the currently active crater (cr4) with the latest eruption of AD 1888–1890 (Mercalli and Silvestri 1891) representing the tail of this prolonged period of activity. This eruption was characterized by a pulsating eruptive column giving rise to discontinuous dilute PDCs and a ballistic fallout of lava blocks and bread-crust bombs (Fig. 27). The eruption produced a metre-thick sheet of loose black dense lapilli-tuffs with isolated bombs (latite to rhyolite) and abundant obsidianaceous bread-crust bombs (trachyte) that form the top portion of the cone (crater cr4). The AD 1888–1890 products have become the archetype for Vulcanian eruptions in the volcanological literature, based on the description of Mercalli and Silvestri (1891).

Fig. 27 – Photographs of the AD 1888-90 explosive eruption showing the development of a 1-2 km-high pulsating eruptive column (a) with a substantial ballistic component of lava blocks and bread-crust bombs (b), and detail of one of the bread-crust bombs (c) (photos from Mercalli).



DAY 3rd: the Vulcano itinerary. Ascent to the summit craters of the active La Fossa cone

Itinerary across the main features of the stratigraphic succession and eruptive activity of the active La Fossa cone (Fig. 28), and discussion about hazard and risk assessment and aspects of risk management and reduction.

STOP 3.1: (38°24'52"N, 14°57'36"E)

Locality: Baia di Levante beach

Focus: La Fossa volcanic system

Description: This is the point of view from which it is possible to appreciate the main features of the active volcanic system of La Fossa (Fig. 29), and introduce its multi-hazard evaluation. The northern flank of La Fossa cone is well visible, together with the traces of the minor (eccentric) Forgia crater. This marked a renewal of activity in 1444 AD following at least 100 years of quiescence, and produced a high-energy steam-blast eruption. The eruption occurred eccentrically with respect to the summit of the Fossa cone, and opened a new stage of the activity of the Fossa cone, characterised by the ascent of viscous plugs of magma that powered at least 8 discrete eruptive

Fig. 28 – Itinerary of the field stops during the first day of activities on Vulcano.



Fig. 29 - Panoramic view of the main features related to the La Fossa volcanic system from the Baia di Levante beach: 1. remains of the Il Faraglione old cone; 2. fumarolic areas (visible sporadically); 3. Forgia crater; 4. zone of the 1988 landslide

events lasting days to years. The scar of the 1988 landslide is also visible along the northern flank of the La Fossa cone.

Along the border of the summit crater of La Fossa, the main fumaroles that characterize the hydrothermal system of La Fossa are evident. Moreover, subordinate points of gas emission and hot springs are present in some submarine areas near the Baia di Levante harbour.

In the foreground, the remains of the Il Faraglione old tuff cone are represented by strongly hydrothermally altered and locally hardened pyroclastic material composed of planar lapilli-tuffs with dense and scoriaceous bombs are visible and make them comparable to deposits from dilute PDCs and associated ballistic fallout



processes. Extreme alteration, together with extensive subaerial and marine erosion and prolonged exploitation of sulphur and alunite during historical times, has resulted in the almost complete dismantling of the original volcanic landform.

It is noteworthy that the main features in this area (La Fossa crater, Forgia crater, Il Faraglione cone and the hydrothermal fields), together with the Vulcanello cone and Mt. Saraceno system, are mostly aligned along a N-S structural system (Ruch et al., 2016).

Points-for-discussion

- Main features of the multihazard volcanic system of La Fossa

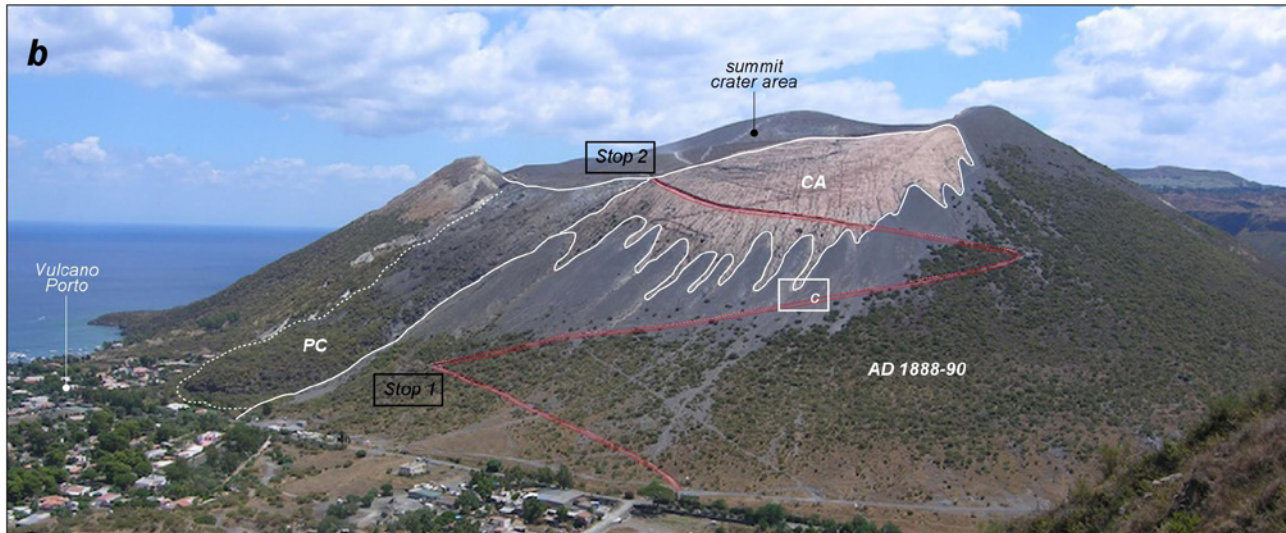
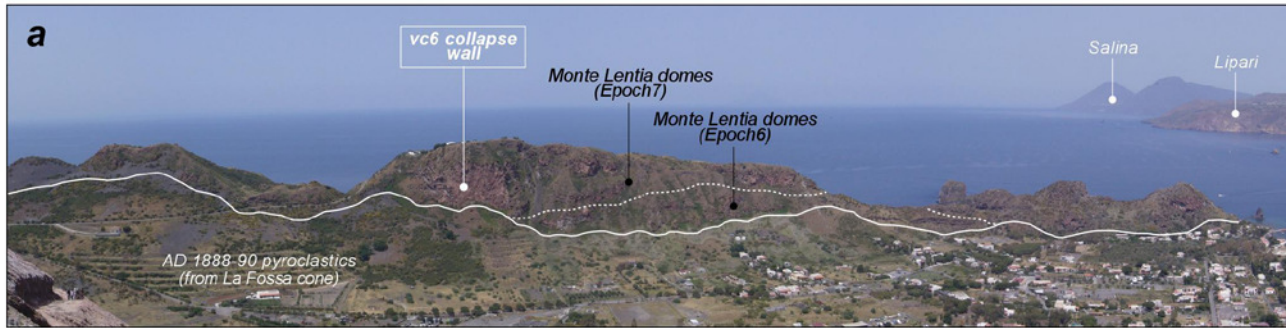
STOP 3.2: (38°24'37"N, 14°57'26"E)

Locality: Pietre Cotte (base of La Fossa cone)

Focus: Morphology and architecture of La Fossa cone

Description: The active La Fossa cone stands out in the middle of La Fossa caldera and represents the dominant morphostructural feature in the northern sector of Vulcano. The latest collapse (vc6, 13-8 ka) leading to development of the western and north-western borders of La Fossa caldera is exposed to the west by a subvertical curvilinear fault truncating the Monte Lentia dome-field (Fig. 30a).

The present-day La Fossa cone is a 391-m-high and c. 2-km-wide steep-sided tuff cone with average slope angles of 30° built up by different pyroclastic successions and lava flows during successive eruptive phases (Fig. 30b). The flanks of the cone are covered by irregular thicknesses of dark grey AD 1888–90 pyroclastic deposits mostly consisting of dense lapilli and blocks, with intercalations of laminated ash layers (Fig. 30c). These deposits overlie the older pyroclastic successions and lava flows mostly related to the XVIII-XIXth centuries. The pink-coloured Caruggi deposits (AD 776) particularly crop out in the upper northwestern slopes of the cone, where are exposed by slope erosion processes affecting the AD 1888–90 unit (Fig. 30b). These processes are largely favoured by the loose feature of AD 1888–90 pyroclastics covering slopes largely free of vegetation and generally overlying an almost impermeable substratum represented by the Caruggi deposits (Fig. 31). Heavy and/or prolonged rainfall can easily affect these loose materials, initiating recurrent episodes of remobilization and mass transfer via small-volume debris flow processes that have invaded the Porto village several times in the last decades (Ferrucci et al., 2005).



To the left, the older Pietre Cotte obsidian lava flow (AD 1739) is also exposed (Fig. 30b), hanging on the Vulcano Porto village. It has a fresh morphology, typically blocky and rough surface. The internal structure

Fig. 30 - (a) View from the cone of La Fossa of the N-S aligned domes and coulees that formed the Monte Lentia dome-field during Epochs 6 and 7. This portion of the dome field is truncated by the vc6 collapse fault representing the current western border of La Fossa caldera. (b) The western flank of La Fossa cone is extensively mantled by the AD 1888-90 pyroclastics, covering the Pietre Cotte lava flow (AD 1739) and the older pink-coloured Caruggi products, the latter exposed in the upper part of the cone by the erosion and reworking of the AD 1888-90 deposits. The footpath of the ascent to the summit craters is highlighted, together with location of Stops 1 and 2 and photograph of Fig. V6c. (c) Detail on the m-thick pyroclastic succession erupted during AD 1888-90 with layers from dilute PDCs and fallout (in places rich in hydrothermalized blocks), showing a substantial component of ballistic blocks particularly towards the upper part of the succession (see Fig. V7b for location); massive deposits by slope reworking crop out at the top.



is characterized by bands of alternating glassy and vesicular layers, flow foliation and folding structures, together with enclaves of latitic magmas evidence of mingling processes.

Points-for-discussion

- Role of the volcano-tectonic collapses in conditioning the localization of the post-collapse eruptive vents and the distribution of the corresponding volcanogenic flows.
- Interaction between eruptive (constructional) and reworking (erosive) processes in the development of an active cone

STOP 3.3: (38°24'23"N, 14°57'31"E)

Locality: External crater rim of La Fossa, elevation of c. 250 m.

Focus: Features of the AD 1888-90 deposits (primary and reworked) and the Caruggi pyroclastics.

Description: Along the footpath the erosive channels lining the western slope of La Fossa cone allow exposure of the pyroclastic succession erupted during the AD 1888-90, represented by massive to thinly-laminated lapilli-tuffs consisting of dark grey dense clasts with loose isolated lava blocks and bombs. The top portion of the succession is made up of massive deposits derived from debris flow reworking of the primary deposits along the steep slopes of the cone (Fig. 30c). The older Caruggi deposits are visible in the lower part of the erosive channels and become dominant in the part at higher elevations of the footpath building up the upper portion of La Fossa cone (Fig. 30b). They are a succession of densely stratified and coherent, pink to varicoloured tuffs deposited from recurrent dilute PDCs.

The flattish area at elevation of c. 250 m is the border of one of the crater rims (cr3) constructed during the evolution of La Fossa, particularly related to the Caruggi and Pietre Cotte activities. The Pietre Cotte lava flow (AD 1739) was erupted from the NW rim of this crater, as presently demonstrated by intense hydrothermalization and the occurrence of lithic-rich pyroclastic deposits (unconformably covering the pink-coloured Caruggi succession). The AD 1888-90 deposits blanket the whole area, consisting of loose, black dense lapilli and blocks, with several obsidianaceous bread-crust bombs ($\varnothing_{\max} > 1\text{m}$) typical of the Vulcanian activity (Fig. 31). These products are the result of intermittent explosive pulses forming transient eruptive columns with a substantial ballistic deposition. Besides the summit of the cone, the fallout deposits of the AD 1888-90 eruption mantle wide sectors of the flanks, together with isolated bread-crust bombs. Di Traglia (2011) reports an accumulation



of 100-500 kg/m² (i.e. 10-50 cm) in the Porto area and <300 kg/m² (i.e. < 30 cm) in the Piano area. Mercalli and Silvestri (1891) also report sedimentation in the southern part of the Italian peninsula (Calabria region) and in the northern coast of Sicily (between Palermo on the west and Catania/Siracusa on the east).

The bread-crust bombs consist of an outer glassy and fractured crust (cm-thick) (Fig. 30b-c) and a more crystallized and degassed inner portion. They are formed by the interplay between contrasting expansion and viscous forces, given that the starting magma is relatively viscous and external part solidifies during the flight of the bomb whereas the internal gas-rich part tries to expand. The competing internal expansion and external viscous forces are responsible of the fracturing of the shell of the bomb. The occurrence of abundant bread-crust bomb ejections during the AD 1888-90 highlights that the shallow plumbing system was at that time represented by reservoir(s) made up of crystal-rich viscous magma plugs. Dellino et al. (2011) report the occurrence of ballistic blocks associated with an impact energy between 10⁵ and 10⁶ J at a distance of <300 m from vent and of 1.4 x 10⁵ J up to Vulcanello in the north of the island and down to the southern caldera rim in the southern part of the island. These observations are related to the Punte Nere and Caruggi eruption units and the latest eruptive cycle including the 1888-90 Vulcanian eruption. Nonetheless, Biass et al. (2016) report impact energies associated with the 1888-90 Vulcanian eruption between 0.06-4 x 10⁶ J at distances between 1000-1500 m from vent along the southern caldera rim. Unfortunately, observations of ballistic blocks that have not been remobilized (mostly by human activity) are rare, with the most reliable being those on the southern caldera rim, which could explain the discrepancy between Dellino et al. (2011) and Biass et al. (2016) observations.

Points-for-discussion

- Characters of the typical Vulcanian activity expected for a future reactivation of La Fossa cone
- Aspects of tephra-fall hazard (ash, lapilli and ballistics)

STOP 3.4: (38°24'21"N, 14°57'38"E)

Locality: Summit crater area of La Fossa, elevation of c. 280 m (helicopter pitch)

Focus: Active crater area and fumarolic field

Description: The present-day crater rim (cr4) is c. 500 m large, has a roughly circular shape and shows at its bottom the traces of the two anastomized vents that originated from the latest AD 1888–1890 eruption



(Fig. 32). Discontinuous outcrops of the older Caruggi and Pietre Cotte (and Grotta dei Palizzi) pyroclastic successions, which built up the framework of the cone, are exposed in its inner south-eastern side.

A well-developed active fumarolic field is present along the northern rim of the summit crater (Fig. 32), as a demonstration of the fumarolic stage of activity (associated with shallow seismicity) in which the La Fossa cone has remained since the AD 1888-90 eruption. Here, the gas output occurs from several high-temperature fumaroles (nowadays at $T \approx 400$ °C) that have been continuously monitored during the last few decades (Nuccio et al. 1999; Granieri et al. 2006). Generally the whole fumarolic system, including Vulcano Porto, shows a range of $T = 100$ - 450 °C. The fumaroles of La Fossa are composed of H_2O (>90%), CO_2 (7-10%), SO_2 (up to 1%), HCl, HF plus several other components (e.g. H_2S , N_2 , H_2 , etc.) in minor proportions (Chiodini et al. 1995). The monitoring system revealed strong chemico-physical variations of the gas output during time. Periods of unrest, called "crisis", episodically occurred (the latest in 2005) with

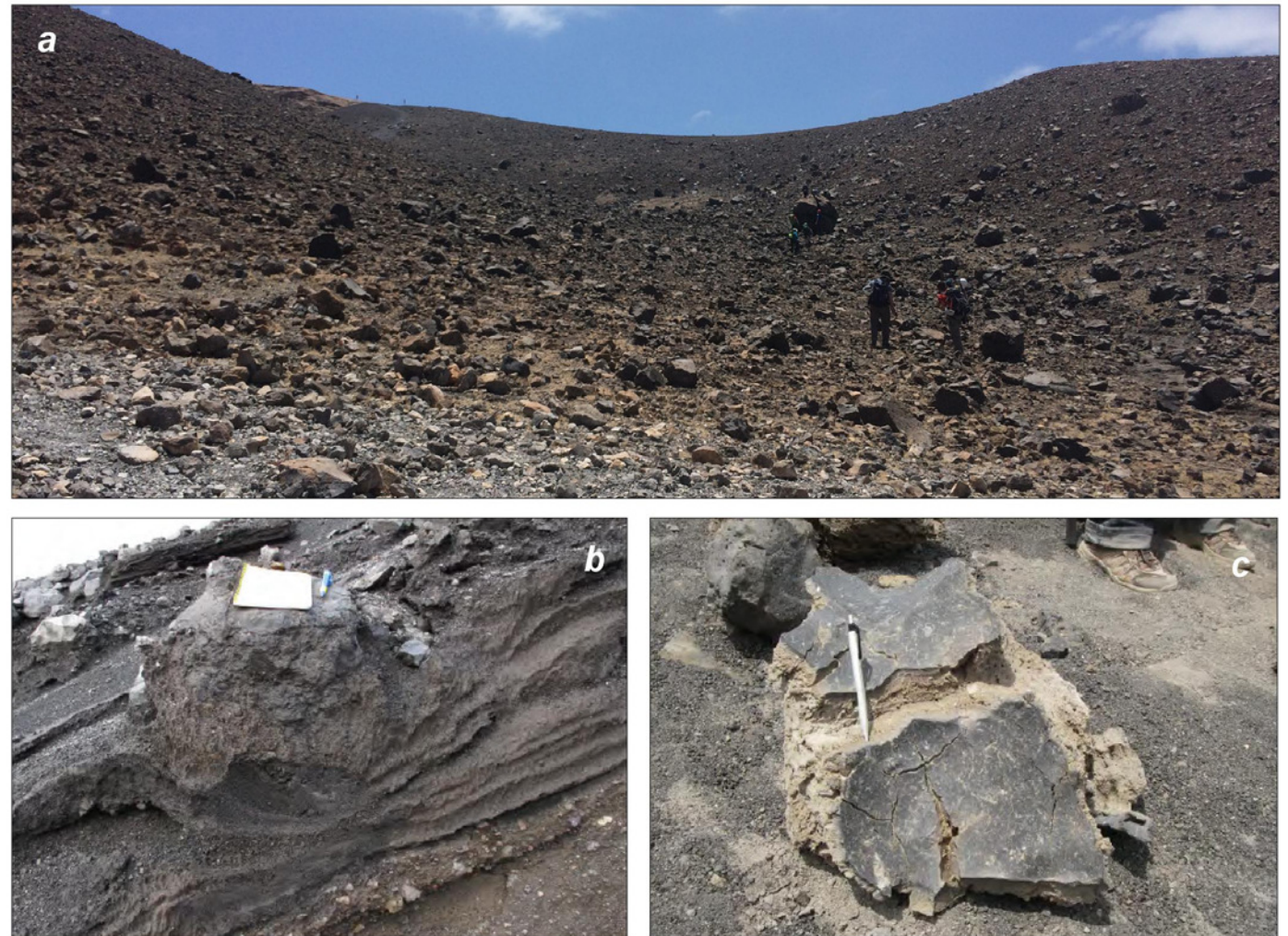


Fig. 31 – Deposits of the 1888-90 Vulcanian eruption: a) Field of bombs covering the surface of the 1888-90 eruption deposits filling the crater rim; b) Impact structures of a bread-crust bomb on underlying layers; c) detail of a breadcrust bomb.

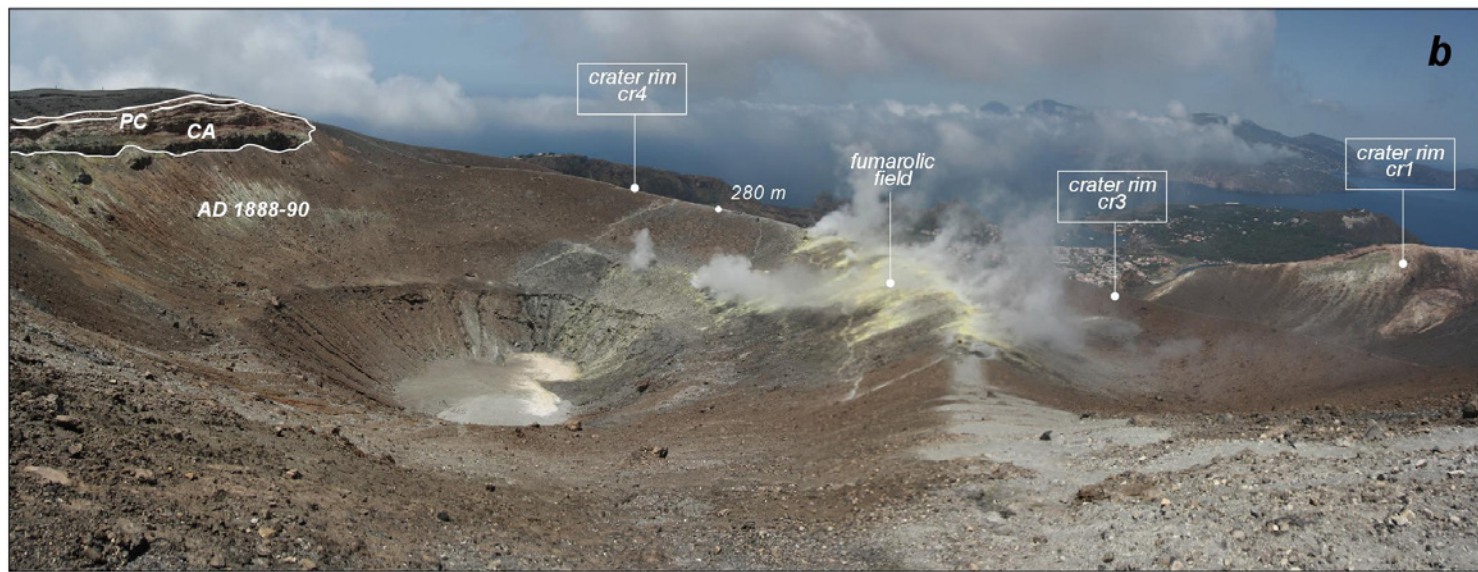


Fig. 32 – Opposite views of the summit crater area of La Fossa cone from the helicopter pitch at elevation of c. 280 m (a) and the peak of Gran Cratere di La Fossa at elevation of c. 390 m (b). The summit crater area is almost entirely covered by the pyroclastic products erupted in AD 1888–1890 characterized by the occurrence of several bread-crust bombs. Discontinuous outcrops of the older pyroclastic products of Caruggi (CA) and Pietre Cotte units (PC), which built up the framework of the cone, are exposed, together with hydrothermally-altered deposits related to the Grotta dei Palizzi series (PA). The morphological evidence for different, coalescent and concentric crater rims (cr1, 3, 4) developing through time is shown in (b), together with the two anastomized vents feeding the AD 1888-90 activity. The active fumarolic field is well visible along the northern rim of crater cr4. Numbered points in the figures indicate metres above sea level.



the fumaroles demonstrating a substantial increase in temperature (e.g from 300 to almost 700°C in the time-span 1988-1993) and the magmatic component of the total gas flux (e.g. T, F/Cl, $^3\text{He}/^4\text{He}$; He/CO₂; CO₂ flux; CO₂/H₂O; Granieri et al. 2006). Paonita et al. (2013) evidence that the detected geochemical changes are consistent with the degassing path of a magma having a latitic composition, through two magma ponding levels at slightly different pressures, where bubble–melt decoupling can occur. This reveals a clear potential for resuming eruptive activity in the future. Moreover, recent studies have provided evidence for dangerous H₂S air concentrations at some sites (usually frequented by tourists), whereas levels of CO₂ in some Vulcano houses may exceed the hazardous thresholds (Carapezza et al. 2011). On the basis of available geochemical data, three possible types of unrest are hypothesized for the future, 1) through the involvement of the surface hydrothermal system, 2) through the involvement of the deep hydrothermal system, or 3) through the potential trigger of movements of magmatic bodies coming from the deepest sources.

Points-for-discussion

- Monitoring of the active La Fossa cone
- Aspects of exposure and systemic vulnerability (e.g. distribution of critical infrastructure and facilities, redundancy, interdependency) (e.g. Galderisi et al. 2013)

STOP 3.5: (38°24'11"N, 14°57'55"E)

Locality: Peak of La Fossa cone, elevation of c. 390 m

Focus: Morphostructural setting of the summit crater area and relationships with the La Fossa caldera.

Description: The peak of La Fossa cone is a spectacular point of view for its summit crater area, which is composed of a number of nested crater rims (cr1-4) constructed during its successive phases of activity under a rough NE–SW alignment. The morphological evidence for three different, coalescent and concentric crater rims (cr1, 3, 4) is represented by curvilinear ridges that are largely covered by the most recent AD 1888-90 products (Fig. 32b). The peak of Gran Cratere di La Fossa also offers the possibility of overlooking the regional setting of the Aeolian Islands from the southernmost island of the archipelago. It is evident the NNW-SSE alignment of the islands of Vulcano, Lipari and Salina along the Tindari–Letojanni strike-slip fault system, together with the parallel preferential elongation of these islands along the same direction. To the left, the Filicudi and Alicudi islands are aligned in a WNW-ESE direction demonstrating the field evidence for the Sisifo-Alicudi fault system that



controls the whole western sector of the Aeolian archipelago. The Panarea and Stromboli islands are visible to the right in a NE-SW alignment expression of an extensional regime that favours the development of active volcanism, which is also developing in the central sector of the archipelago (Lipari and Vulcano) mostly along N-S tectonic structures (Ruch et al., 2016). It is noteworthy that all the inactive volcanoes in the Aeolian Arc are located in the central-western sector (Salina, Filicudi and Alicudi) to the west of the Tindari–Letojanni fault system representing the lateral termination of the Ionian slab.

To the south, along the steep cliff of Rio Grande, a subvertical collapse wall is the eastern branch of the La Fossa caldera, encircling the La Fossa cone. This collapse (vc2) truncates the Scoglio Conigliara lava flows (c. 99 ka) and offset the older Il Piano caldera (visible in the background), and is unconformably covered by pyroclastic products and lava flows relative to the Monte Aria fissure (c. 78 ka). These stratigraphic relationships constrain the time-interval of the early stages of formation of La Fossa caldera. The collapse vc4 (which occurred at some point between 42 and 24 ka) formed the central-eastern part of La Fossa caldera. This collapse is made evident by a curvilinear fault in the area of Monte Luccia (crosscutting the scoriaceous products of the Monte Luccia fissure) and in the middle sector of the Rio Grande gully (truncating the Monte Rosso scoria cone). The latest collapse vc6 (13–8 ka) along the western and north-western borders of the caldera is also visible in the area of Monte Lentia. The continuation of the La Fossa caldera rims in the NE sector of Vulcano is documented by abrupt escarpments found in the submarine areas near Punta Luccia and Vulcanello (Casalbore et al., 2018). It is noteworthy that the steep wall of La Fossa caldera is a substantial topographic obstacle for the lateral distribution of PDCs spreading along the flanks of La Fossa cone, as shown by thick accumulations of pyroclastic products at the foot of the main fault.

Points-for-discussion:

- Influence of caldera wall on the distribution of pyroclastic deposits produced from La Fossa cone



DAY 4th: primary school of Vulcano

STOP 4.1: (38°22'55"N, 14°59'0"E)

Locality: Il Piano primary school

Focus: Crisis management simulation at Vulcano

Description: Meeting with the teachers and the children of the primary school of Vulcano located on the area of Il Piano to discuss aspects of hazard, vulnerability and risk assessment and both risk and crisis management together with representatives of the CERG-C program of the University of Geneva and of the Italian Civil Protection. A dedicated experiential learning school exercise on volcanic crisis management that has been running at the school for the last 7 years will also be presented and discussed in details. The fieldtrip participants will have the chance to directly interact with the teachers and the children that participated in the exercise to better familiarize with the activity.



4. Mount Etna volcano

Mount Etna is the highest (3330 m a.s.l.) and largest (about 1200 km²) volcano of Europe, and one of the most active volcanoes on the Earth. It lies on the densely inhabited Ionian coast of eastern Sicily, and represents a classical example of how an active volcano interacts with resident population and tourists.

The structural framework of Etna volcano is the result of a complex interaction between regional tectonics, flank instability processes and basement morphology (Lo Giudice and Rasà, 1992; Rust and Neri, 1996; Monaco et al., 1997; Bousquet and Lanzafame, 2004; Neri et al., 2004).

The main structural lineaments (Fig. 33), reported from Branca et al. (2011a) and Azzaro et al. (2012), are:

- the E–W oriented Pernicana transtensive fault system, extending from the upper northeast flank to the Ionian coast, characterised by a left strike-slip displacement rate of 2 cm/y (Rasà et al., 1996).
- the NNW–SSE to NW–SE Tremestieri–Trecastagni fault system, formed by two normal faults with right-lateral component representing the southern boundary of the unstable eastern flank (Lo Giudice and Rasà, 1992; Solaro et al., 2010).
- the Timpe normal fault system with a right-lateral component, associated with an intense seismicity, dissecting the lower eastern flank. It is formed by several main segments (e.g. Acireale, S. Tecla, Moscarello and S. Leonardello faults), showing slip-rates ranging from 1.0 to 2.7 mm/y with NW–SE to NNW–SSE oriented and up to 180 m high scarps.

The morphostructural setting of Etna volcano is strongly influenced by the presence of the wide Valle del Bove formed, about 10 ka ago, as a consequence slope failures that involved a large portion of the eastern flank (Calvari et al., 2004; Guest et al., 1984) (see STOP 5.1 for more information).

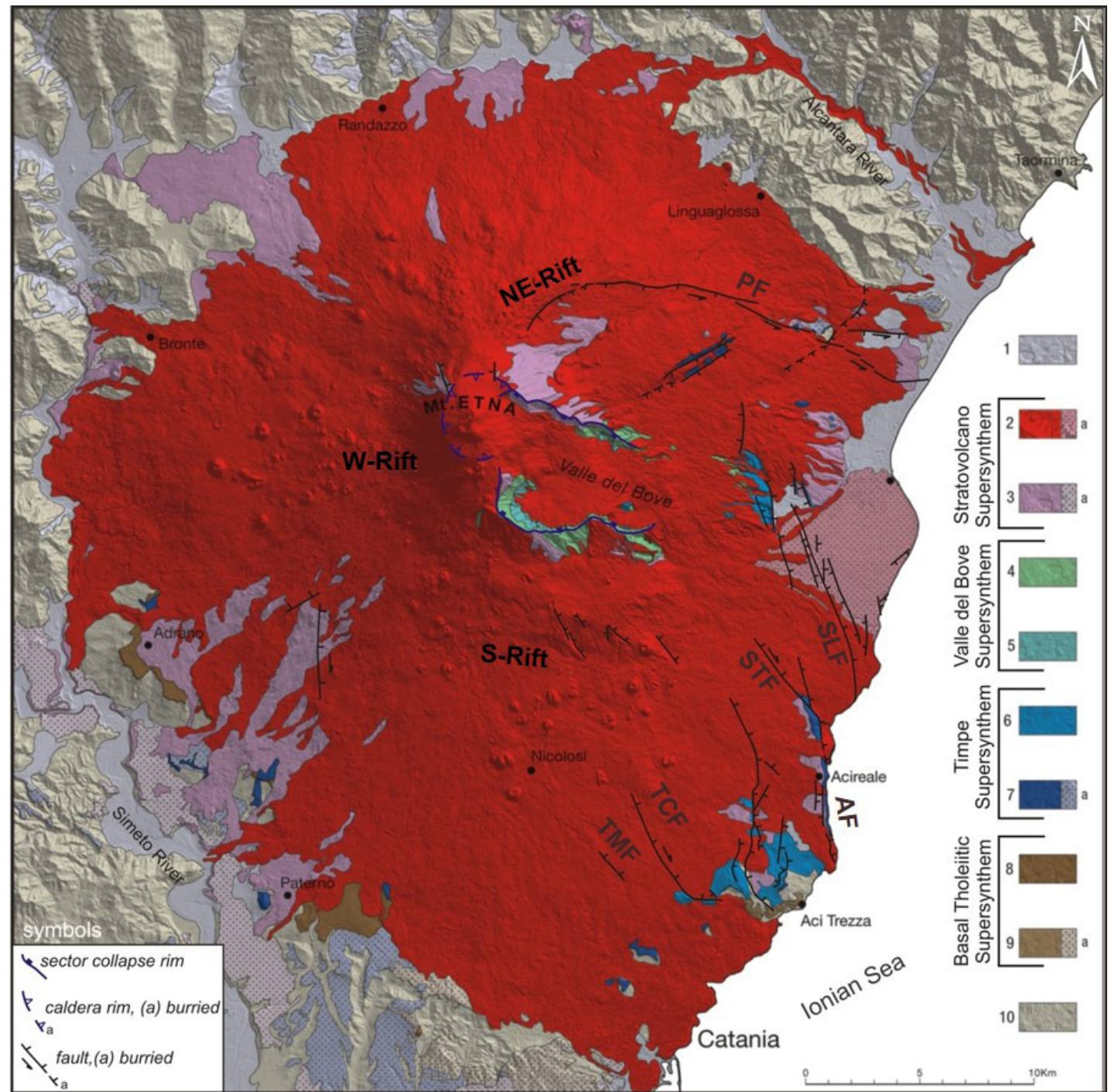
The eastern flank of Etna is involved in a seaward gravitational sliding (Borgia et al. 1992; Lo Giudice and Rasà 1992; McGuire et al., 1996; Rust and Neri 1996) resulting from the interaction between gravity, regional tectonics and recurrent dike intrusions (Rasà et al. 1996; Azzaro et al., 2013). Based on marine geological and geophysical data, Chiocci et al. (2011) highlighted the active role of the gravitational instability affecting the continental margin instability offshore Etna to drive the seaward sliding of the volcano's eastern flank.

Bonforte et al., (2011), based on Permanent Scatterers data, proposed the occurrence of an uniform and diffuse inflation of the northern and western flanks, related to the magma accumulation at depth and the consequent pressurization of the entire feeding system of the volcano, from the intermediate storage zones up to the central



conduits. This deformation is mainly visible on the northern and western slopes of the volcano, because they lie over the orogenic chain and are thus not disturbed by gravitational spreading process. The seaward motion of the southern and eastern flanks of the volcano is

Fig. 33 - Semplified tectonic and geologic map of Mount Etna (1:250.000 scale) based on the main unconformity-bounded units (Branca et al, 2011a). Symbols: PF, Pernicana fault; SLF, S. Leonardello fault; STF, S. Tecla fault; AF, Acireale fault; TCF, Trecastagni fault; TMF, Tremestieri fault. Legend: 1, Present and recent covers; 2, Il Piano Synthem (Mongibello volcano) (a, sedimentary deposits); 3, Concazze Synthem (Ellittico volcano) (a, sedimentary deposits); 4, Zappini Synthem (Cuvigghiuni, Salifizio, Giannicola and Monte Cerasa volcanoes); 5, Croce Menza Synthem (Trifoglietto, Rocche and Tarderia volcanoes); 6, S. Alfio Synthem; 7, Acireale Synthem (a, sedimentary deposits); 8, Adrano Synthem; 9, Aci Trezza Synthem (a, sedimentary deposits); 10, sedimentary and metamorphic basement



<https://doi.org/10.3301/GFT.2018.02>



instead not related to its magmatic and eruptive dynamics. Horizontal seaward velocities progressively increase from higher to lower elevations, while subsidence decreases, consistent with a wide rotational decollement. The seaward motion of this sector of the volcano, also detected through different geophysical techniques (Lundgren et al., 2004; Puglisi and Bonforte, 2004; Rust et al., 2005) is segmented into different blocks showing distinct velocities and kinematics (Bonforte et al., 2011).

Based on the distribution of eruptive fissures and scoria cones on the Etna flanks, three main weakness zones (S-, NE- and W-Rift) were identified, favouring magma intrusion and eruptions at greater distance from the central volcanic conduit (Fig. 33):

- the S-Rift comprises scoria cones and eruptive fissures mostly developed over the last 2 ka (Del Carlo and Branca, 1998) and distributed from the summit craters to the S-SE down to elevations of 600 m asl. The latest eccentric scoria cones formed during the 2002-2003 eruption lie on this rift.
- the NE-Rift consists of a network of N- to NE-striking sub-parallel eruptive fissures that are clustered, together with spatter ramparts, scoria cones and pit craters, in a restricted area about 2 km wide extending from elevations of 2500 m down to 1700 m asl (Garduño et al. 1997; Branca et al., 2003). This rift is affected by a strong (eastward) extensional tectonic activity linked with the Pernicana Fault System.
- the W-Rift comprises about 60 scoria cones and among them some of the largest of the whole Etna volcano (e.g. Mt. Minardo and Mt. Ruvolo). The latest flank eruption in this rift occurred in 1974 when several eruptive fissures produced two small scoria cones at 1650 m asl (Monti De Fiore).

From a petrochemical point of view, with the exception of the early (500–200 ka) subalkaline volcanic products (Gillot et al., 1994; Corsaro et al., 2002), the Etna's volcanic products belong to an alkali suite, spanning a composition from picritic basalts to trachytes, with mugearitic and the most abundant hawaiitic rocks (Le Maitre, 1989; Corsaro and Pompilio, 2004) (Fig. 34A).

The Etna volcano is known as one of the largest contributors of magmatic gases such as CO₂, SO₂, HCl and HF to the atmosphere (10-15 % of global volcanogenic budget, Allard et al., 1991). Continuous plume emissions occur from the four summit craters, which provide almost the totality of the emitted SO₂ (Fig. 34B), HCl and HF and the large majority of CO₂ (Allard et al., 1991; Francis et al., 1998; Caltabiano et al., 2004). Temporary emissions additionally take place during the flank eruptions, while remarkable outgassing of CO₂ occurs from the flanks of the volcano, mainly through active faults (Giammanco et al., 1997) and groundwater transport (Aiuppa et al., 2000).

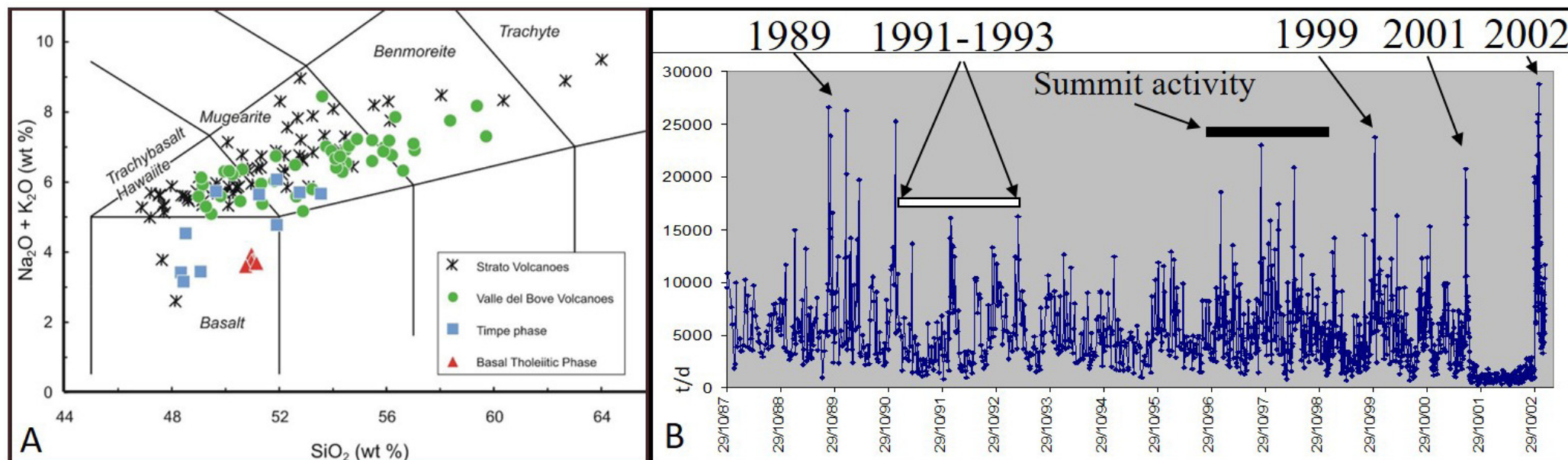


Fig. 34 – A) TAS diagram of Etna volcanics (modified from Corsaro and Pompilio, 2004). B) SO₂ fluxes (t/d) during 1987-2002. Numbers indicate the most important eruptions within the interval, during which a remarkable increasing of SO₂ flux was recorded (from INGV - Osservatorio Etno).

4.1. Eruptive History

The eruptive, magmatic and volcano-tectonic history of Etna volcano is synthetically described according to the most recent stratigraphy and geological map at 1:50.000 scale by Branca et al. (2011a). Stratigraphic analysis of the classical lithostratigraphic units, supported by radioisotopic datings and tephrostratigraphic data, allow the authors of the geological map to organize the succession into unconformity-bounded units (synthem) and informal lithosomes (Fig. 33), useful to represent the different eruptive centres. Branca et al. (2011b) interpreted the almost continuous evolution of Etnean volcanism into four main phases (Basal Tholeiitic, Timpe, Valle del Bove and Stratovolcano; Fig. 35) corresponding to the four supersynthem in which the stratigraphy of the Mt. Etna is subdivided (Fig. 33).

The oldest Basal Tholeiitic phase corresponds to a long period, from about 580 up to 260 ka, of scattered fissure-type tholeiitic volcanism, which represents the northward extension of the Plio-Pleistocene Hyblean

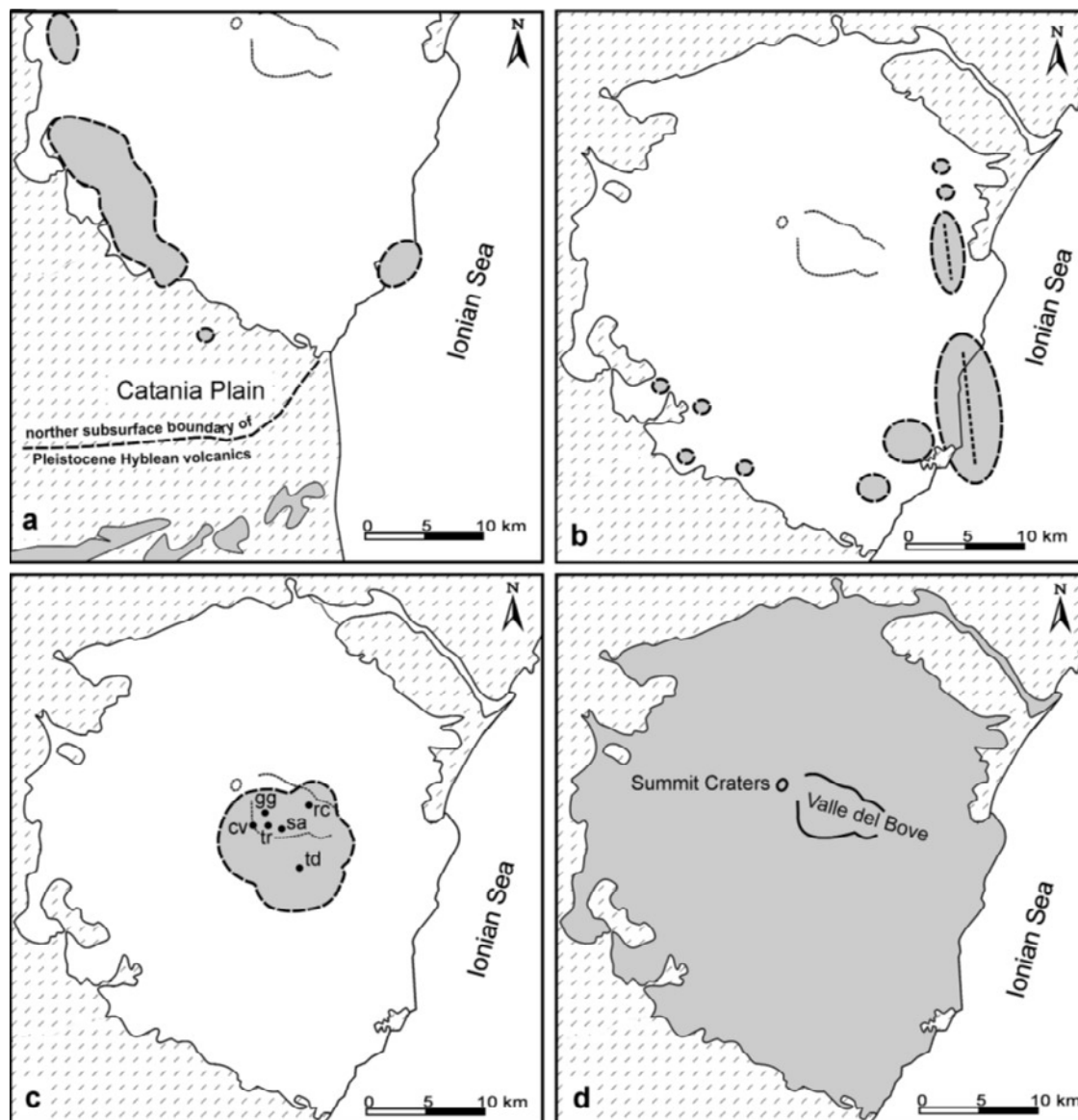


Fig. 35 - Schematic representation of the main evolutionary phases of Etna volcano: a) Basal Tholeiitic phase; b) Timpe phase; c) Valle del Bove Centres phase (td=Tarderìa, rc=Rocche, tr=Trifoglietto, gg=Giannicola, sa=Salifizio, cv=Cuvigghiuni volcanoes); d) Stratovolcano phase (Branca et al., 2004).

volcanism to the Etna region. The second phase (Timpe) started about 220 ka ago when eruptive activity was mainly concentrated in the Ionian coast along the NNW-SSE oriented Timpe fault system, where fissure-type eruptions formed a small shield volcano and the passage from tholeiitic to alkaline volcanics occurred. The third phase of the Valle del Bove Centres is marked by a main westward shift of the feeding system in the area presently occupied by the Valle del Bove depression, where some nested volcanic centres were formed. The earliest volcanic edifices in this phase were Tarderìa and Rocche, followed by the Trifoglietto volcano along the southwestern side of Valle del Bove. A local shifting of the magmatic feeder then induced the formation of the Giannicola, Salifizio and Cuvigghiuni volcanic centres (Fig. 36).

The fourth phase (Stratovolcano) is that leading to the definitive stabilization of the plumbing system and the construction of the main Ellittico stratovolcano, which forms the bulk of the present edifice. Five caldera-forming Plinian eruptions, occurred between 19 and 17 ka, marked the end of Ellittico activity (Coltelli et al., 2000; Del Carlo et al., 2017). During the Holocene, a persistent basaltic volcanic activity formed the Mongibello volcano (2 in Fig. 33), whose products cover at least 85% of the Mount Etna area. Its frequent, often continuous for long time, eruptive activity

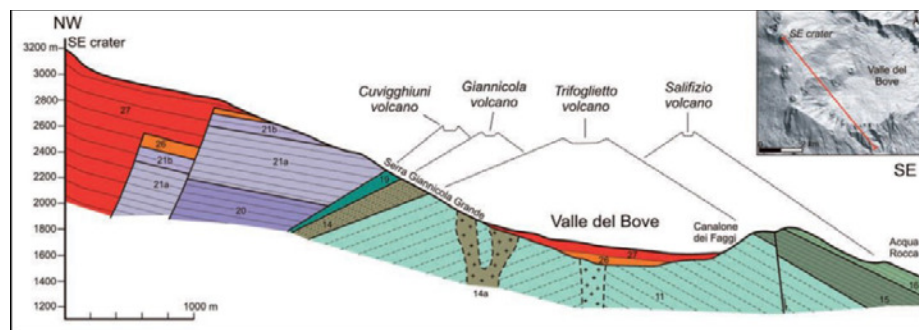


Fig. 36 – Schematic geologic section from the summit toward SE reconstructing the paleo-morphology of the main volcanic centres of Valle del Bove (Branca et al., 2011a and Fig. 32). The numbers of the lithostratigraphic units as on the geological map of Mount Etna (Branca et al., 2011a): 14, 14a, 15, 16 and 19 units belong to Zappini Synthem; 20, 21a and 21b units to Concasse Synthem (Ellittico volcano); 26 and 27 units to Il Piano Synthem (Mongibello volcano).

has occurred from both the summit area and the volcano flanks down to elevations of 400 meters asl. Presently, the summit area is characterized by four craters, the Voragine and the Bocca Nuova, which lie in the area of the former Central Crater, and the Northeast Crater and Southeast Crater, located on the Central Crater's cone flanks (see Stop 5.2 for more information).

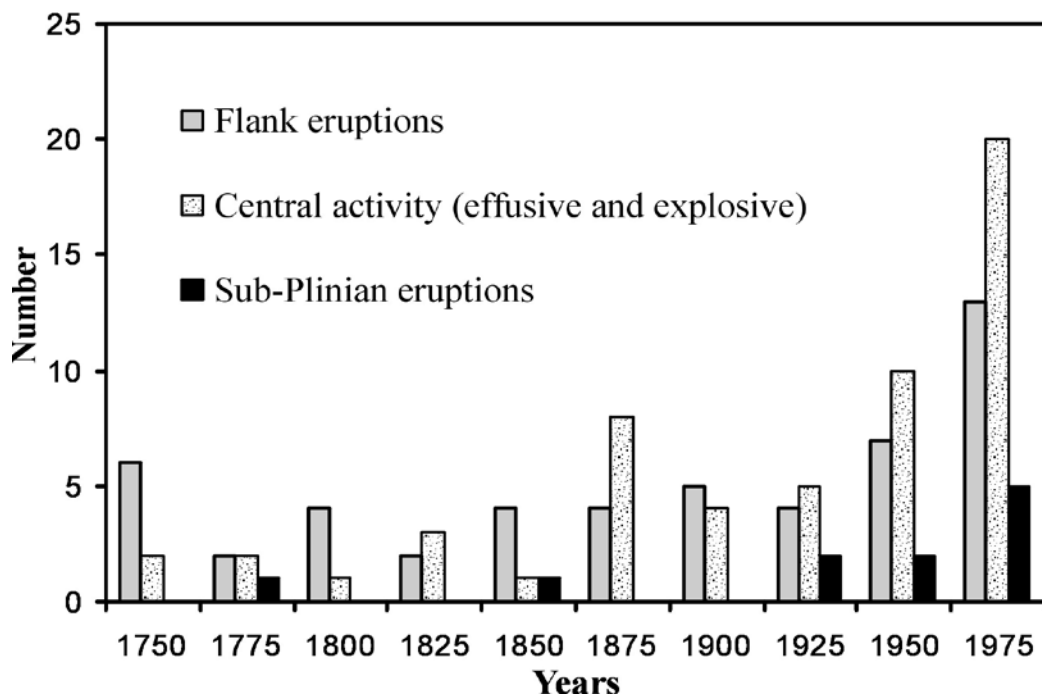


Fig. 37 - Histogram of the frequency of the eruptions from 1670 to 2003 (Branca and Del Carlo, 2005).

The well-documented activity of Etna volcano during the last 3 centuries shows the coexistence of three main types of eruptions: central (explosive and effusive), flank and Subplinian (Fig. 37). Subplinian eruptions are short-lived events, generally occurring in periods of intense central activity. The summit activity can go on continuously for many months up to years or even decades (e.g., 1955-1971; 1995-2001; 2011-2016), during the time intervals between flank eruptions. In recent years, especially since the late 1970s, a significant increase in the frequency of summit explosive eruptive episodes was observed. In particular, between 1998 and 2013 more than 150 episodes of lava fountaining (paroxysms) occurred, many of which generated high columns of volcanic ash. Flank activity at Etna produced 319 monogenic scoria and spatter cones (Mazzarini and Armienti, 2001), scattered across its slopes at altitudes ranging



from 2990 to 475 m asl. They are clustered along the NE-, S- and W-Rift zones (Rittmann, 1973; Mazzarini and Armienti, 2001). The duration of flank eruptions can be as short as a few hours, but in some cases they exceed one year (e.g. 1614-1624, 1651-1654, 1991-1993 and 2008-2009 eruptions).

Lava flows can cause serious damage but do not represent a direct threat to the ~900,000 people living in the area potentially threatened by eruptions. From 1669 to present, 58 flank eruptions were emitted by vents located between elevations of 2500 and 400 m asl (Fig. 38). Among these, the lowest ones, located near the inhabited areas, were also the most dangerous even for their unusual high effusion rates (e.g. 1669, 1928 and 1981 eruptions). The 1669 flank eruption, well studied by Branca et al. (2013), was the largest effusive event of Etna volcano in historical times. It was an exceptional event among Etna eruptions in terms of the length, covered area and volume of the emitted lava flows, the high (maximum) effusion rate and the widespread damage. The eruption lasted 122 days producing $607 \pm 105 \times 10^6$ m³ of lava. A aa flow-field was formed, representing the widest and longest lava field produced by Etna volcano in its eruptive history, extending for 17 km from the vent located in the Nicolosi area at elevation of 800 m asl, and reaching Catania, where it created new land presently occupied by the southern part of the town. The average estimated effusion rate of 58 ± 10 m³/s and the maximum effusion rate of ~640 m³/s are the highest over the past 400 years.

After 1669, the most destructive flank eruption occurred in November 1928 on the (lower) eastern sector of Etna (Fig. 39). The eruption started on 2nd November and lasted 18 days. The first brief phase (3 days) was characterized by strong explosive activity and minor lava flow output from two fissures located in Valle del Leone (2600 m asl) and Serra delle Concazze (between 2200 and 1550 m asl). On 4th November the fissure system migrated downward to Ripa della Naca (1200 m asl) and in the following two days the lava flow travelled some 6.5 kms entering in the town of Mascali, situated at elevations of only 100 m asl. Most of Mascali was overwhelmed by lava flows on 7th November. Then the velocity of the lava flow decreased and the most advanced flow front stopped at an altitude of about 30 m asl, reaching a maximum length of 9.4 km with a totale volume of 53 Mm³ (Branca et al., 2017). The destruction of Mascali had a great impact in the popular culture of the Fascism period in Italy, and showed again the vulnerability of the Etnean territory during the volcano eruptions. Another short lived but important flank eruption occurred between 17th and 23th March 1981 from a very long fissure system at elevations ranging from 2595 to 1117 m asl (Fig. 40A). The upper segment of the fissure (above 2200 m asl) produced lava fountaining and small lava flows, while from the lower part of the fissure a fast moving lava flow invaded the forest and agricultural lands above Randazzo town, reaching a length of 5 km in a few hours with an unusually high effusion rate (up to 640 m³/s, Fig. 40B). The cumulate volume of lava

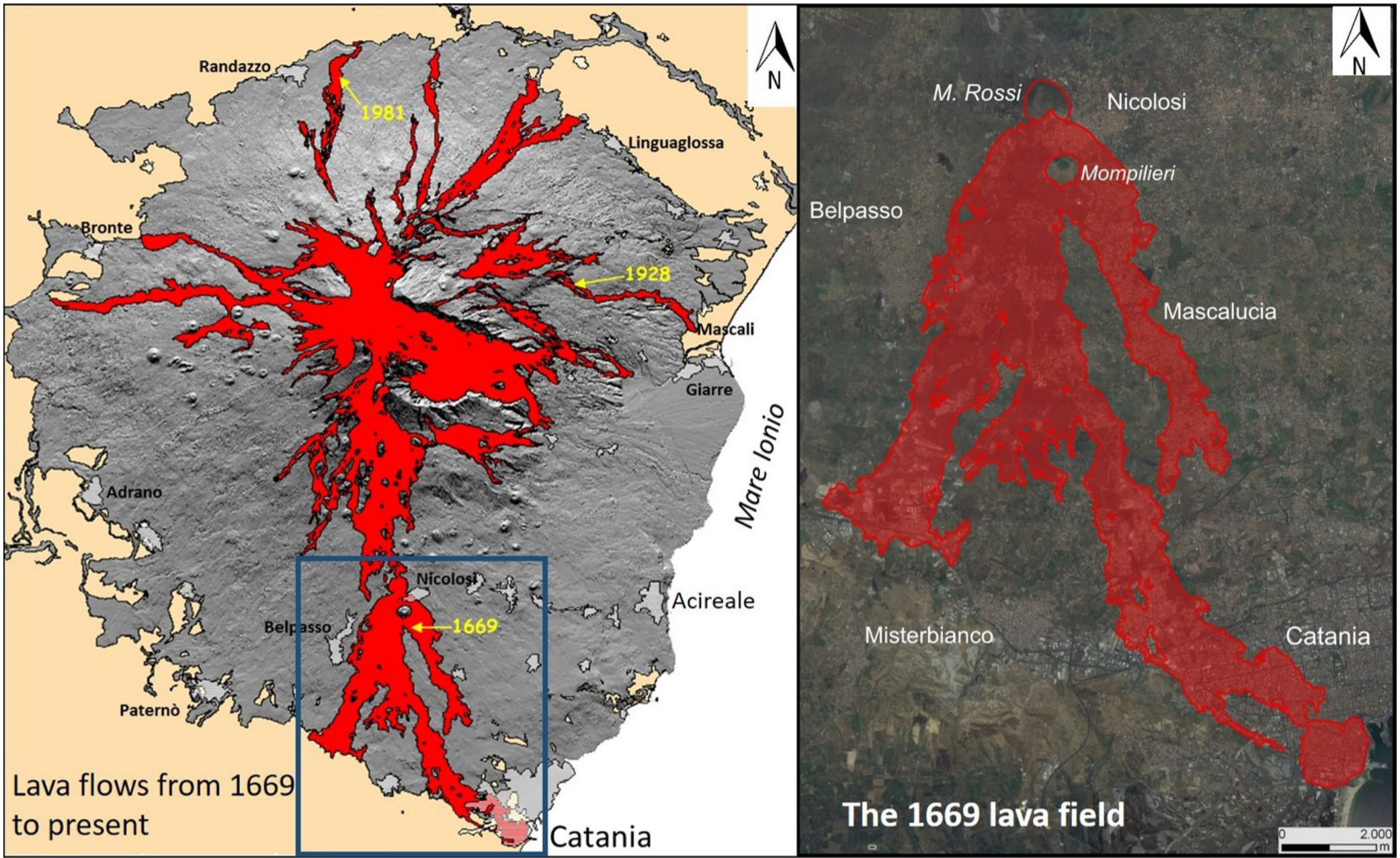


Fig. 38 – Areal distribution of the lava flow fields from 1669 to the present (left), and the wide 1669 lava flow (right) (from Branca et al., 2013).

<https://doi.org/10.3301/GFT.2018.02>

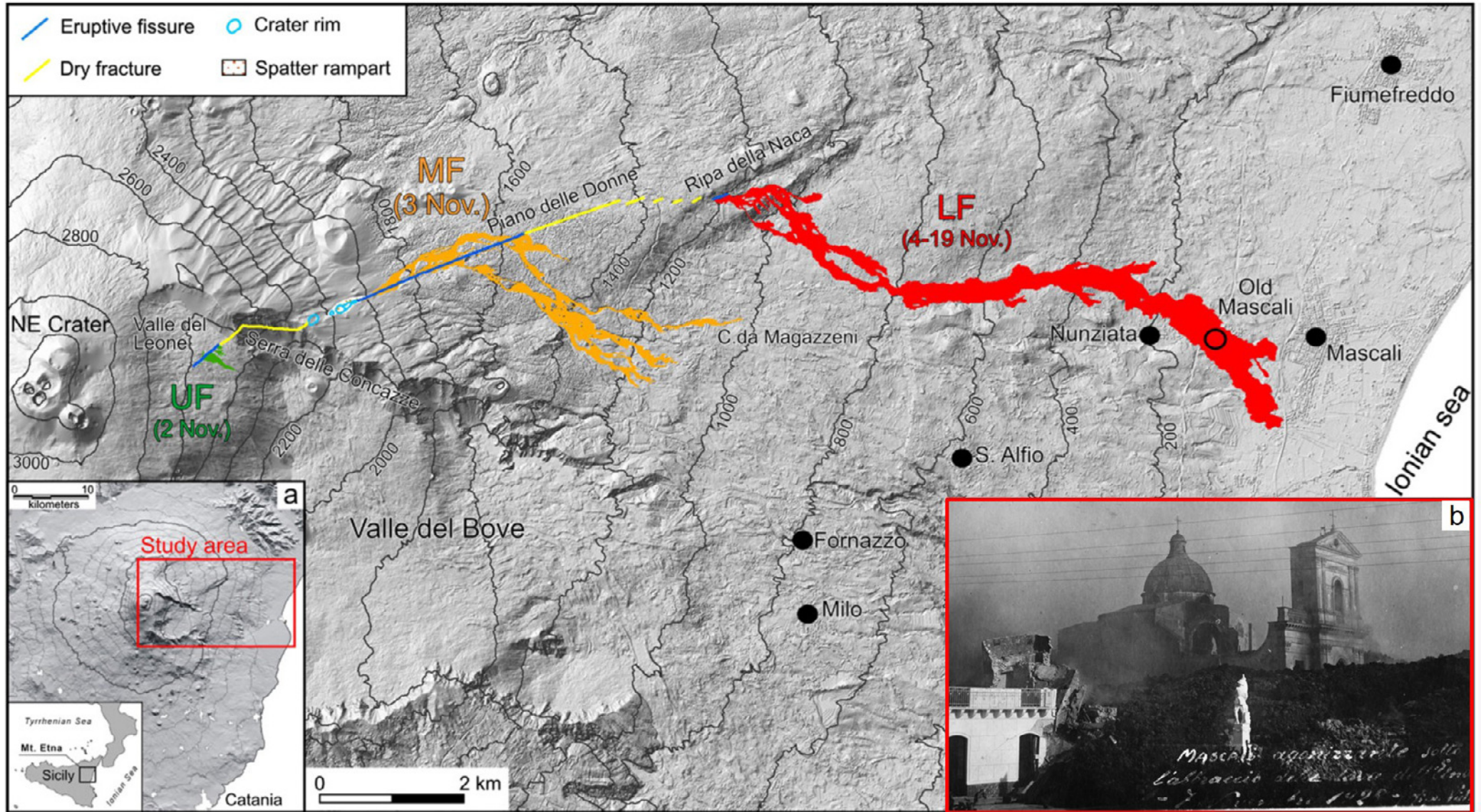


Fig. 39 - Map of the fissures and products of the 1928 eruption along the NE flank of Etna. The colored areas represent lavas produced from the lower (LF), middle (MF) and upper (UF) fissures (from Branca et al., 2017). a) Location of the study area within the Etna region. b) Photograph taken on 7th November, showing lava destroying the Mascali village (Photo courtesy of Archivio Fotografico Toscano of Prato).

<https://doi.org/10.3301/GFT.2018.02>



erupted was only 22.75 Mm^3 (Coltelli et al., 2012), with a final length of the lava flow of 10 km. Randazzo was not invaded by the lava only because the lower vent decreased its activity a few hours after the opening. This eruption highlights how the Etna's lower fissures, which often produce fast moving and dangerous lava flows, represent a less frequent but not rare event, which can threaten the inhabited areas representing a serious concern for their safety (Coltelli et al., 2012).

The Etna volcano, in spite of its predominant effusive activity, is characterized by many tephra deposits in its volcanic succession, which have revealed how the volcano has been also able to perform large explosive

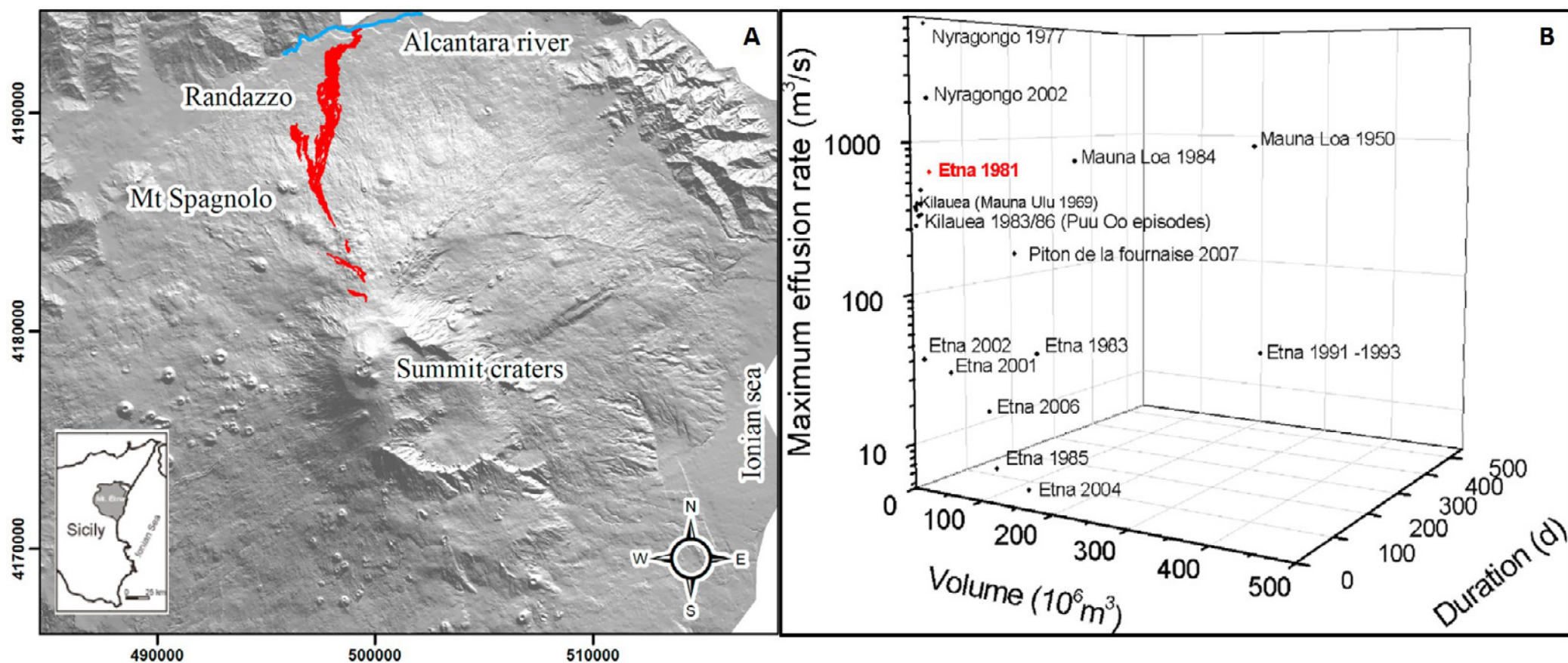


Fig. 40 - A) Map of the lava flow field of the 1981 eruption (Coltelli et al., 2012). B) Diagram comparing the duration, maximum effusion rate and volume of the 1981 eruption with those of the post-1971 eruptions of Etna and selected eruptions from other volcanoes (Coltelli et al., 2012).



eruptions (Coltelli et al., 1998, 2000, 2005). Pyroclastic deposits related to eruptions from more than 100 ka to the Present have been correlated over the whole volcanic edifice (Coltelli et al., 2000). Within this time interval, five main periods of explosive activity have been identified: a) >100 ka (Strombolian to Subplinian activity); b) ~100 ka (Plinian benmoreitic eruption); c) 80 to 19 ka (Strombolian to Subplinian events of basaltic to mugearitic magmas); d) 19-17 ka (Plinian benmoreitic eruptions forming the Ellittico caldera); e) <13 ka (basaltic and hawaiitic explosive activity ranging from Strombolian to Plinian). The last period includes the 3930 ± 60 ka BP Subplinian eruption of picritic basalts, and the 122 B.C. Plinian basaltic eruption, which represent two main marker beds for the Holocene stratigraphy of the volcano. The 3930 ka Subplinian eruption was fed by a picritic magma and produced a fallout deposit of 0.183 km³, widely dispersed eastwards (Coltelli et al., 2005; Fig. 41). The 122 B.C. eruption was the largest explosive eruption of the Mongibello volcano in Holocene times (Coltelli et al., 1998). Its eruptive vent was located on Etna's summit where it was associated to the formation of a large caldera named "Cratere del Piano". The column height has been estimated to 24-26 kms based on the features of the widespread pyroclastic scoria fall deposit recognized along the southeastern flank of Etna, with thickness ranging from 2 m on the summit area to 10 cm along the Catania coast (Fig. 41). This deposit caused roof collapses and huge damages to the ancient town of Catania as reported in Roman Age chronicles.

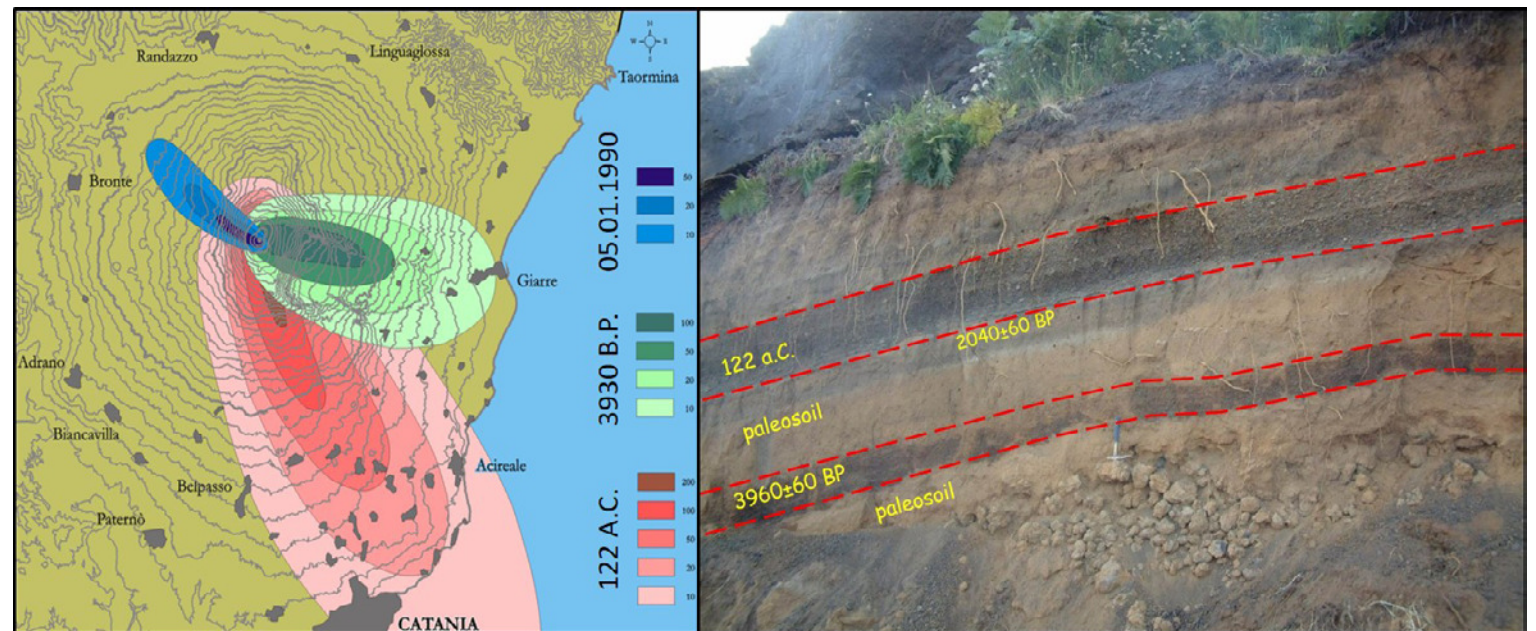
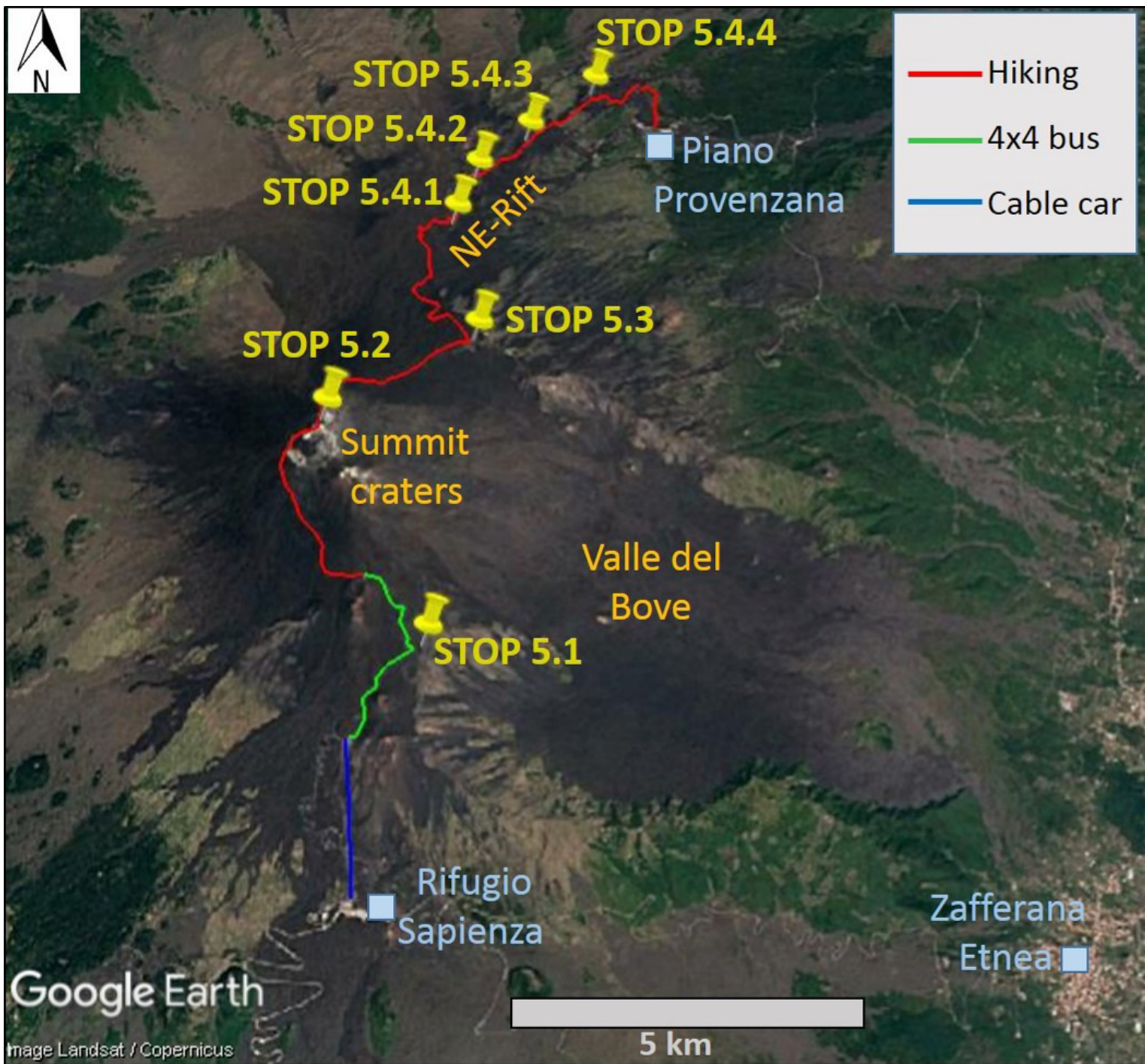


Fig. 41 – Isopach map (in centimeters) of the fall deposits produced during the 3930 ka Subplinian, 122 B.C. Plinian and 1990 fallout deposits (on the left; Coltelli et al., 1998; Coltelli et al., 2005; Scollo et al., 2013). On the right, a stratigraphic section in the surroundings of Mt. Solfizio along the southern flank of Etna at 1800 m asl, showing the 3930 ka and 122 B.C. fall deposits (photo by M. Coltelli).



DAY 5th: field itinerary to the summit craters of Etna and the NE-Rift volcanic system

The Etna field itinerary is focused on the main features of the volcano, including the Valle del Bove collapse depression, the summit craters and Ellittico caldera and the NE-rift volcanic system. The itinerary initially runs along the southern flank of the volcano (Fig. 42), starting from the Rifugio Sapienza ski area (1900 m asl). By cable car, the spectacular Belvedere viewpoint at 2650 m asl is reached, providing an impressive view of the Valle del Bove depression from its western rim. Then, by

Fig. 42 - Field itinerary and stop points of the 5th day on Etna volcano merged on a Google Earth map.



means of 4x4 bus we will ascend to an elevation of 2900 m asl, from where the footpath to the Etna summit craters (3300 m a.s.l.) starts. The second part of the itinerary is along the northern flank of the volcano, starting from a viewpoint of the remnants of the Ellittico caldera, and continuing through the NE-Rift zone, where it can be observed the upper, middle and lower segment of the 2002 eruptive fissure and the vents of the 1809 eruption, before reaching the Piano Provenzana ski area (1800 m asl).

The sixth day is devoted to the Osservatorio Etneo, which is the Catania Section of INGV, where the seismic and volcanic monitoring of Etna and other active volcanoes in Sicily is developed.

STOP 5.1: (37°43'41"N, 15°00'34"E)

Locality: "Belvedere" area, elevation of 2650 m asl (western rim of Valle del Bove).

Focus: Valle del Bove collapse depression, volcanic dikes, lava flow fields of 1991-1993, 2011-2017, 1763, and 2001 and 2002-2003 scoria cones.

Description: Valle del Bove is a 7x5 wide, horseshoe-shaped morphostructural depression located along the eastern flank of Etna, with up to 1000 m high sub-vertical walls (Fig. 43). It is the result of lateral collapses affecting the eastern flank of the volcano since 9-10 ka ago, not directly associated to eruptive activity (Calvari et al., 2004). At the mouth



1991-1993
lava field

Fig. 43 - Panoramic view of the impressive Valle del Bove collapse depression from its western rim. On the right, it can be recognized the (darker) 1991-93 lava flow field filling the southern portion of the depression.

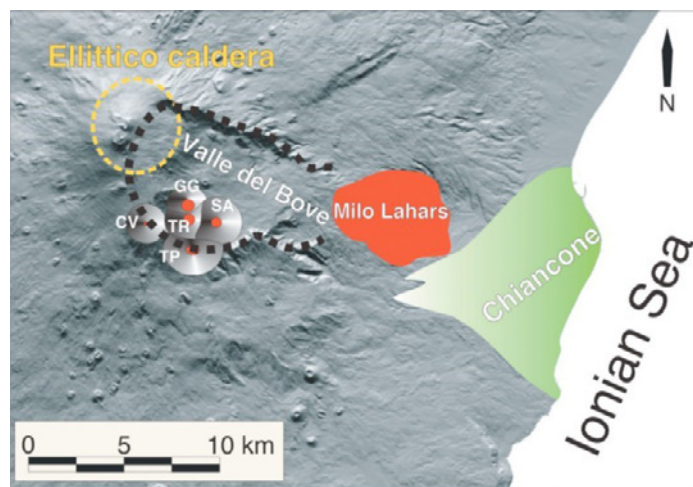


Fig. 44 - Sketch map of the summit and eastern flank of Etna showing the Valle del Bove outline (black dotted line) related to the Ellittico caldera (yellow), the Milo Lahars (red) and the Chiancone deposits (green). The position of the older volcanoes related to the Valle del Bove eruptive phase is also shown: TR = Trifoglietto; GG = Giannicola Grande; SA = Salifizio; CV = Cuvigghiuni; TP = Tripodo (Calvari et al., 2004).

of Valle del Bove the debris avalanche deposit related to the collapses (Milo lahars or Milo member, Calvari et al., 1998) crops out, whereas its fluvial reworking counterpart constitutes the Chiancone member, a fan-shaped volcanoclastic deposit extending along the coast (Calvari and Groppelli, 1996) and offshore (Bousquet et al., 1998; Del Negro and Napoli, 2002; Chiocci et al., 2011) (Fig. 44).

Along the Valle del Bove collapse walls, lava flows, tephra layers and dikes (Fig. 45A) belonging to the ancient volcanic centres preceding the present Etna volcano (Mongibello) are well exposed, putting in evidence spectacular stratigraphic relationships and angular to erosional unconformities (Fig. 45B). Along the northern wall of Valle del Bove, the

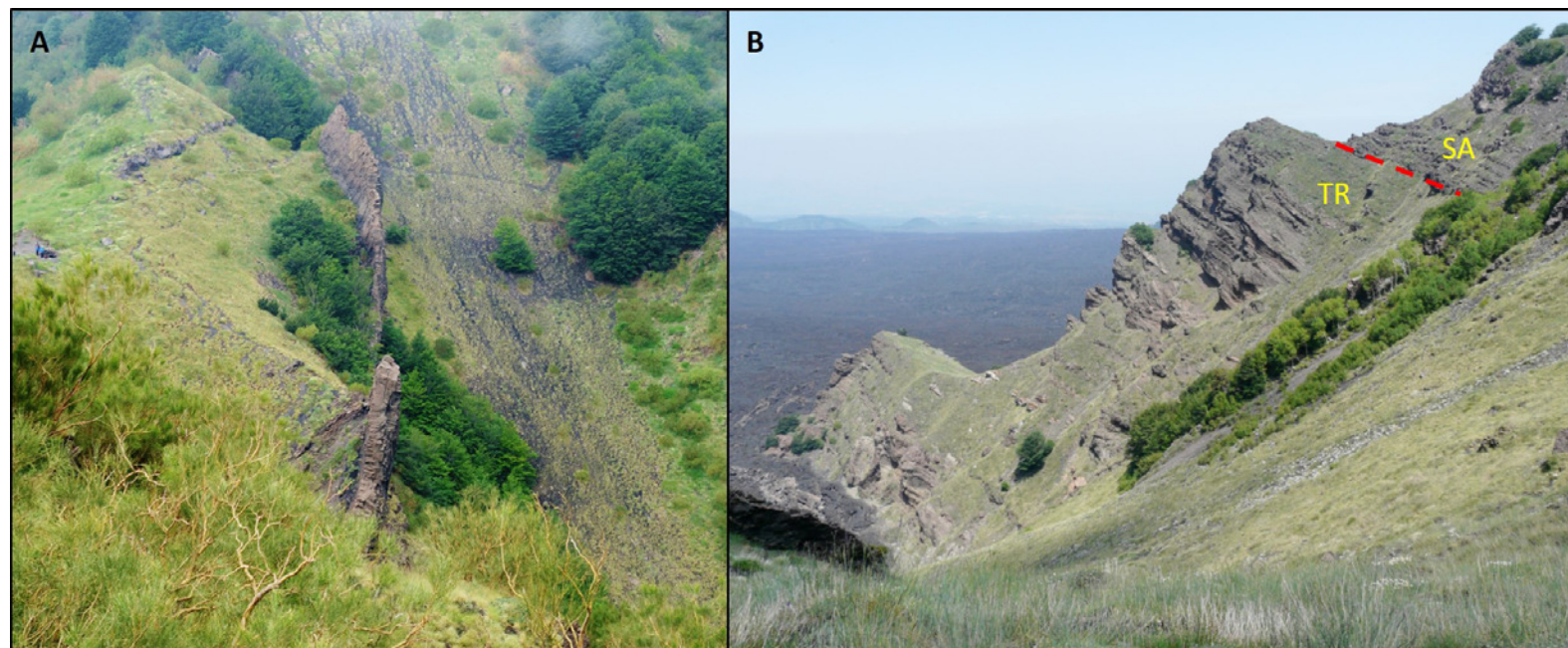


Fig. 45 - A) View of the magnificent dikes cutting the Valle del Bove southern wall (photo by M. Catania) B) Panoramic view of the Valle del Bove southern collapse wall near the saddle of Serra dell'Acqua showing an angular unconformity between the Trifoglietto volcano (TR) and the younger Salifizio volcano (SA) associated to quiescence and a slight shifting of feeding system.



remnants of the Ellittico volcano crop out, whereas along the western and southern walls the deposits related to the Trifoglietto, Salifizio, Giannicola and Cuvigghiuni volcanoes are exposed (Branca et al., 2011a,b). The Valle del Bove collapse depression represents the preferred area where most of the historical lava flows has streamed and piled up. From this viewpoint, the 1991-1993 (Figs. 43, 46A) and 2011-2017 lava flow fields are well recognizable, because of their darker color in comparison with the surrounding older lava flows. The 1991-1993 eruption occurred from December 1991 to March 1993 from an eruptive fissure located below the stop point, between 2400-2200 m asl, and represents the largest effusive eruption since 1669. It produced a final volume of $235 \times 10^6 \text{ m}^3$ of lava, covering an area of 7.6 km^2 from the source down to Piano dell'Acqua (only one km far from the Zafferana Etnea village), having travelled for more than 8 km (Calvari et al., 1994). During this eruption, a

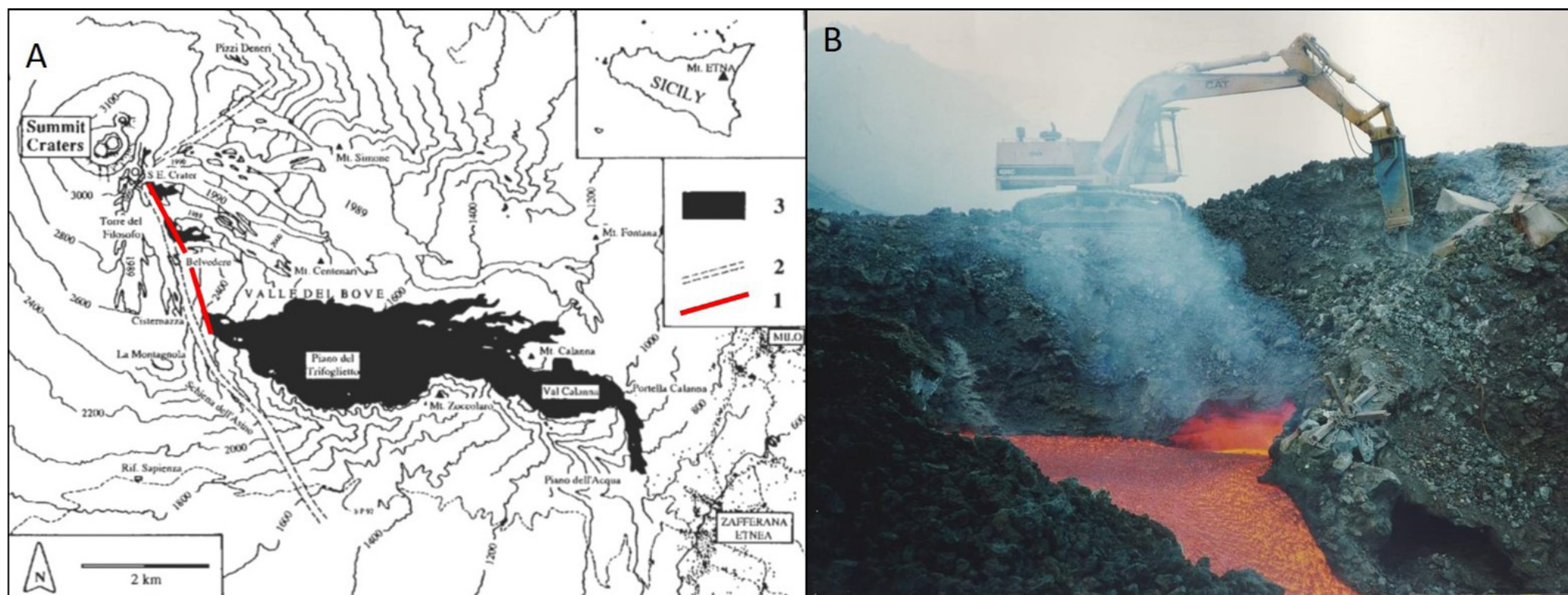


Fig. 46 – A) Schematic map of the 1991-1993 lava flow field (3) with the corresponding eruptive fissures (1) almost parallel to the ones (2) feeding the 1989 eruption (modified from Calvari et al., 1994). B) Photograph showing the attempt of diversion of a lava flow in Valle del Bove during the 1991-1993 eruption.



man-made diversion of the natural flow from its lava tube was performed (Fig. 46B). Southwestward from the stop point, it is possible to observe the La Montagnola cinder cone (1763 eruption), the 2001 upper cone, the two coalescent scoria cones of the 2002-2003 eruption and the Cisternazza pit crater related to the same 1763 eruption, all located along the S-Rift volcanic system. The 2001 flank eruption caused significant damage to tourist facilities and for several days threatened the town of Nicolosi on the southern flank of Etna. This eruption was characterized by a highly dynamic evolution with a complex interaction between different eruptive fissures, changing eruptive styles and contemporaneous summit and eccentric activity (Behncke and Neri, 2003) (Fig. 47). Seven eruptive fissures were active, five located on the S flank between 3050 and 2100 m asl (Fig. 48A), and two on the NE flank between 3080 and 2600 m asl. All of them emitted lava flows, the most voluminous of which reached a length of 7 km. The 2570 m vent produced a vigorous phreatomagmatic activity as the dike cut through a shallow aquifer. The total volume of the eruption was estimated in $\sim 25 \times 10^6 \text{ m}^3$ of lava and $5\text{--}10 \times 10^6 \text{ m}^3$ of pyroclastics (Behncke and Neri, 2003). The 2002-2003 eruption was characterized by an extraordinary and continuous explosive activity with abundant ash emission, which caused damage to agriculture, housing and the local economy and reached the coasts of Greece and Libya (Fig. 48B), and discontinuous lava flow output. The eruption involved the opening of eruptive fissures on both the NE and S flanks of the volcano (Fig. 48A). Magma erupted from the S fissure was the relatively undegassed, volatile-rich, buoyant fraction which drained the deep feeding system bypassing the central conduits, as typical for the Etna eccentric

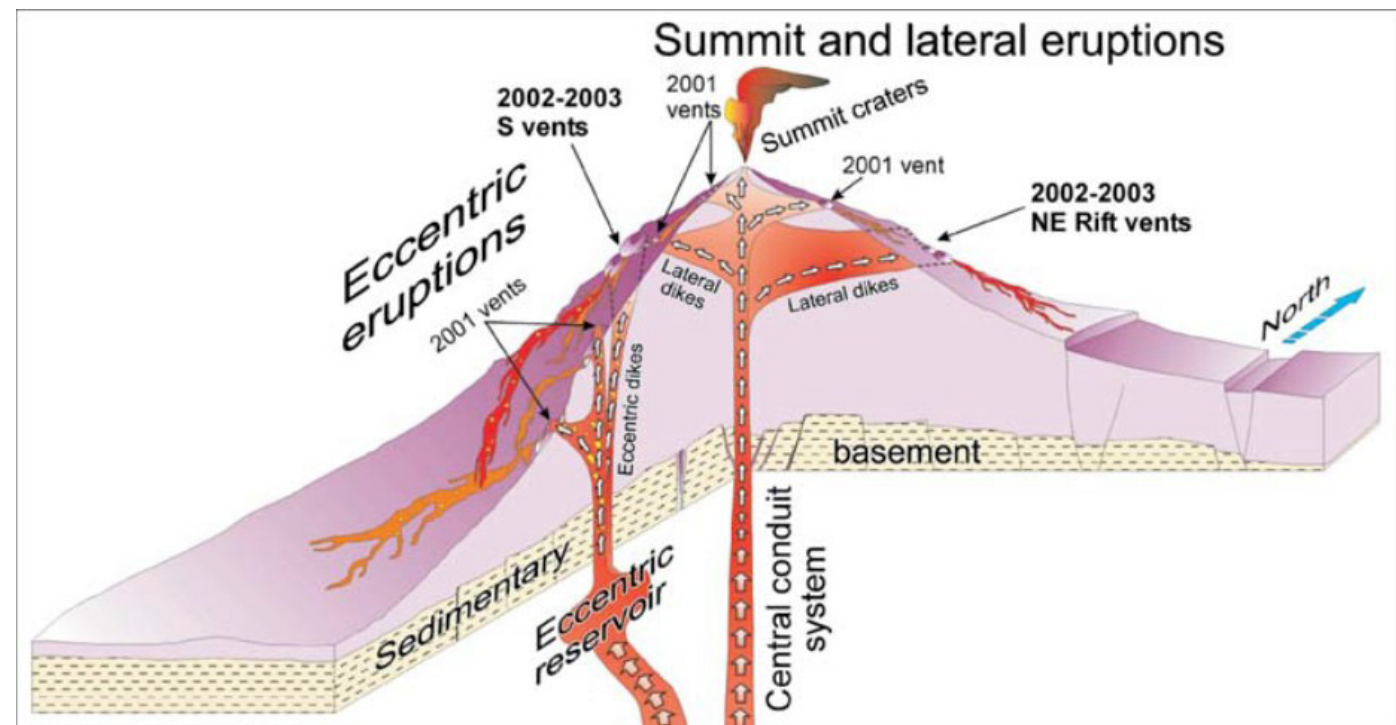


Fig. 47 - Schematic diagram of the magma feeding system feeding the 2001 and 2002-03 eruptions (Behncke and Neri, 2003; Andronico et al., 2005).

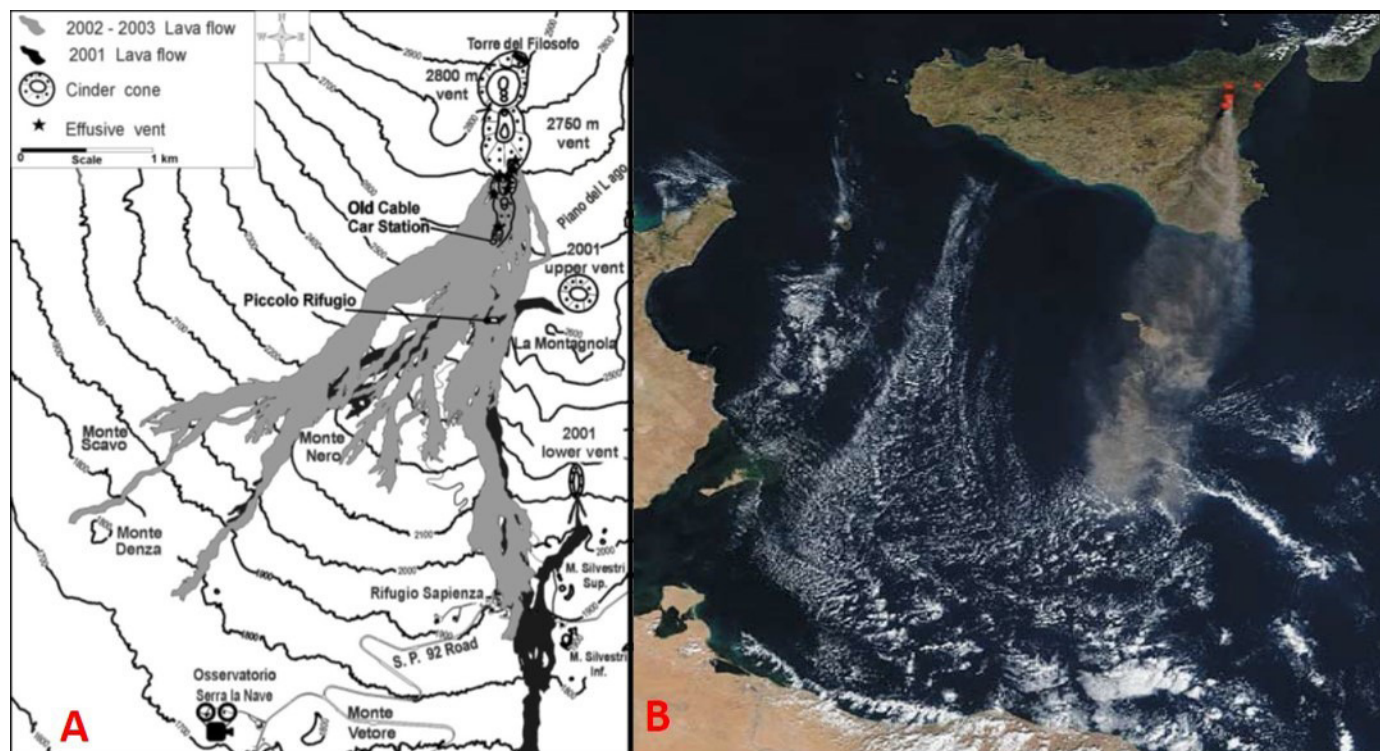


Fig. 48 – A) Schematic map of the 2001 and 2002–2003 lava flow fields along the southern flank of Etna, with location of their effusive vents (from Andronico et al., 2005). B) Volcanic plume formed on 27 October 2002 (satellite image by MODIS Rapid Response Team at NASA GSFC Goddard Space Flight Center).

STOP 5.2: (37°45'09"N, 14°59'45"E)

Locality: Summit craters (3300 m asl).

Focus: Summit eruptive activity and "Cratere del Piano" caldera.

Description: The summit area of Etna is currently characterized by four craters: Voragine, Bocca Nuova, Northeast Crater and Southeast Crater (Fig. 49A). This crater configuration contrasts strongly with that of one century ago, when at the summit there was only a 250 m high cone with a 500 m large diameter, called "Central Crater". Historical records indicate that this cone formed in about one century of activity following the collapse of the preceding summit cone during the catastrophic 1669 eruption.

eruptions (Andronico et al., 2005). The 2001 and 2002-2003 eruptions have demonstrated that significant amounts of pyroclastic rocks (ash, lapilli, bombs and blocks) can be also generated by flank eruptive activity. Differently from the commonly short-lived summit paroxysms, pyroclastic fallout during flank eruptions can go on for weeks or even months, and impact life in the populated areas, representing a serious threat for traffic both on the ground and in the air.

Points-for-discussion

- Recent lava flow fields
- Summit, lateral and eccentric eruptive activity and shiftings of feeding system

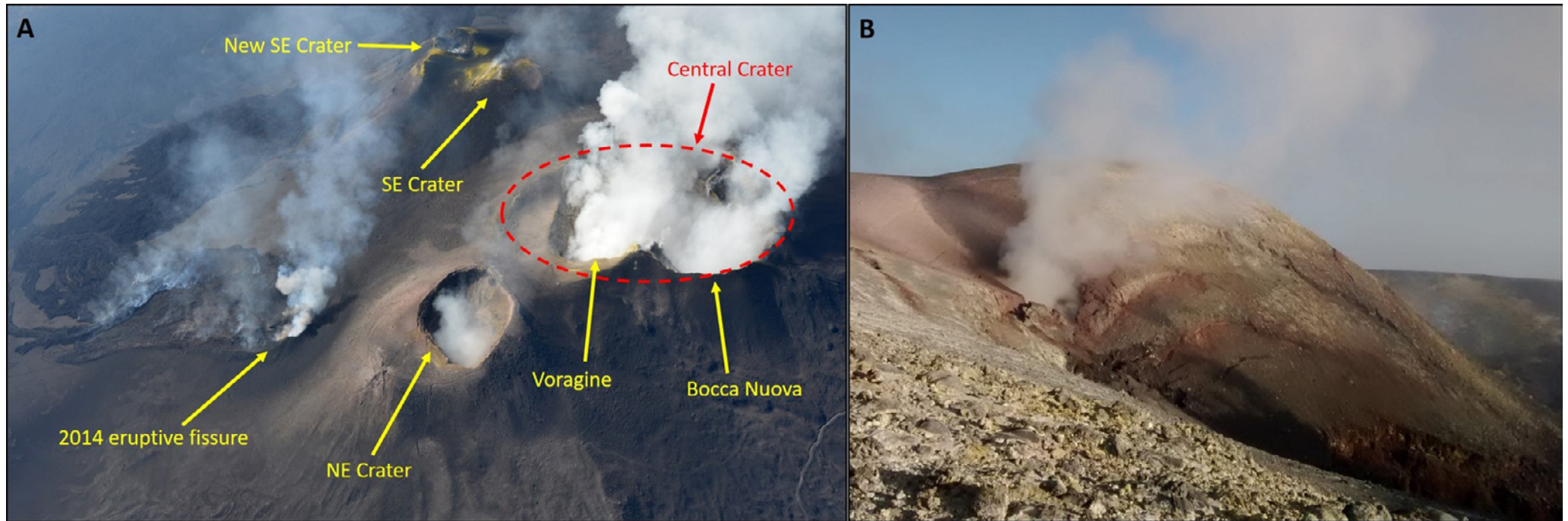


Fig. 49 – A) Helicopter view of the summit craters during the 2014 eruption (photo by M. Coltelli). B) Outgassing vent along the border of the Voragine crater (photo by D. Cavallaro).

The NE Crater, born in 1911, currently represents the highest point (3330 m asl) of Etna volcano. Its growth was accompanied by voluminous outflows of lava and repeated collapses throughout the 1950s. Vigorous growth phases of the cone occurred from 1966 to 1971 and from 1974 to 1977, two eruptive periods characterized by Strombolian activity and slow lava effusion, mostly from vents on the flanks or at the base of the growing pyroclastic cone. In 1977-1978 and 1980-1981, the crater changed its behavior, producing a series of short-lived violent explosive eruptions with high lava fountains and voluminous lava flows extending few kms downslope. The most violent eruption occurred in 1986 and ended with the partial destruction of the cone. Other series of paroxysmal eruptions with high lava fountains occurred in 1995-1996, producing a partial filling of the crater with subsequent collapses of portions of the cone. During the May 2016 eruption the crater largely collapsed. Actually, it is characterized by an intense and almost continuous steam activity.



The Voragine is a funnel-shaped crater formed in 1945 in the NE sector of the previous "Central Crater" at the end of a 15-years long and strong explosive activity alternated with gravitational collapses. During the following decades the crater gradually enlarged by collapse and/or explosive activity. A powerful explosive eruption occurred in July 1960, and produced heavy tephra fall (its volume was estimated at $10 \times 10^6 \text{ m}^3$) causing forest fires and considerable damage to agricultural land especially on the NE side of the volcano. Since its growth, collapses have alternated with the partial infilling of the crater. In a few cases (e.g. in 1980) magma rose within the Voragine crater almost to its border. A remarkable series of four paroxysmal events occurred in December 2015, one of which produced a "pine"-like plume higher than 14 km. After the last eruptive activity occurred in May 2016, it has been characterized by an intense and almost continuous steam activity from a degassing vent located in the eastern portion of the crater (Fig. 49B).

The Bocca Nuova is a 250x300 m wide and about 100 m deep crater, born in 1968 as a small "pit crater" of the main Voragine crater, and then enlarged by numerous collapses and explosive episodes during the next decades until the present structure. During the '70s, it was the most active among the summit craters, generating strong Strombolian events throwing large bombs out of the rim. The last important eruption occurred in 1999 when, accompanied by an intense Strombolian phase, a series of lava overflows from the western rim of the crater extended until the middle western slopes of the volcano down to 1750 m asl. From the beginning of the 21st century, it has been characterized by two main degassing vents.

The SE Crater is the youngest among the summit craters, born in 1971 as a "pit crater", while its eruptive activity started in 1978. In the last 20 years it has been the most active among the four craters, producing paroxysmal events characterized by Strombolian activity with episodic lava fountains, sometimes associated with lava overflows, over periods lasting from a few weeks to months. During its growth, several periods of activity have been observed (Andronico and Corsaro, 2011): 1989 (16 lava fountains), 1998–99 (22), 2000 (64), 2001 (15), 2006–2007 (24). More recently, the activity of the SE Crater moved along its eastern flank, with the formation in 2010 of a "pit crater". During the next years, this new edifice evolved and formed a new crater called New SE Crater that produced 45 paroxysmal events between 2011 and 2013, often characterized by few kms high eruptive columns. These caused the fallout of pyroclastic rocks (from ash to lapilli) down to the coast creating copious damage to the agriculture and the closure of Catania airport for several days. In the last 5 years, it has produced some explosive eruptions associated with lava overflows, the last one in April 2017. The four summit craters are characterized by a nearly continuous plume emission constituted by SO_2 (up to 25 t/d and about 2 Mt/y), HC1 and HF and CO_2 (Allard et al., 1991; Francis et al., 1998; Caltabiano et al., 2004).



The crater rims are affected by an intense fumarole activity with conspicuous presence of yellowish sulphur sublimation deposits. Two types of fumaroles are identified: (i) low-temperature fumaroles dominated by CO_2 with minor amounts of SO_2 and H_2S , and negligible chlorine contents; (ii) high-temperature fumaroles strongly air-contaminated and characterized by appreciable amounts of volcanogenic carbon, sulfur and chlorine (Liotta et al., 2010). The fumarole fields of the summit area reflect the outgassing of fractures that are directly fed by different portions of the shallow plumbing system.

The whole summit area of Etna volcano rises above 2900 m asl and rests on a flattish area formed by the filling up of two almost concentric calderas (Fig. 50). The smaller and younger one is the "Cratere del Piano" caldera, whereas the larger and older one is the Ellittico caldera. The 2-km wide "Cratere del Piano" caldera was formed in association to the 122 B.C. Plinian eruption of basaltic composition (Coltelli et al., 1998), which represents the largest explosive eruption of Mongibello volcano in Holocene times. The buried rim of this caldera is morphologically recognizable between Torre del Filosofo and Punta Lucia at about 2900 m asl. The formation of this caldera caused the disruption of the older Ellittico caldera southern rim. The eruptive activity of the past 2 ka produced the filling of the "Cratere del Piano" caldera, building the present Etna summit cone (Branca et al., 2011a, b).



Fig. 50 – Panoramic view of the northern flank of Etna volcano where the Ellittico caldera rim (dashed red line) can be recognized (Branca et al., 2011).



Points-for-discussion

- Features of the present-day eruptive and outgassing activity from the summit craters.
- Processes of caldera development.

STOP 5.3: (37°45'53"N, 15°01'02"E)

Locality: Piano delle Concazze (2800 m asl)

Focus: Ellittico caldera

Description: The northern rim of the Ellittico caldera is recognized near to Punta Lucia (2930 m asl) and Pizzi Deneri (2847 m asl), along the northern flank of Etna (Fig. 51). This caldera has been formed during a rather short eruptive period dated at 19-17 ka through five Plinian eruptions, and ended the activity of the Ellittico volcano (Coltelli et al., 2000; Del Carlo et al., 2017). A stratigraphic unit made up by layers of pumice lapilli

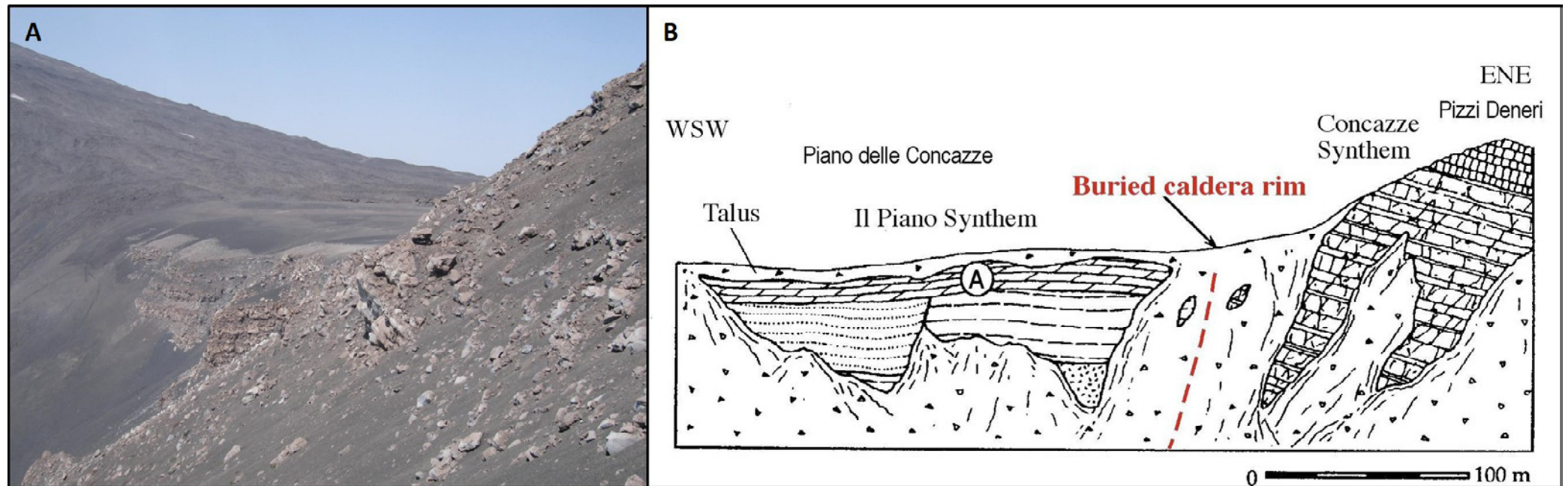


Fig. 51 – A) Panoramic view and schematic cross-section showing the Ellittico caldera NW rim and B) the corresponding angular unconformity in the area of Valle del Leone and Piano delle Concazze area (modified from Coltelli et al., 1994).



found in the northern and eastern sectors of the volcano indicates that the Ellittico caldera collapse could be related to a series of strong explosive eruptions, characterized by a repeated eruptive scenario like the following: 1) early Plinian eruptive column erupting the more silicic magma and producing widespread pumice fallout; 2) decreasing explosive intensity erupting less silicic magma and feeding lava fountains that produced thick spatter agglomerate deposits around the vent; 3) collapse of the thick hot spatter deposit along the steep slopes near the summit forming both block-and-ash flows and scoria pyroclastic flows that travelled down the flanks of the volcano; one of these eruptions formed the Biancavilla-Montalto ignimbrite deposits. The sub-horizontal lava flow units of the younger Mongibello volcano filled the Ellittico caldera collapse depression and onlap the older lava flows truncated by the collapse (Coltelli et al., 1994) (Fig. 51). The present morphostructural setting of this area is exposed by the flank collapse of Valle del Bove.

Points-for-discussion

- Processes of caldera developing
- Building up of the present Etna volcano

Stop 5.4.1: (37°46'52"N, 15°00'38"E)

Locality: NE-Rift

Focus: Morphostructural features and eruptive activity along the NE-Rift, and upper section of the 2002 eruption

Description: The NE-Rift is one of the main intrusion zones of the Etna volcano. It extends for about 7 km from the summit craters down to 1500 m asl, and consists of a network of N to NE-striking sub-parallel eruptive fissures closely spaced in an area about 1–2 km wide (Garduno et al. 1997; Andronico et al., 2005). These fissures have produced spatter ramparts and scoria cones during the last 15 ka. The eruptive events along the NE-Rift during the last 300 years have been characterized by short duration and comparable low volume of erupted lava (Branca and Del Carlo, 2003). The onsets of the eruptions are preceded by seismic sequences, marking the opening of several km-long fissure systems that develop from the summit craters down to the NE-Rift zone (e.g., in 1809, 1911, 1923, 1947 and 2002 eruptions).

The last eruption in the NE-Rift occurred in 2002. A seismic swarm with its epicentre in the summit area began on 26 October 2002. The day after a set of extensional fractures trending N-S (horizontal displacements between 10 and 50 cm), formed in the Piano delle Concazze area (2800 m asl). Subsequently, a N-S trending fissure at the base of the NE Crater (3000 m asl) produced a short-lived explosive event. The downslope propagation of

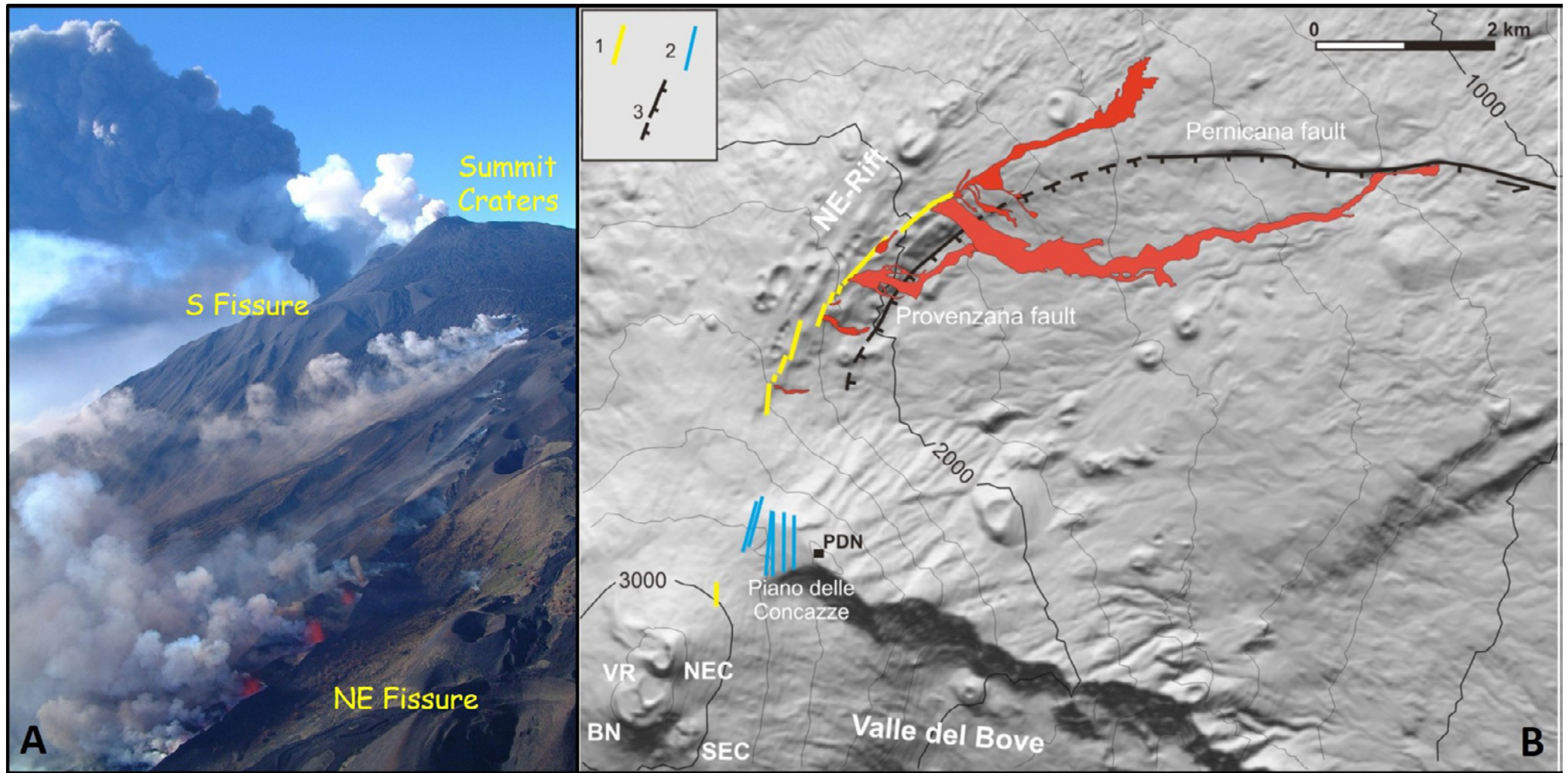


Fig. 52 – A) Helicopter view of the 2002 eruptive fissure along the NE-Rift. In the background the contemporaneous activity on the southern flank is visible. B) Map showing the fissure system and the lava flow of the 2002 eruption (Branca et al., 2003). Symbols: VR = Voragine; BN = Bocca Nuova; NEC = NE Crater; SEC = SE Crater. Inset Legend: 1, eruptive fissure; 2, dry fractures; 3, fault (the arrow indicates lateral slip movement).

the dike was marked by the opening of an eruptive fissure system at 2470 m asl. It extended along the eastern border of the NE-Rift, covering a distance of 3.5 km until 1900 m asl. The upper portion of the NE rift (2470–2150 m asl) consists of a set of dry and eruptive fissures (Fig. 52A), striking from N5°E to N20°E in a right



en-echelon arrangement, producing both explosive and effusive activity. These segments are characterized by a series of spatter ramparts and pit craters in which the volcanic succession of the rift is exposed (Branca et al., 2003) (Fig. 52B).

Stop 5.4.2: (37°47'15"N, 15°00'43"E)

Locality: NE-Rift (2350 m asl)

Focus: The 1809 eruptive fissure

Description: The 1809 eruption, well-described by Geshi and Neri (2014), was one of the major flank eruptions of Etna during the 19th Century. It was characterized by earthquake swarms, exceptionally long and fast-propagating eruptive fissures and highly fed lava flows. A NNE-aligned eruptive fissure opened along the northern side of the former "Central Crater" (3200 m asl) and rapidly propagated for about 4 km downward until 2300 m asl producing a 5 km long lava flow. During the days after the fracture propagated westward and then downward, reaching 1400 m asl and generating several eruptive and explosive vents, and a 5.5 km long lava flow, which stopped at 670 m asl (Fig. 53A). Along the lower fracture, some pit craters formed as a consequence of hydromagmatic explosive activity and allowed to closely observe the internal structure of the shallow feeder system of an effusive vent related to the early stage of the eruption (Fig. 53B). The feeder dike in its lower part shows evidence of temporal arrest and rupturing at the base of the layers of host rock before the dike opened to the surface. After the feeder dike reached the surface, an oblique lava fountain formed an asymmetric scoria

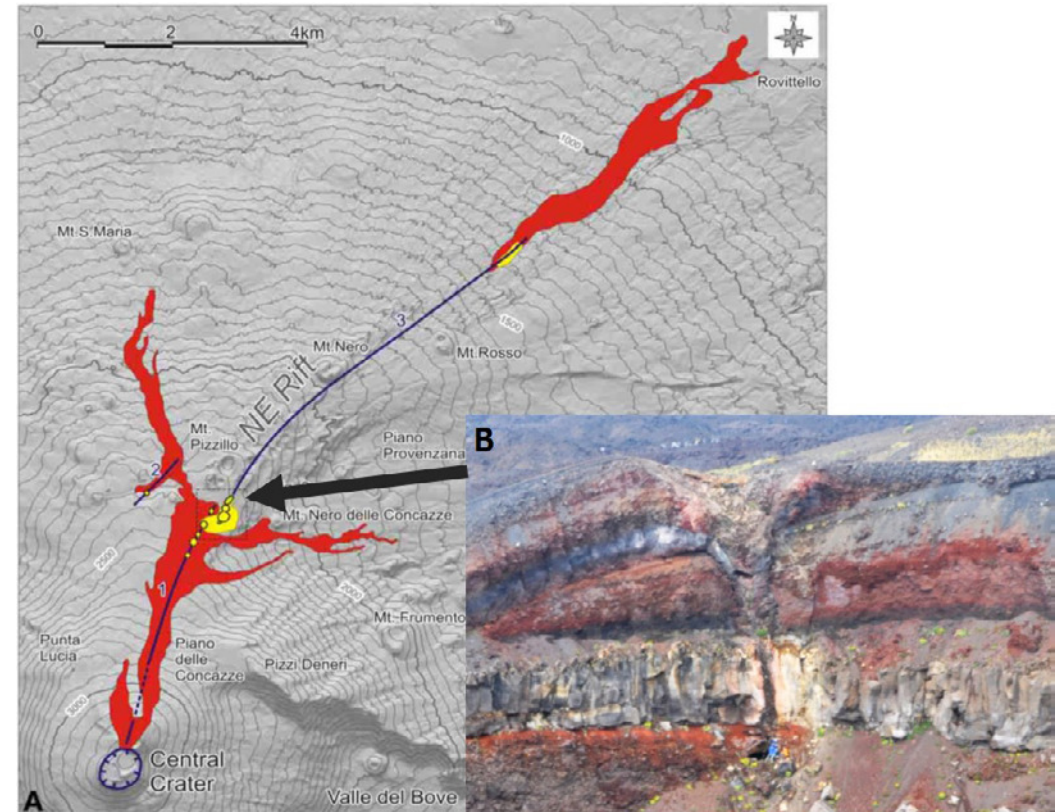


Fig. 53 – A) Map of the 1809 eruption along the NE-Rift (from Geshi and Neri, 2014). Eruptive fissures, numbered 1 to 3 from the top to the bottom according to the chronology of opening, are in blue. Yellow areas highlight the main cinder cones and explosive vents. B) Outcrop photograph showing a natural cross section of the feeder dike and vent of the 1809 eruption, exposed in the wall of a pit crater related to the later stage of the eruption.



cone. The eruption style shifted to a more violent hydromagmatic eruption as the propagation of the eruptive fissure to the lower NE-Rift withdrew magma from the upper portion of the rift zone. Drop of the excess magmatic pressure within the upper portion of the fissure conduit caused to entrain external groundwater into the system.

Stop 5.4.3: (37°47'37"N - 15°01'09"E)

Locality: NE-Rift (2200 m asl)

Focus: Middle sector of the 2002 eruptive fissure.

Description: Along the NE-Rift several explosive vents related to the 2002 eruptive fissure are visible. Among them, some are very deep pit craters, along the walls of which it is possible to observe the feeder dike (Fig. 54).

Stop 5.4.4: (37°48'03"N, 15°01'44"E)

Locality: NE-Rift (2000 m asl)

Focus: Lower segment of the 2002 eruptive fissure.

Description: The lower segment (2030-1900 m asl) of the 2002 fissure along the NE-Rift is characterized by a series of coalescent scoria cones forming two main segments striking from N40°E to N60°E in a right en-echelon arrangement. The scoria cones show breaching in correspondence of the main lava flow outpouring. Overall, about $10 \times 10^6 \text{ m}^3$ of lava were emitted during the 9 days of the eruption, forming two narrow lava flow fields, 2.8 and 6.2 km-long (Andronico et al., 2005), partially covering the Piano

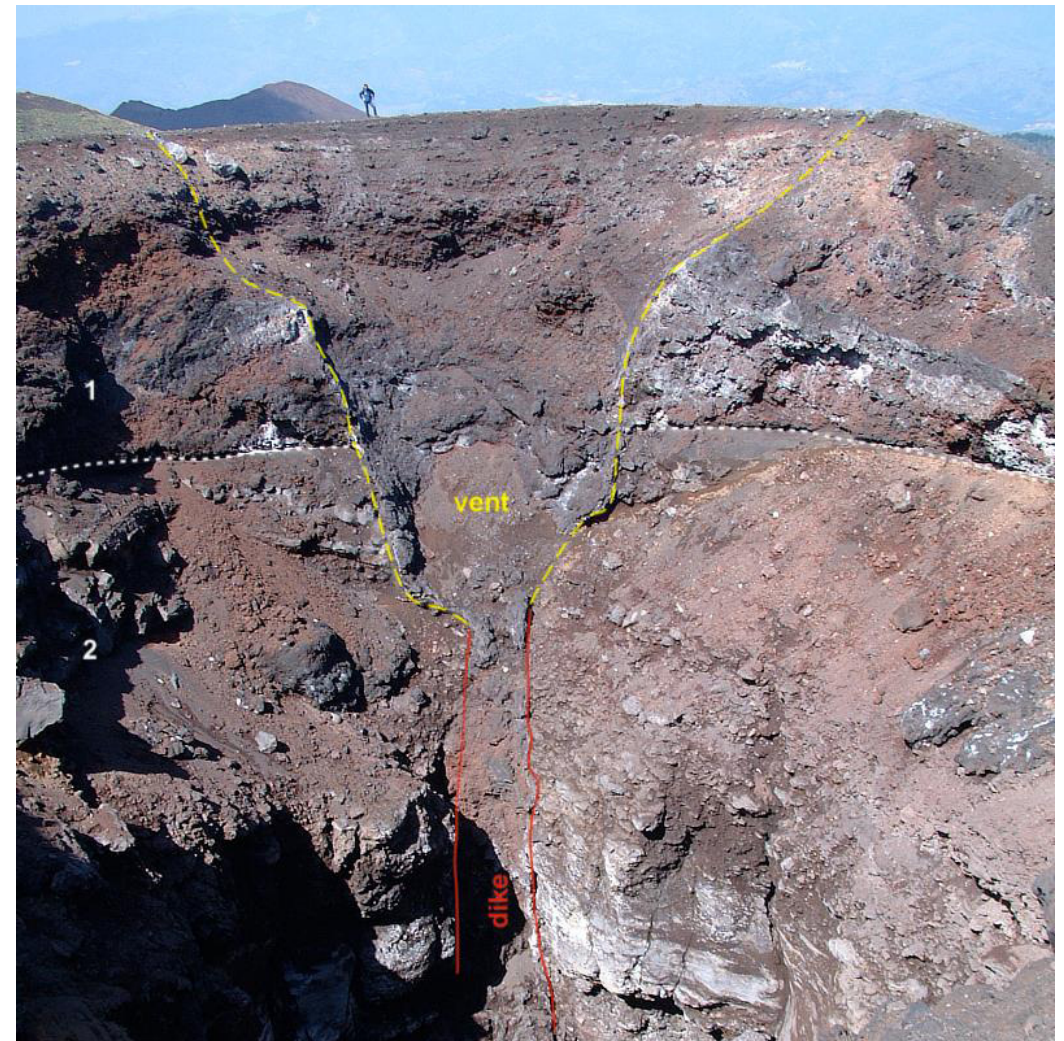


Fig. 54 – Natural section of an explosive vent of the 2002 eruption along the NE-Rift, which is exposed along the inner walls of a pit crater. The yellow dashed lines marks the shape of the explosive vent, while the white dotted lines mark the base of the scoria cone. The feeder dike (red solid line) is 3-4 m wide. The 2002 pyroclastic deposit (1), about 16 m thick, made of welded reddish scoriaceous bombs cover the pre-historic volcanics of the NE-Rift (2) (Branca et al., 2003).



Provenzana ski area infrastructure (Fig. 55). Magma erupted from the eruptive fissure represented the partially degassed magma fraction normally residing within the central conduits and the shallow plumbing system (Andronico et al., 2005).

Points-for-discussion

- Flank eruptive activity
- Migration of magma in the rift zones and propagation of eruptive fissures

Fig. 55 - Lower segment of the 2002 eruptive fissure along the NE-Rift. In the background, the ash column emitted from the simultaneous activity in the southern flank is visible.

DAY 6th: Osservatorio Etneo

STOP 6.1: (37°30'49"N, 15°04'56"E)

Locality: Osservatorio Etneo, Catania Section of INGV

Focus: Monitoring of Italian active volcanoes

Description: The seismic and volcanic monitoring of the Italian territory is one the main tasks of the INGV, for natural disasters prevention and management. This objective has a high priority in Sicily, where the peculiarity of the geodynamic context, characterized by a high seismic and volcanic hazard, amplifies the need to provide adequate and up-to-date surveillance of these natural phenomena. In order to cope with this activity it is essential to have adequate monitoring networks of volcanic and seismically active areas, with instruments operating in real-time that allow the prompt knowing of phenomena in progress. The surveillance of the active volcanic areas of Sicily (Etna, Stromboli and Vulcano) aims to:

- understand through accurate studies the volcanic events of the past and their eruptive mechanisms;
- acquire data from monitoring systems (permanent sensor networks as well as periodic measurement campaigns) aimed at identifying any phenomena that significantly change the state of volcano activity;
- use computer codes to process the acquired data in real-time, refine these results offline, and then use in numerical models of the processes of intrusion, ascent and eruption of magmas, to predict the possible evolution of in progress phenomena.

The Control Room of Osservatorio Etneo, Catania Section of INGV, is managed by two staff units working in 24/7 surveillance shifts, assisted by an expert volcanologist always on call; data are acquired in real-time, automatically pre-processed and displayed on dedicated monitors (Fig. 56A). The staff on duty controls the main parameters of volcanic activity in the areas of competence, recorded by the continuous monitoring networks. All significant changes are promptly communicated to the competent national and local offices of the Italian Civil Protection.

The monitoring system consists of a multi-parameter network of geophysical and geochemical sensors that transmit the acquired data (seismic, infrasonic, ground deformation, gravimetric and magnetic signals, and gas composition) through different transmission systems (satellite, radio, microwave and wireless bridges). These signals, suitably treated, are displayed on monitors with different processing levels. In addition, a permanent video surveillance system, carried out by means of cameras operating in both visible and thermal bands

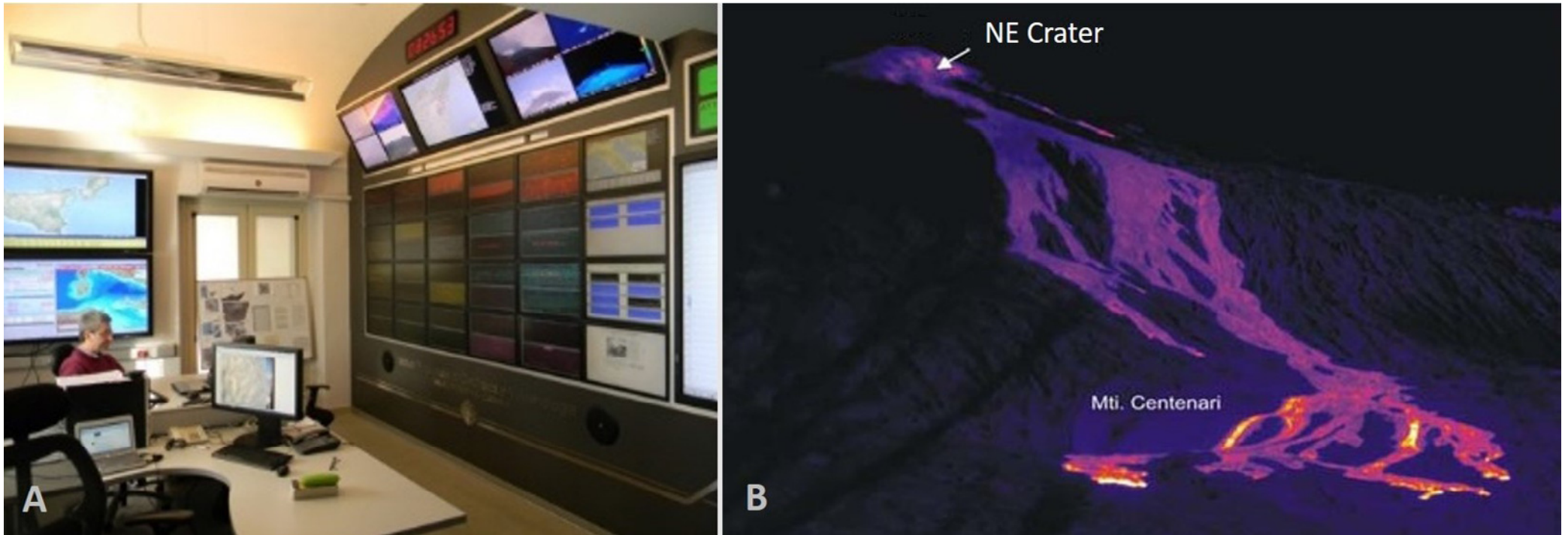


Fig. 56 – A) Control Room of the Osservatorio Etneo of INGV in Catania. B) Example of a thermal camera image showing a lava flow field erupted from the NE crater and flowing along the western wall of Valle del Bove.

(Fig. 56B), allows to check the state of the volcanic vents of Etna, Stromboli and Vulcano, and to record the images of the ongoing eruptive phenomena. Moreover, the Osservatorio Etneo of INGV carries out surveillance activities by monitoring and forecasting the dispersion of volcanic ash clouds in coordination with the Volcanic Ash Advisor Center in Toulouse, the Meteorological Watch Office of the Italian Air Force and the Air-traffic Control Centre of ENAV S.p.A. (the last two are national centers in charge of issuing security notices for air navigation: NOTAM and SIGMET) and the airports near Etna volcano (Catania International Airport; Reggio Calabria and Comiso regional airports). According to the ICAO Doc 9766-AN968 Handbook on the International Aircraft Volcano Watch (IAVW) and the ENAC Meteorology for Air Navigation, Osservatorio Etneo of INGV is endowed for the monitoring of the volcanic phenomena of Etna, Stromboli and Vulcano. To comply with this task, in addition to the aforementioned surveillance systems, new tools have been developed for observation of volcanic plumes such as Lidar and Radar. The acquired dataset allows to report, by means of VONA (Volcano



Observatory Notices for Aviation) messages, any eruptive event that may cause disturbance or damage to airplanes passing through the central Mediterranean airspace to the abovementioned aeronautical operators involved in the control and safety of air traffic and airport operations.

Points-for-discussion

- Volcano monitoring and surveillance
- Volcanic ash and aviation safety

Acknowledgements

The Authors are grateful to Andrea Zanchi (editor in chief) and Guido Giordano (associate editor) for their kind and careful handling of the manuscript. Paola Donato and Claudio Tranne are also thanked for their constructive reviews.

List of References

- Aiuppa A., Allard P., D'Alessandro W., Michel A., Parello F., Treuil M., Valenza M. (2000) - Mobility and fluxes of major, minor and trace metals during basalt weathering and groundwater transport at Mt. Etna volcano (Sicily). *Geochim. Cosmochim. Acta*, 64, 1827-1841.
- Allard P., Carbonnelle J., Dajlevic D., Le Bronec J., Morel P., Robe M.C., Maurenas J.M., Faivre-Pierret R., Martin D., Sabroux J.C., Zettwoog P. (1991) - Eruptive and diffuse emissions of CO₂ from Mount Etna. *Nature*, 351, 387-391.
- Andronico D. and Corsaro R.A. (2011) - Lava fountains during the episodic eruption of South-East Crater (Mt. Etna), 2000: insights into magma-gas dynamics within the shallow volcano plumbing system. *Bull. Volcanol.*, 73, 1165-1178, <http://dx.doi.org/10.1007/s00445-011-0467-y>.
- Andronico D., Branca S., Calvari S., Burton M.R., Caltabiano T., Corsaro R.A., et al. (2005) - A multi-disciplinary study of the 2002-03 Etna eruption: insights for a complex plumbing system. *Bull. Volcanol.*, 67, 314-330. doi:10.1007/s00445-004-0372-8.
- Azzaro R., Bonforte A., Branca S., Guglielmino F. (2013) - Geometry and kinematics of the fault systems controlling the unstable flank of Etna volcano (Sicily). *J. Volcan. Geother. Res.*, 251, 5-15.
- Azzaro R., Branca S., Gwinner K., Coltelli M. (2012) - The volcano-tectonic map of Etna volcano, 1:100.000 scale: morphotectonic analysis from high-resolution DEM integrated with geologic, active faulting and seismotectonic data. *Italian Journal of Geosciences (Boll. Soc. Geol. It.)*, 131(1), 153-170.
- Beccaluva L., Gabbianelli G., Lucchini F., Rossi P.L., Savelli C. (1985) - Petrology and K/Ar ages of volcanic dredged from the Aeolian seamounts: implications for geodynamic evolution of the Southern Tyrrhenian basin. *Earth Planet. Sci. Lett.*, 74, 187-208.
- Behncke B. and Neri M. (2003) - The July-August 2001 eruption of Mt. Etna (Sicily). *Bull. Volcanol.*, 65, 461-476. <http://dx.doi.org/10.1007/s00445-003-0274-1>.
- Bertagnini A., Metrich N., Francalanci L., Landi P., Tommasini S., Conticelli S. (2008) - Volcanology and magma geochemistry of the present-day activity: constraints on the feeding system. In: Calvari S., Inguaggiato S., Puglisi G., Ripepe M., Rosi M. (eds) *The Stromboli Volcano. An Integrated Study of the 2002-2003 Eruption*. AGU, Washington, Geophysical Monograph, 182, 19-37.
- Biass S., Falcone J.L., Bonadonna C., Di Traglia F., Pistolesi M., Rosi M., Lestuzzi P. (2016) - Great Balls of Fire: A probabilistic approach to quantify the hazard related to ballistics — A case study at La Fossa volcano, Vulcano Island, Italy, *J. of Volcanol. And Geotherm. Res.*, 325, 1-14.
- Bigazzi G. and Bonadonna F.P. (1973) - Fission track dating of the obsidian of Lipari Island (Italy). *Nature*, 242, 322-323.
- Bonforte A., Guglielmino F., Coltelli M., Ferretti A., Puglisi G. (2011) - Structural assessment of Mount Etna volcano from Permanent Scatterers analysis. *Geochemistry, Geophysics, Geosystems* 12, Q02002. <http://dx.doi.org/10.1029/2010GC003213>.
- Borgia A., Ferrari L., Pasquarè G. (1992) - Importance of gravitational spreading in the tectonic and volcanic evolution of Mount Etna. *Nature*, 357, 231-235.
- Bousquet J.C., Gabbianelli G., Lanzafame G., Sartori R. (1998) - Evolution volcanotectonique de l'Etna (Sicile): nouvelles données de géologie marine et terrestre. *Rapport de la Commission Internationale pour l'Exploration Scientifique de la Mer Méditerranée*, 35, 56-57.

- Bousquet J.C. and Lanzafame G. (2004) - The tectonics and geodynamics of Mt. Etna: synthesis and interpretation of geological and geophysical data. In: Bonaccorso A., Calvari S., Coltelli M., Del Negro C., Falsaperla S. (Eds.), Mt. Etna: Volcano Laboratory: American Geophysical Union, Geophysical Monograph, 143, 29–47.
- Branca S., De Beni E., Chester D., Duncan A., Lotteri A. (2017) - The 1928 eruption of Mount Etna (Italy): Reconstructing lava flow evolution and the destruction and recovery of the town of Mascali. *Journal of Volcanology and Geothermal Research* 335, 54–70.
- Branca S., De Beni E., Proietti C. (2013) - The large and destructive 1669 AD Etna eruption: reconstruction of the lava flow field evolution and effusion rate trend. *Bull. Volcanol.*, 75 (694), 2–16. <http://dx.doi.org/10.1007/s00445-013-0694-5>.
- Branca S., Coltelli M., Groppelli G., Lentini F. (2011a) - Geological Map Of Etna Volcano, 1:50,000 Scale. *Ital. J. Geosci.*, 130 (3), 265–291. <http://dx.doi.org/10.3301/IJG.2011.15>.
- Branca S., Coltelli M., Groppelli G. (2011b) - Geological evolution of a complex basaltic stratovolcano: Mount Etna, Italy. *It. J. Geosci. (Boll. Soc. Geol. It.)*, 130(3), <http://dx.doi.org/10.3301/IJG.2011.13>.
- Branca S., Coltelli M., Groppelli G. (2004) - Geological evolution of Etna volcano. In: "Etna Volcano Laboratory", Bonaccorso, Calvari, Coltelli, Del Negro, Falsaperla (Eds), AGU (Geophy - sical monograph series), 143, 49-63.
- Branca S., Carbone D., Greco F. (2003) - Intrusive mechanism of the 2002 NE-Rift eruption at Mt. Etna (Italy) inferred through continuous microgravity data and volcanological evidences. *Geophys. Res. Lett.*, 30(20), 2077, <http://dx.doi.org/10.1029/2003GL018250>.
- Branca S. and Del Carlo P. (2005) - Types of eruptions of Etna Volcano AD 1670-2003: Implications for short-term eruptive behaviour. *Bull. Volcanol.*, 67, 732-742.
- Calanchi N., De Rosa R., Mazzuoli R., Rossi P.L., Santacroce R., Ventura G. (1993) - Silicic magma entering a basaltic magma chamber: eruptive dynamics and magma mixing-an example from Salina (Aeolian islands, Southern Tyrrhenian Sea). *Bull. Volcanol.*, 55, 504-522.
- Caltabiano T., Burton M., Giammanco S., Allard P., Bruno N., Murè F., Romano R (2004) - Volcanic gas emissions from the summit craters and flanks of Mt. Etna, 1987 – 2000. In: Bonaccorso A, Calvari S, Coltelli M, Del Negro C, Falsaperla S (eds) Mt. Etna Volcano Laboratory, *Geophys. Monogr. Ser.*, AGU, Washington, D.C., 143, 111–128.
- Calvari S. and Groppelli G. (1996) - Relevance of the Chiancone volcanoclastic deposit in the recent history of Etna Volcano (Italy). *J. Volcanol. Geother. Res.*, 72, 239-258.
- Calvari S., Lodato L., Steffke A., Cristaldi A., Harris A.J.L., Spampinato L., Boschi E. (2010) - The 2007 Stromboli eruption: event chronology and effusion rates using thermal infrared data. *J. of Geophys. Res. – Solid Earth*, 115, B04201.
- Calvari S., Spampinato L., Lodato L., Harris A.J.L., Patrick M.R., Dehn J., Burton M.R., Andronico D. (2005) - Chronology and complex volcanic processes during the 2002–2003 flank eruption at Stromboli volcano (Italy) reconstructed from direct observations and surveys with a handheld thermal camera. *J. of Geophys. Res. – Solid Earth*, 110, B02201.
- Calvari S., Tanner L.H., Groppelli G., Norini G. (2004) – A comprehensive model for the opening of the Valle del Bove depression and hazard evaluation for the eastern flank of Etna volcano. In: "Etna Volcano Laboratory", Bonaccorso A., Calvari S., Coltelli M., Del Negro C., Falsaperla S. (Eds.), AGU (Geophysical monograph), 143, 65-75.

- Calvari S., Tanner L.H., Groppelli G. (1998) - Debris-avalanche deposits of the Milo-Lahar sequence and the opening of the Valle del Bove on Etna volcano (Italy). *J. Volcanol. Geother. Res.*, 87, 193-209.
- Calvari S., Coltelli M., Neri M., Pompilio M., Scribano V. (1994) - The 1991-1993 Etna eruption: Chronology and lava flow-field evolution, *Acta Vulcanol.*, 4, 1-14.
- Carapezza M.L., Barberi F., Ranaldi M., Ricci T., Tarchini L., Barrancos J., Fischer C., Perez N., Weber K., Di Piazza A., Gattuso A. (2011) - Diffuse CO₂ soil degassing and CO₂ and H₂S concentrations in air and related hazards at Vulcano Island (Aeolian arc, Italy). *J. Volcanol. Geotherm. Res.*, 207, 130-144.
- Carbone S., Lentini F., Grasso M. (1982) - Considerazioni sull'evoluzione geodinamica della Sicilia sud-orientale dal Cretaceo al Quaternario. *Mem. Soc. Geol. It.*, 24, 367-386.
- Cas R.A.F. and Wright J.V. (1987) - *Volcanic Successions*. Unwin Hyman, London.
- Casalbore D., Romagnoli C., Bosman A., De Astis G., Lucchi F., Tranne C.A., Chiocci F.L. (2018) - Multi-stage formation of La Fossa Caldera (Vulcano Island, Italy) from an integrated subaerial and submarine analysis. *Marine Geophys. Res.*, 1-14.
- Chappell J. and Shackleton N.J. (1986) - Oxygen isotopes and sea level. *Nature*, 324, 137-140.
- Chiocci F.L., Coltelli M., Bosman A., Cavallaro D. (2011) - Continental margin large-scale instability controlling the flank sliding of Etna volcano. *Earth and Planetary Science Letters*, 305, 57-64, <http://dx.doi.org/10.1016/j.epsl.2011.02.040>.
- Chiodini G., Cioni R., Marini L., Panichi C. (1995) - Origin of the fumarolic fluids of Vulcano Island, Italy, and implications for volcanic surveillance. *Bull. Volcanol.*, 57, 99-110.
- Colella A. and Hiscott R.N. (1997) - Pyroclastic surges of the Pleistocene Monte Guardia sequence (Lipari Island, Italy): depositional processes. *Sedimentology*, 44, 47-66.
- Coltelli M., Marsella M., Proietti C., Scifoni S. (2012) - The case of the 1981 eruption of Mount Etna: An example of very fast moving lava flows, *Geochem. Geophys. Geosyst.*, 13, Q01004, <http://dx.doi.org/10.1029/2011GC003876>.
- Coltelli M., Del Carlo P., Pompilio M., Vezzoli L. (2005) - Explosive eruption of a picrite: the 3930 BP subplinian eruption of Etna volcano (Italy). *Geophys. Res. Lett.*, 32, L23307, <http://dx.doi.org/10.1019/2005GL024271R>.
- Coltelli M., Del Carlo P., Vezzoli L. (1998) - The discovery of a Plinian basaltic eruption of Roman age at Etna volcano, Italy. *Geology*, 26, 1095-1098.
- Coltelli M., Del Carlo P., Vezzoli L. (2000) - Stratigraphic constrains for explosive activity in the last 100 ka at Etna volcano. Italy. *Inter. J. Earth Sciences*, 89, 665-677.
- Coltelli M., Garduño V.H., Neri M., Pasquaré G., M. Pompilio (1994) - Geology of the northern wall of Valle del Bove, Mt. Etna (Sicily). *Acta Vulcanologica*, 5, 55-68.
- Corazzato C., Francalanci L., Menna M., Petrone C.M., Renzulli A., Tibaldi A., Vezzoli L. (2008) - What controls sheet intrusion in volcanoes? Structure and petrology of the Stromboli sheet complex, Italy. *J. Volcanol. Geotherm. Res.*, 173, 26-54.
- Corsaro R.A. and Pompilio M. (2004) - Dynamics of magmas at Mount Etna. In: Bonaccorso A, Calvari S, Coltelli M, Del Negro C, Falsaperla S (eds) *Mt Etna Volcano Laboratory*. AGU (Geophysical monograph series), 143, 91-110.

- Corsaro R.A., Neri M., Pompilio M. (2002) - Paleo-environmental and volcano-tectonic evolution of the southeastern flank of Mt. Etna during the last 225 ka inferred from the volcanic succession of the "Timpe", Acireale, Sicily. *J. Volcanol. Geotherm. Res.*, 113, 289–306.
- Crisci G.M., Delibrias G., De Rosa R., Mazzuoli R., Sheridan M.F. (1983) - Age and petrology of the Late-Pleistocene Brown Tuffs on Lipari, Italy. *Bull. Volcanol.*, 46, 381–391.
- Crisci G.M., De Rosa R., Lanzafame G., Mazzuoli R., Sheridan M.F., Zuffa G.G. (1981) - Monte Guardia Sequence: a Late-Pleistocene Eruptive Cycle on Lipari (Italy). *Bull. Volcanol.*, 44, 241–255.
- Davì M., De Rosa R., Barca D. (2009) - A LA-ICP-MS study of minerals in the Rocche Rosse magmatic enclaves: evidence of a mafic input triggering the latest silicic eruption of Lipari Island (Aeolian Arc, Italy). *J. Volcanol. Geotherm. Res.*, 182, 45–56.
- De Astis G., Dellino P., La Volpe L., Lucchi F., Tranne C.A. (2013a) - Geological map of the island of Vulcano, scale 1:10,000 (Aeolian archipelago). In: Lucchi F., Peccerillo A., Keller J., Tranne C.A., Rossi P.L. (eds) *The Aeolian Islands Volcanoes*. Geological Society, London, Memoirs, 37, enclosed DVD.
- De Astis G., Lucchi F., Dellino P., La Volpe L., Tranne C.A., Frezzotti M.L., Peccerillo, A. (2013b) - Geology, volcanic history and petrology of Vulcano (central Aeolian archipelago). In: Lucchi F., Peccerillo A., Keller J., Tranne C.A., Rossi P.L. (eds) *The Aeolian Islands Volcanoes*. Geological Society, London, Memoirs, 37, 281–348.
- De Beni E., Branca S., Coltelli M., GropPELLI G., Wijbrans J. (2011) - ³⁹Ar/⁴⁰Ar isotopic dating of Etna volcanic succession. *Italian Journal of Geosciences* 130 (3), 292–305 <http://dx.doi.org/10.3301/IJG.2011.14>.
- Del Carlo P., Branca S., D'Orlando C. (2017) - New findings of Late Glacial Etna pumice fall deposits in NE Sicily and implications for distal tephra correlations in the Mediterranean area. *Bull. Volcanol.* 79:50, <http://dx.doi.org/10.1007/s00445-017-1135-7>.
- Del Carlo P. and Branca S. (1998) - Tephrostratigraphic dating of the pre-1300 AD SE flank eruptions of Mt Etna. *Acta Vulcanol.*, 10, 33–37.
- Delle Donne D., Marchetti E., Ripepe M., Ulivieri G., Lacanna G. (2006) - Monitoring explosive volcanic activity using thermal images, Stromboli volcano, Italy. *EOS Transact., AGU*, 79, 1975.
- Dellino P. and La Volpe L. (1995) - Fragmentation versus transportation mechanisms in the pyroclastic sequence of Monte Pilato – Rocche Rosse (Lipari, Italy). *J. Volcanol. Geotherm. Res.*, 64, 211–232.
- Dellino P. and La Volpe L. (1997) - Stratigrafia, dinamiche eruttive e deposizionali, scenario eruttivo e valutazioni di pericolosità a La Fossa di Vulcano. In: La Volpe L., Dellino P., Nuccio M., Privitera E., Sbrana A. (eds) *Progetto Vulcano: Risultati dell'attività di ricerca 1993–1995*. CNR – Gruppo Nazionale per la Vulcanologia, Felici Editore, Pisa, 214–237.
- Dellino P., De Astis G., La Volpe L., Mele D., Sulpizio R. (2011) - Quantitative hazard assessment of phreatomagmatic eruptions at Vulcano (Aeolian Islands – Southern Italy) as obtained by combining stratigraphy, event statistics and physical modelling. *J. Volcanol. Geotherm. Res.*, 201, 364–384.
- Del Negro C. and Napoli R. (2002) - Ground and marine magnetic surveys of the lower eastern flank of Etna volcano (Italy). *J. Volcanol. Geotherm. Res.*, 114, 357–372.

- De Rosa R., Donato P., Gioncada A., Masetti M., Santacroce R. (2003) - The Monte Guardia eruption (Lipari, Aeolian islands): an unusual example of magma mixing sequence. *Bull. Volcanol.*, <http://dx.doi.org/10.1007/s00445-003-0281-2>.
- De Rosa R., Donato P., Scarciglia F. (2016) - On the origin and post-depositional history of widespread massive ash deposits: the case of Intermediate Brown Tuffs (IBT) of Lipari (Aeolian Islands, Italy). *J. Volcanol. Geotherm. Res.*, 327, 135-151.
- Di Martino C., Frezzotti M.L., Lucchi F., Peccerillo A., Tranne C.A., Diamond L.W. (2010) - Magma storage and ascent at Lipari Island (Aeolian archipelago, southern Italy) during the old stages (223–81 ka): role of crustal processes and tectonic influence. *Bull. Volcanol.*, 72, 1061–1076.
- Di Martino C., Forni F., Frezzotti M.L., Palmeri R., Webster J.D., Ayuso R.A., Lucchi F., Tranne C.A. (2011) - Formation of cordierite-bearing lavas during anatexis in the lower crust beneath Lipari Island (Aeolian arc, Italy). *Contrib. Mineral. Petrol.*, 162, 1011–1030.
- Di Stefano A., Branca S. (2002) - Long-term uplift rate of the Etna volcano basement (Southern Italy) from biochronological data of the Pleistocene sediments. *Terra Nova*, 14, 61–68.
- Di Traglia F. (2011) - The last 1000 years of eruptive activity at the Fossa Cone (Island of Vulcano, Southern Italy). Phd Thesis, University of Pisa, Italy.
- Di Traglia F., Pistolesi M., Rosi M., Bonadonna C., Fusillo R., Roverato M. (2013) - Growth and erosion: The volcanic geology and morphological evolution of La Fossa (Island of Vulcano, Southern Italy) in the last 1000 years. *Geomorphology*, 194, 94–107.
- Ferrucci M., Pertusati S., Sulpizio R., Zanchetta G., Pareschi M.T., Santacroce R. (2005) - Volcaniclastic debris flows at La Fossa Volcano (Vulcano Island, southern Italy): Insights for erosion behaviour of loose pyroclastic material on steep slopes. *J. Volcanol. Geotherm. Res.*, 145, 173–191.
- Forni F., Lucchi F., Peccerillo A., Tranne C.A., Rossi P.L., Frezzotti M.L. (2013) - Stratigraphy and geological evolution of the Lipari volcanic complex (central Aeolian archipelago). In: Lucchi F., Peccerillo A., Keller J., Tranne C.A. and Rossi P.L. (eds) *The Aeolian Islands Volcanoes*. Geological Society, London, *Memoirs*, 37, 213–279.
- Forni F., Ellis B.S., Bachmann O., Lucchi F., Tranne C.A., Agostini S., Dallai L. (2015) - Erupted cumulate fragments in rhyolites from Lipari (Aeolian Islands). *Contr. Mineral. Petrol.*, 170, 49.
- Francalanci L., Braschi E., Di Salvo S., Lucchi F., Petrone C.M. (2014) - When magmas do not interact: paired Roman-age activity revealed by tephra studies at Stromboli volcano. *Bull. Volcanol.*, 76, 884.
- Francalanci L., Lucchi F., Keller J., De Astis G., Tranne C.A. (2013) - Eruptive, volcano-tectonic and magmatic history of the Stromboli volcano (north-eastern Aeolian archipelago). In: Lucchi F., Peccerillo A., Keller J., Tranne C.A. and Rossi P.L. (eds) *The Aeolian Islands Volcanoes*. Geological Society, London, *Memoirs*, 37, 395–469.
- Francalanci L., Tommasini L., Conticelli S., Davies G.R. (1999) - Sr isotope evidence for new magma input and short residence time in the XX century activity of Stromboli volcano. *Earth Planet. Sci. Lett.*, 167, 61–69.
- Francis P., Burton M.R., Oppenheimer C. (1998) - Remote measurements of volcanic gas compositions by solar occultation spectroscopy. *Nature*, 396, 567-570.

- Fusillo R., Di Traglia F., Gioncada A., Pistolesi M., Wallace P.J., Rosi M. (2015) - Deciphering post-caldera volcanism: insight into the Vulcanello (Island of Vulcano, Southern Italy) eruptive activity based on geological and petrological constraints. *Bulletin of Volcanology*, <http://dx.doi.org/10.1007/s00445-015-0963-6>.
- Galderisi A., Bonadonna C., Delmonaco G., Ferrara F.F., Menoni S., Ceudech A., Biass S., Frischknecht C., Manzella I., Minucci G., Gregg C. (2013) - Vulnerability Assessment and Risk Mitigation: The Case of Vulcano Island, Italy, *Landslide Science and Practice*, Volume 7: Social and Economic Impact and Policies, Springer Berlin Heidelberg, 55-64, http://dx.doi.org/10.1007/978-3-642-31313-4_8.
- Gamberi F., Marani M., Savelli C. (1997) - Tectonic, volcanic and hydrothermal features of a submarine portion of the Aeolian arc (Tyrrhenian sea). *Marine Geol.*, 140, 1-2, 167-181.
- Gamberi F. and Marani M.P. (1997) - Detailed bathymetric mapping of the eastern offshore slope of Lipari island (Tyrrhenian Sea): insight into the dark side of an arc volcano. *Marine Geophys. Res.*, 19, 363-377.
- Guarduño V.H., Neri M., Pasquarè G., Borgia A., Tibaldi A. (1997) - Geology of the NE-Rift of Mount Etna (Sicily, Italy). *Acta Vulcanol.*, 9, 91-100.
- Geshi N. and Neri M. (2014) - Dynamic feeder dike systems in basaltic volcanoes: the exceptional example of the 1809 Etna eruption (Italy). *Front. Earth Sci.*, 2, 13, <http://dx.doi.org/10.3389/feart.2014.00013>.
- Giammanco S., Gurrieri S., Valenza M. (1997) - Soil CO₂ degassing along tectonic structures of Mount Etna (Sicily): the Pernicana fault. *Applied Geochem.*, 12, 429, 13.
- Gillot P.Y., Kieffer G., Romano R. (1994) - The evolution of Mount Etna in the light of potassium-argon dating. *Acta Vulcanologica*, 5, 81-87.
- Gioncada A., Mazzuoli R., Bisson M., Pareschi M.T. (2003) Petrology of volcanic products younger than 42 ka on the Lipari-Vulcano complex (Aeolian Islands, Italy): an example of volcanism controlled by tectonics. *J. Volcanol. Geotherm. Res.*, 122, 191-220.
- Gioncada A. and Sbrana A. (1991) - 'La Fossa caldera', Vulcano: inferences from deep drillings. *Acta Vulcanologica*, 1, 115-125.
- Granieri D., Carapezza M.L., Chiodini G., Avino R., Caliro S., Ranaldi M., Ricci T., Tarchini L. (2006) - Correlated increase in CO₂ fumarolic content and diffuse emission from La Fossa crater (Vulcano, Italy): Evidence of volcanic unrest or increasing gas release from a stationary deep magma body? *Geophys. Res. Lett.*, 33, L13316, <http://dx.doi.org/10.1029/2006GL026460>.
- Grasso M., Ben Avraham Z. (1992) - Magnetic study of the northern margin of the Hyblean Plateau, southern Sicily: structural implication. *Ann. Tectonicae*, 6, 202-213.
- Guest J.E., Chester D.K., Duncan A.M. (1984) - The Valle del Bove, Mount Etna: its origin and relation to the stratigraphy and structure of the volcano. *Journal of Volcanology and Geothermal Research*, 21, 1-23.
- Harris A. and Ripepe M. (2007) - Temperature and dynamics of degassing at Stromboli. *J. Geophys. Res. - Solid Earth*, 112, B03205.
- Hornig-Kjarsgaard I., Keller J., Koberski U., Stadlbauer E., Francalanci L., Lenhart R. (1993) - Geology, stratigraphy and volcanological evolution of the island of Stromboli, Aeolian arc, Italy. *Acta Vulcanologica*, 3, 21-68.
- Keller J. (1980) - The island of Salina. *Rend. Soc. It. Mineral. Petrol.*, 36, 489-524.

- Keller J. (1981) - Quaternary tephrochronology in the Mediterranean region. In: Self S., Sparks S.R.J. (eds) Tephra Studies. NATO, Advanced Study Institutes Series C 75, D. Reidel Publishing Company, Dordrecht, 227–244.
- Keller J. (2002) - Lipari's fiery past: dating the medieval pumice eruption of Monte Pelato: International Conference 'The fire between air and water', UNESCO-Regione Siciliana, Lipari, September 29th–October 2nd, oral presentation.
- Keller J., Ryan W.B.F., Ninkovich D., Altherr R. (1978) - Explosive volcanic activity in the Mediterranean over the past 200.000 yr as recorded in deep-sea sediment. *Geol. Americ. Soc. Bull.*, 89, 591–604.
- Kraml M., Keller J., Henjes-Kunst F. (1997) - Dating of Upper Quaternary deep-sea sediments from the Ionian Sea (Eastern Mediterranean) with laser $^{40}\text{Ar}/^{39}\text{Ar}$ analyses on prominent tephra layers. EUG 9 (European Union of Geosciences), Strasbourg (France) 23–27 March 1997, *Terra Nova* 9, Abstract Supplement 1, 406.
- Laiolo M. and Cigolini C. (2006) - Mafic and ultramafic xenoliths in San Bartolo lava field: new insights on the ascent and storage of Stromboli magmas. *Bull. Volcanol.*, 68, 653–670.
- Le Maitre, R. W., Streckeisen A., Zanettin B., Le Bas M.J., Bonin B., Bateman P. (2010) – *Igneous Rocks – A classification and Glossary of terms*. Cambridge University Press, UK.
- Le Maitre, R. W., Streckeisen A., Zanettin B., Le Bas M.J., Bonin B., Bateman P. (2010) – *Igneous Rocks – A classification and Glossary of terms*. Cambridge University Press, UK.
- Lentini F., Carbone S., Guarnieri P. (2006) - Collisional and postcollisional tectonics of the Apenninic–Maghrebien orogen (southern Italy). In: Dilek, Y., Pavlides, S. (Eds.), *Postcollisional tectonics and magmatism in the Mediterranean region and Asia*: GSA Special Paper, 409, 57–81.
- Liotta M., Paonita A., Caracausi A., Martelli M., Rizzo A., Favara R. (2010) - Hydrothermal processes governing the geochemistry of the crater fumaroles at Mount Etna volcano (Italy). *Chemical Geology*, 278, 92–104.
- Lo Giudice E. and Rasà R. (1992) - Very shallow earthquakes and brittle deformation in active volcanic areas: the Etnean region as an example. *Tectonophysics*, 202, 257–268.
- Longaretti G., Rocchi S. (1991) - Il magmatismo dell'Avampese Ibleo (Sicilia orientale) tra il trias e il Quaternario: dati stratigrafici e petrologici di sottosuolo. *Mem. Soc. Geol. It.*, 45, 911–925.
- Lucchi F. (2009) - Late-Quaternary marine terrace deposits as tools for wide-scale correlation of unconformity-bounded units in the volcanic Aeolian archipelago (southern Italy). *Sediment. Geol.*, 216, 158–178.
- Lucchi F. (2013) - Stratigraphic methodology for the geological mapping of volcanic areas: insights from the Aeolian archipelago (Southern Italy). In: Lucchi F., Peccerillo A., Keller J., Tranne C.A., Rossi P.L. (eds) *The Aeolian Islands Volcanoes*. Geological Society, London, *Memoirs*, 37, 37–53.
- Lucchi F., Gertisser R., Keller J., Forni F., De Astis G., Tranne C.A. (2013a) - Eruptive history and magmatic evolution of the island of Salina (central Aeolian archipelago). In: Lucchi F., Peccerillo A., Keller J., Tranne C.A., Rossi P.L. (eds) *The Aeolian Islands Volcanoes*. Geological Society, London, *Memoirs*, 37, 155–211.
- Lucchi F., Keller J., De Astis G., Francalanci L., Tranne C.A. (2013b) - Geological map of Stromboli, scale 1:10 000 (Aeolian archipelago). In: Lucchi F., Peccerillo A., Keller J., Tranne C.A., Rossi P.L. (eds) *The Aeolian Islands Volcanoes*. Geological Society, London, *Memoirs*, 37, enclosed DVD.

- Lucchi F., Keller J., Tranne C.A. (2013c) - Regional stratigraphic correlations across the Aeolian archipelago (southern Italy). In: Lucchi F., Peccerillo A., Keller J., Tranne C.A., Rossi P.L. (eds) *The Aeolian Islands Volcanoes*. Geological Society, London, *Memoirs*, 37, 57–81.
- Lucchi F., Tranne C.A., De Astis G., Keller J., Losito R., Morche W. (2008) - Stratigraphy and significance of Brown Tuffs on the Aeolian Islands (southern Italy). *J. Volcanol. Geotherm. Res.*, 177, 49–70.
- Lucchi F., Tranne C.A., Calanchi N. Rossi P.L. (2004) - Stratigraphic constraints to date late Quaternary ancient shorelines and to evaluate vertical movements at Lipari (Aeolian Islands). *Quatern. Int.*, 115/116, 105–115.
- Lucchi F., Tranne C.A., Forni F., Rossi P.L. (2013d) - Geological map of the island of Lipari, scale 1:10 000 (Aeolian archipelago). In: Lucchi F., Peccerillo A., Keller J., Tranne C.A., Rossi P.L. (eds) *The Aeolian Islands Volcanoes*. Geological Society, London, *Memoirs*, 37, enclosed DVD.
- Lundgren P., Casu F., Manzo M., Pepe, A., Berardino P., Sansosti E., Lanari R. (2004) - Gravity and magma induced spreading of Mount Etna volcano revealed by satellite radar interferometry. *Geophysical Research Letters* 31, L04602. <http://dx.doi.org/10.1029/2003GL018736>.
- Marsella M., Baldi P., Coltelli M., Fabris M. (2012) - The morphological evolution of the Sciara del Fuoco since 1868: reconstructing the effusive activity at Stromboli volcano. *Bull. Volcanol.*, 74, 231–248.
- Mazzarini F. and Armienti P. (2001) - Flank cones at Mount Etna Volcano: do they have a power-law distribution? *Bull. Volcanol.*, 62, 420–430.
- Mazzuoli R., Tortorici L., Ventura G. (1995) - Oblique rifting in Salina, Lipari and Vulcano Islands (Aeolian Islands, Southern Tyrrhenian Sea, Italy). *Terra Nova*, 7, 444–452.
- McGuire W.J., Moss J.L., Saunder, S.J., Stewart I.S. (1996) - Dike-induced rifting and edifice instability at Mount Etna. In: Gravestock, P.J., McGuire, W.J. (Eds.), *Etna: 15 Years On*. ODA/Cheltenham & Gloucester College of Higher Education, 20–24.
- Mercalli G. and Silvestri O. (1891) - L'eruzione dell'Isola di Vulcano incominciata il 3 agosto 1888 e terminata il 22 marzo 1890. *Ann. Uff. Centr. Metereol. Geodinam.*, 10, 71–281.
- Monaco C., Tapponnier P., Tortorici L., Gillot P.Y. (1997) - Late Quaternary slip rates on the Acireale–Piedimonte normal faults and tectonic origin of Mt. Etna (Sicily). *Earth and Planetary Science Letters*, 147, 125–139.
- Neri M., Acocella V., Behncke B. (2004) -The role of the Pernicana fault system in the spreading of Mount Etna (Italy) during the 2002–2003 eruption. *Bulletin of Volcanology*, 66, 417–430.
- Nicotra E., Giuffrida M., Viccaro M., Donato P., D'Oriano C., Paonita A., De Rosa R. (in press) - Timescales of pre-eruptive magmatic processes at Vulcano (Aeolian Islands, Italy) during the last 1000 years. *Lithos*.
- Nuccio P.M., Paonita A., Sortino F. (1999) - Geochemical modeling of mixing between magmatic and hydrothermal gases: the case of Vulcano, Italy. *Earth Plan. Sci. Lett.*, 167, 321–333.
- Paonita A., Federico C., Bonfanti P., Capasso G., Inguaggiato S., Italiano F., Madonia P., Pecoraino G., Sortino F. (2013) - The episodic and abrupt geochemical changes at La Fossa fumaroles (Vulcano Island, Italy) and related constraints on the dynamics, structure, and compositions of the magmatic system. *Geochim. et Cosmochim. Acta*, 120, 158–178.

- Patrick M.R., Harris A.J.L., Ripepe M., Dehn J., Rothery D.A., Calvari S. (2007) - Strombolian explosive styles and source conditions: insights from thermal (FLIR) video. *Bull. Volcanol.*, 69, 769–784.
- Peccerillo A., De Astis G., Faraone D., Forni F., Frezzotti M.L. (2013) - Compositional variations of magmas in the Aeolian arc: implications for petrogenesis and geodynamics. In: Lucchi F., Peccerillo A., Keller J., Tranne C.A., Rossi P.L. (eds) *The Aeolian Islands Volcanoes*. Geological Society, London, *Memoirs*, 37, 489–508.
- Peccerillo A. and Taylor S.R. (1976) - Geochemistry of the Eocene calc-alkaline volcanic rocks from the Kastamonu area, northern Turkey. *Contr. Mineral. Petrol.*, 58, 63–81.
- Puglisi G. and Bonforte A. (2004) - Dynamics of Mount Etna volcano inferred from static and kinematic GPS measurements. *Geophysical Research Letters* 109, B11404. <http://dx.doi.org/10.1029/2003jb002878>.
- Rasà R., Azzaro R., Leonardi O. (1996) - Aseismic creep on faults and flank instability at Mount Etna volcano, Sicily. In: McGuire W.J., Jones A.P., Neuberg J. (Eds.), *Volcano Instability on the Earth and Other Planets*: Geological Society of London, *Special Publications*, 110, 179–192.
- Ricci Lucchi F., Calanchi N., Lanzafame G., Rossi P.L. (1988) - Plant-rich pyroclastic deposits of Monte S. Angelo, Lipari (Aeolian Island). *Rend. Soc. Mineral. Petrol.*, 43, 1227–1251.
- Ripepe M. (1996) - Evidence for gas influence on volcanic seismic signals recorded at Stromboli. *J. Volcanol. Geotherm. Res.*, 70, 3–4, 221–233.
- Rittmann A. (1973.) - Structure and evolution of Mount Etna. *Philos. Trans. R. Soc. Lond.*, 274A, 5–16.
- Romagnoli C., Calanchi C., Gabbianelli G., Lanzafame G., Rossi P.L. (1989) - Contributi delle ricerche di geologia marina alla caratterizzazione morfostrutturale ed evolutiva dei complessi vulcanici di Salina, Lipari e Vulcano (Isole Eolie). *Boll. GNV (Gruppo Nazionale di Vulcanologia)*, 2, 971–978.
- Romagnoli C., Casalbore D., Bortoluzzi G., Bosman A., Chiocci F.L., D’Oriano F., Gamberi F., Ligi M., Marani M. (2013) - Bathymorphological setting of the Aeolian islands. In: Lucchi F., Peccerillo A., Keller J., Tranne C.A., Rossi P.L. (eds) *The Aeolian Islands Volcanoes*. Geological Society, London, *Memoirs*, 37, 27–36.
- Rosi M., Bertagnini A., Landi P. (2000) - Onset of the persistent activity at Stromboli volcano (Italy). *Bull. Volcanol.*, 62, 294–300.
- Rosi M., Pistolesi M., Bertagnini A., Landi P., Pompilio M., Di Roberto A. (2013) - Stromboli Volcano, Aeolian Islands (Italy): present eruptive activity and hazards. In: Lucchi F., Peccerillo A., Keller J., Tranne C.A., Rossi P.L. (eds) *The Aeolian Islands Volcanoes*. Geological Society, London, *Memoirs*, 37, 471–488.
- Ruch J., Vezzoli L., De Rosa R., Di Lorenzo R., Acocella R. (2016). Magmatic control along a strike-slip volcanic arc: The central Aeolian arc (Italy). *Tectonics*, 35, 2, 407–424.
- Rust D. and Neri M. (1996) - The boundaries of large-scale collapse on the flanks of Mount Etna, Sicily. In: McGuire W.J., Jones A.P., Neuberg J. (Eds.), *Volcano Instability on the Earth and Other Planets*: Geological Society of London, *Special Publications*, 110, 193–208.
- Scollo S., Coltelli M., Bonadonna C., Del Carlo P. (2013) - Tephra hazard assessment at Mt. Etna (Italy). *Nat. Hazards Earth Syst. Sci.*, 13, 12, 3221–3233.

- Sheridan M.F., Frazzetta G., La Volpe L. (1987) - Eruptive histories of Lipari and Vulcano, Italy, during the past 22.000 years. In: J.H. Fink (Editor), The emplacement of silicic domes and lava flows. Geol. Soc. Am., Special Papers, 212, 29-34.
- Solaro G., Acocella V., Pepe S., Ruch J., Neri M., Sansosti E. (2010) - Anatomy of an unstable volcano from InSAR: multiple processes affecting flank instability at Mt. Etna, 1994–2008. Journal of Geophysical Research 115, B10405. <http://dx.doi.org/10.1029/2009JB000820>.
- Spampinato L., Calvari S., Harris A.J.L., Dehn J. (2008) - Evolution of the lava flow field by daily thermal and visible airborne surveys. In: Calvari S., Inguaggiato S., Puglisi G., Ripepe M., Rosi M. (eds) The Stromboli Volcano. An Integrated Study of the 2002–2003 eruption. AGU, Washington, Geophysical Monograph, 182, 201–211.
- Speranza F., Pompilio M., D’Ajello Caracciolo F., Sagnotti L. (2008) - Holocene eruptive history of the Stromboli volcano: constraints from paleomagnetic dating. J. Geophys. Res. – Sol. Earth, 113, B09101.
- Tibaldi A. (2001) - Multiple sector collapses at Stromboli volcano, Italy: how they work. Bull. Volcanol., 63, 112–125.
- Ventura G. (2013) - Kinematics of the Aeolian volcanism (Southern Tyrrhenian Sea) from geophysical and geological data. In: Lucchi F., Peccerillo A., Keller J., Tranne C.A., Rossi P.L. (eds) The Aeolian Islands Volcanoes. Geological Society, London, Memoirs, 37, 3–11.
- Waelbroeck C., Labeyrie L., Michel E., Duplessy J.C., McManus J.F., Lambeck K., Balbon E., Labracherie M. (2002) - Sea-level and deep water temperature changes derived from foraminifera isotopic records. Quat. Sci. Rev., 21, 295–305.
- Wulf S., Kraml M., Brauer A., Keller J., Negendank J.F.W. (2004) - Tephrochronology of the 100 ka lacustrine sediment record of Lago Grande di Monticchio (southern Italy). Quatern. Int., 122, 7–30.
- Zanchetta G., Sulpizio R., Neils R., Cioni R., Eastwood W.J., Siani G., Caron B., Paterne M., Santacroce R. (2011) - Tephrostratigraphy, chronology and climatic events of the Mediterranean basin during the Holocene: an overview. The Holocene, 21, 33–52.